Université de Montréal

Nitrate metabolism in the dinoflagellate *Lingulodinium polyedrum*

par
Steve Dagenais Bellefeuille

Département de sciences biologiques
Faculté des arts et sciences

Thèse présentée à la Faculté des études supérieures et postdoctorales
en vue de l'obtention du grade de Ph.D
en sciences biologiques

Décembre, 2015

© Steve Dagenais Bellefeuille, 2015

Résumé

Les dinoflagellés sont des eucaryotes unicellulaires retrouvés dans la plupart des écosystèmes aquatiques du globe. Ces organismes amènent une contribution substantielle à la production primaire des océans, soit en tant que membre du phytoplancton, soit en tant que symbiontes des anthozoaires formant les récifs coralliens. Malheureusement, ce rôle écologique majeur est souvent négligé face à la capacité de certaines espèces de dinoflagellés à former des fleurs d'eau, parfois d'étendue et de durée spectaculaires. Ces floraisons d'algues, communément appelées "marées rouges", peuvent avoir de graves conséquences sur les écosystèmes côtiers, sur les industries de la pêche et du tourisme, ainsi que sur la santé humaine. Un des facteurs souvent corrélé avec la formation des fleurs d'eau est une augmentation dans la concentration de nutriments, notamment l'azote et le phosphore. Le nitrate est un des composants principaux retrouvés dans les eaux de ruissellement agricoles, mais également la forme d'azote bioaccessible la plus abondante dans les écosystèmes marins. Ainsi, l'agriculture humaine a contribué à magnifier significativement les problèmes associés aux marées rouges au niveau mondial. Cependant, la pollution ne peut pas expliquer à elle seule la formation et la persistance des fleurs d'eau, qui impliquent plusieurs facteurs biotiques et abiotiques. Il est particulièrement difficile d'évaluer l'importance relative qu'ont les ajouts de nitrate par rapport à ces autres facteurs, parce que le métabolisme du nitrate chez les dinoflagellés est largement méconnu. Le but principal de cette thèse vise à remédier à cette lacune. J'ai choisi *Lingulodinium polyedrum* comme modèle pour l'étude du métabolisme du nitrate, parce que ce dinoflagellé est facilement cultivable en laboratoire et qu'une étude transcriptomique a récemment fourni une liste de gènes pratiquement complète pour cette espèce. Il est également intéressant que certaines composantes moléculaires de la voie du nitrate chez cet organisme soient sous contrôle circadien. Ainsi, dans ce projet, j'ai utilisé des analyses physiologiques, biochimiques, transcriptomiques et bioinformatiques pour enrichir nos connaissances sur le métabolisme du nitrate des dinoflagellés et nous permettre de mieux apprécier le rôle de l'horloge circadienne dans la régulation de cette importante voie métabolique primaire.

Je me suis tout d'abord penché sur les cas particuliers où des floraisons de dinoflagellés sont observées dans des conditions de carence en azote. Cette idée peut sembler contre-intuitive, parce que l'ajout de nitrate plutôt que son épuisement dans le milieu est généralement associé aux floraisons d'algues. Cependant, j'ai découvert que lorsque du nitrate était ajouté à des cultures initialement carencées ou enrichies en azote, celles qui s'étaient acclimatées au stress d'azote arrivaient à survivre près de deux mois à haute densité cellulaire, alors que les cellules qui n'étaient pas acclimatées mourraient après deux semaines. En condition de carence d'azote sévère, les cellules arrivaient à survivre un peu plus de deux semaines et ce, en arrêtant leur cycle cellulaire et en diminuant leur activité photosynthétique. L'incapacité pour ces cellules carencées à synthétiser de nouveaux acides aminés dans un contexte où la photosynthèse était toujours active a mené à l'accumulation de carbone réduit sous forme de granules d'amidon et corps lipidiques. Curieusement, ces deux réserves de carbone se trouvaient à des pôles opposés de la cellule, suggérant un rôle fonctionnel à cette polarisation.

La deuxième contribution de ma thèse fut d'identifier et de caractériser les premiers transporteurs de nitrate chez les dinoflagellés. J'ai découvert que *Lingulodinium* ne possédait que très peu de transporteurs comparativement à ce qui est observé chez les plantes et j'ai suggéré que seuls les membres de la famille des transporteurs de nitrate de haute affinité 2 (NRT2) étaient réellement impliqués dans le transport du nitrate. Le principal transporteur chez *Lingulodinium* était exprimé constitutivement, suggérant que l'acquisition du nitrate chez ce dinoflagellé se fondait majoritairement sur un système constitutif plutôt qu'inductible. Enfin, j'ai démontré que l'acquisition du nitrate chez *Lingulodinium* était régulée par la lumière et non par l'horloge circadienne, tel qu'il avait été proposé dans une étude antérieure.

Finalement, j'ai utilisé une approche RNA-seq pour vérifier si certains transcrits de composantes impliquées dans le métabolisme du nitrate de *Lingulodinium* étaient sous contrôle circadien. Non seulement ai-je découvert qu'il n'y avait aucune variation journalière dans les niveaux des transcrits impliqués dans le métabolisme du nitrate, j'ai aussi constaté qu'il n'y avait aucune variation journalière pour n'importe quel ARN du transcriptome de *Lingulodinium*. Cette découverte a démontré que l'horloge de ce dinoflagellé n'avait pas besoin de transcription rythmique pour générer des rythmes physiologiques comme observé chez les autres eukaryotes.

Mots-clés : acclimatation, amidon, boucles de rétrocontrôle transcription-traduction, carbone, corps lipidiques, dinoflagellé, floraisons d'algues, horloge circadienne, *Lingulodinium polyedrum*, photosynthèse, rythmes journaliers, nitrate, transcriptome, transporteurs de nitrate de haute affinité, stress d'azote

Abstract

Dinoflagellates are unicellular eukaryotes found in most aquatic ecosystems of the world. They are major contributors to carbon fixation in the oceans, either as free-living phytoplankton or as symbionts to corals. Dinoflagellates are also infamous because some species can form spectacular blooms called red tides, which can cause serious damage to ecosystems, human health, fisheries and tourism. One of the factors often correlated with algal blooms are increases in nutrients, particularly nitrogen and phosphorus. Nitrate is one of the main components of agricultural runoffs, but also the most abundant bioavailable form of nitrogen in marine environments. Thus, agricultural activities have globally contributed to the magnification of the problems associated with red tides. However, bloom formation and persistence cannot be ascribed to human pollution alone, because other biotic and abiotic factors are at play. Particularly, it is difficult to assess the relative importance of nitrate addition over these other factors, because nitrate metabolism in dinoflagellate is mostly unknown. Filling part of this gap was the main goal of this thesis. I selected *Lingulodinium polyedrum* as a model for studying nitrate metabolism, because this dinoflagellate can easily be cultured in the lab and a recent transcriptomic survey has provided an almost complete gene catalogue for this species. It is also interesting that some molecular components of the nitrate pathway in this organism have been reported to be under circadian control. Thus, in this project, I used physiological, biochemical, transcriptomic and bioinformatic approaches to enrich our understanding of dinoflagellate nitrate metabolism and to increase our appreciation of the role of the circadian clock in regulating this important primary metabolic pathway.

I first studied the particular case of dinoflagellate blooms that occur and persist in conditions of nitrogen depletion. This idea may seems counterintuitive, because nitrogen addition rather than depletion, is generally associated with algal blooms. However, I discovered that when nitrate was added to nitrogen-deficient or nitrogen-sufficient cultures, those that had been acclimated to nitrogen stress were able to survive for about two months at high cell densities, while non-acclimated cells died after two weeks. In conditions of severe nitrogen limitation, cells could survive a little bit more than two weeks by arresting cell division and reducing photosynthetic rates. The incapacity to synthesize new amino acids for

these deprived cells in a context of on-going photosynthesis led to the accumulation of reduced carbon in the form of starch granules and lipid bodies. Interestingly, both of these carbon storage compounds were polarized in *Lingulodinium* cells, suggesting a functional role.

The second contribution of my thesis was to identify and characterize the first nitrate transporters in dinoflagellates. I found that in contrast to plants, *Lingulodinium* had a reduced suite of nitrate transporters and only members of the high-affinity nitrate transporter 2 (NRT2) family were predicted to be functionally relevant in the transport of nitrate. The main transporter was constitutively expressed, which suggested that nitrate uptake in *Lingulodinium* was mostly a constitutive process rather than an inducible one. I also discovered that nitrate uptake in this organism was light-dependent and not a circadian-regulated process, as previously suggested.

Finally, I used RNA-seq to verify if any transcripts involved in the nitrate metabolism of *Lingulodinium* were under circadian control. Not only did I discovered that there were no daily variations in the level of transcripts involved in nitrate metabolism, but also that there were no changes for any transcripts present in the whole transcriptome of *Lingulodinium*. This discovery showed that the circadian timer in this species did not require rhythmic transcription to generate biological rhythms, as observed in other eukaryotes.

Keywords : acclimation, carbon, circadian clock, daily rhythms, dinoflagellate, harmful algal blooms, high-affinity nitrate tranporters, *Lingulodinium polyedrum*, lipid bodies, nitrate, nitrate uptake, nitrogen stress, photosynthesis, starch, transcription-translation feedback loops, transcriptome

Table of contents

List of tables

List of figures

List of abbreviations

A: adenine

ADP: adenine diphosphate

AMT: ammonium transporter

An: *Aspergillus nidulans*

Arg: arginase

Asl: argininosuccinate lyase

AsuS: argininosuccinate synthase

At: *Arabidopsis thaliana*

Ata: *Alexandrium tamarense*

ATP: adenosine triphosphate

ATX: Ataxin-2

BLAST: Basic Local Alignment Search Tool

bp: base pair

C: carbon

CA: carbonic anhydrase

$CaCl_2$: calcium chloride

CCM: CO_2-concentrating mechanisms

cDNA: complementary DNA

CHAPS: 3-[(3-Cholamidopropyl)dimethylammonio]-1-propanesulfonate hydrate

CK2: casein kinase 2

Cl: chloride

CLCs: chloride channels

CO_2: carbon dioxide

CPS: carbamoyl phosphate synthase

Cr: *Chlamydomonas reinhardtii*

cRNA: complementary RNA

CT: Circadian Time

DEPC: diethylpyrocarbonate

DIC: differential interference contrast

DIN: dissolved inorganic nitrogen

DMSO: dimethyl sulfoxide

DNA: deoxyribonucleic acid

DNRA: dissimilatory NO_3^- reduction to ammonium

DON: dissolved organic nitrogen

DPM: disintegrations per minute

DTT: dithiothreitol

DVM: diurnal vertical migration

DW: dry weight

EDTA: ethylenediaminetetraacetic acid

ER: endoplasmic reticulum

FAA: free amino acid

FAV: flavine adenine dinucleotide

Fd: ferredoxins

FW: fresh weight

G: guanine

G6PDH: glucose-6-phosphate dehydrogenase

Gln: glutamine

Glu: glutamate

GOGAT: glutamine oxoglutarate aminotransferase (also known as glutamate synthase)

GS: glutamine synthetase

HABs harmful algal blooms

HCl: hydrogen chloride

HEPES: 4-(2-hydroxyethyl)-1-piperazineethanesulfonic acid

HK: hexokinase

HLP: histone-like proteins

HPLC: high performance liquid chromatography

HTDs: heterotrophic dinoflagellates

I_2: iodine

IEF: isoelectric focusing

K: potassium

Kb: kilobase

KCl: potassium chloride

kD: kilodalton

KI: potassium iodide

KOH: potassium hydroxide

LBP: luciferin-binding protein

LCF: luciferase

LD: light/dark

Lp: *Lingulodinium polyedrum*

Mes: 2-(*N*-morpholino) ethanesulfonic acid

MFS: major facilitator superfamily

mg: milligram

$MgSO_4^-$: magnesium sulfate

MIPs: major intrinsic proteins

mL: milliliter

mM: millimolar

MPSS: massively parallel signature sequencing

mRNA: messenger RNA

MS: mass spectrometry

MSX: L-methionine sulfoximine

MTDs: mixotrophic dinoflagellates

MYA: millions years ago

N: nitrogen

N_2: dinitrogen gas

N_2O: nitrous oxide

Na: sodium

NaCl: sodium chloride

NAD(P)H: nicotinamide adenine dinucleotide (phosphate)

$NaHCO_3$: bicarbonate

$NaNO_3$: sodium nitrate

NanoSIMS: nanoscale secondary ion mass spectrometry

NAR2: nitrate assimilation related

NH_3: ammonia

NH_4^+: ammonium

NiR: nitrite réductase

nm: nanometer

NO_2^-: nitrite

NO_3^-: nitrate

NPF: nitrate transporter 1/ peptide transporter

NR: nitrate reductase

NRT1: nitrate transporter 1

NRT2: nitrate transporter 2

NS: nitrate signature

O_2: oxygen

ORF: open reading frame

OTC: ornithine carbamoyltransferase

OUC: ornithine-urea cycle

P: phosphorus

PAS: Periodic acid-Schiff

PBS: phosphate-buffered saline

PCP: peridinin-chlorophyll *a*-protein

Per: Period

pg: picogram

PMF: proton motive force

PMSF: phenylmethanesulfonyl fluoride

PO_4^{3-}: phosphate

PON: particulate organic nitrogen

PSII: photosystem II

PST: paralytic shellfish toxin

RACE: rapid amplification of cDNA ends

RNA: ribonucleic acid

RNAi: RNA interference

RNA-seq: RNA sequencing

rRNA: ribosomal RNA

RPKM: Reads Per Kilobase per Million mapped reads

RuBisCO: ribulose-1,5-bisphosphate-carboxylase-oxygenase

SD: standard deviation

SDS: sodium dodecyl sulfate

SE: standard error

Si: silicium

SL: spliced leader

SLAC/SLAH: slow anion channel-associated 1 homologues

Ssp: *Symbiodinium* sp. Freudenthal

T: thymine

TAGs: triacylglycerols

TCA: tricarboxylic acid cycle (also known as Krebs cycle and citric acid cycle)

TEM: transmission electron microscope

TM: transmembrane domain

ToL: Tree of Life Web Project

Tris: 2-amino-2-hydroxymethyl-1,3-propanediol

tRNA: transfer RNA

TSA: Transcriptome Shotgun Assembly

TTFL: transcriptional/translational feedback loops

TYF: Twenty-four

µg: microgram

µL: microliter

µM: micromolar

µmol: micromole

Ure: urease

v/v: volume/volume

ZT: *Zeitgeber* Time

Je dédie cette thèse à ma grand-mère Lucie Bouchard et à mon grand-père Laurent Bellefeuille, qui ont tous les deux contracté l'Alzheimer durant mes études doctorales. En souvenir de votre acharnement au travail, de votre indépendance et de votre tendresse sans équivoque

Remerciements

Je prends souvent des décisions sur le vif. Cette stratégie bien qu'elle amène beaucoup de surprises dans ma vie, vient également avec son lot de déceptions. Chose certaine, je n'ai jamais regretté avoir choisi David Morse comme directeur de recherche et ce, en me basant strictement sur la qualité de sa performance en tant qu'orateur lors des 15 premières minutes d'un cours d'introduction à la biologie cellulaire, il y a près de 8 ans. C'est pourquoi, j'aimerais tout d'abord offrir mes plus sincères remerciements à ce professeur qui m'a accueilli dans son laboratoire dès ma deuxième année de baccalauréat et qui a suivi ma progression depuis toutes ces années. J'apprécie qu'il m'ait donné la liberté de piloter mon projet de recherche dans ses montées, ses vrilles et ses descentes. Dans tout le processus, j'ai reçu conseils, encouragements et critiques constructives, qui ont solidifié ma réflexion et mon autonomie scientifiques. Aussi, je tiens à souligner le plaisir que j'ai eu à écrire conjointement avec le professeur Morse. Au passage de sa plume, les idées conservent leur essence tout en devenant plus concrètes, plus colorées et tout simplement plus attrayantes. Travailler dans son laboratoire a été pour moi une expérience remarquable qui a accentué ma compréhension et mon amour de la biologie.

Cette expérience n'aurait pas été la même si elle n'avait pas été accompagnée d'excellents collègues comme Mathieu Beauchemin et Sougata Roy. Par leur intelligence et leur créativité, ils ont contribué à enrichir mon projet de recherche. Je leur suis également reconnaissant pour les nombreuses discussions stimulantes que nous avons eues sur la science en générale et sur nos vies au quotidien.

J'aimerais aussi remercier Sonia Dorion et le professeur Jean Rivoal avec qui j'ai eu la chance de travailler dans le cadre de l'article présenté au chapitre 2 de cette thèse. J'ai bénéficié de leur expertise en biochimie dans une ambiance à la fois rigoureuse et conviviale. Toujours ils m'ont offert une aide technique précieuse et un intérêt honnête dans mes démarches scientifiques

Sur un plan psychologique et plus personnel, je remercie tous les membres de ma famille pour leur patience et leur soutien, surtout dans les derniers mois de rédaction. En particulier, je souligne la présence dans ma vie de mon amoureux Alexis Laurin, qui par son

tempérament calme, son humour créatif et sa curiosité aigüe, tant pour la science que pour les arts, a atténué de beaucoup le stress de mes études.

Finalement, je remercie le FQRNT et le CRSNG qui m'ont soutenu financièrement durant la majeure partie de mon doctorat.

Chapter 1- Introduction

1.1. Overview of dinoflagellates

1.1.1. Phylogeny

Dinoflagellates are unicellular organisms that can be found in most aquatic ecosystems of the world. They display a tremendous diversity in morphology, nutritional strategies and ecological functions. Phylogenetically, dinoflagellates cluster with ciliates and apicomplexans within the well-supported superphylum Alveolata (Fig. 1.1.1), named for the flattened vesicles (cortical alveoli) that form a continuous layer just under the plasma membrane in these organisms [1]. The apicomplexans are sister to dinoflagellates and molecular clock analyses estimated their divergence at about 800-900 million years ago [2,3]. These analyses are consistent with the discovery of the oldest dinoflagellate fossils in late Mesoproterozoic rocks [4]. Molecular phylogenetics has divided the dinoflagellates in three groups: the Oxyrrhinales, the Syndiniales and the core dinoflagellates (Fig. 1.1.1) [5,6]. While not a true dinoflagellate, the oyster pathogen *Perkinsus marinus* has been useful in inferring ancestral conditions in dinoflagellates, because this organism possesses some distinctive dinoflagellate features, while retaining more general eukaryotic characteristics (Fig 1.1.1). The free-living Oxyrrhinales and parasitic Syndiniales are also heterotrophic and localized at the base of the tree [7,8,9,10]. The core dinoflagellates contain the majority of characterized species, which are heterotrophic, phototrophic or mixotrophic. Fensome et al, initially classified the core dinoflagellates into 14 orders based on morphological data, such as the patterns of thecal plates or the absence of a theca altogether [11]. However, molecular and ultrastructural phylogenies showed that thecal characteristics evolved multiple times within the core dinoflagellates [5,9] and as a result, many of the orders previously described were poly- and paraphyletic. Thus, relationships among dinoflagellates are still being investigated and future classifications will most likely introduce major changes [5].

1.1.2. Plastid origin and distinctive features

About half of the ~2000 dinoflagellate species that have been described are photosynthetic [12]. Most of these have distinctive chloroplasts surrounded by three membranes and contain chlorophylls *a* and *c*, in addition to the xanthophyll peridinin, which is

a photopigment unique to dinoflagellates and responsible for the characteristic red colour of most species [13]. The peridinin chloroplast is thought to result from an endosymbiotic event involving a red alga. However, it was a matter of debate if this event occurred ancestrally, through a single secondary endosymbiotic event or rather recently through, serial tertiary endosymbiosis [14,15], the latter occurring by engulfment of an alga containing a secondary plastid. On one hand, the "Chromoalveolata hypothesis" suggested that all members within this supergroup, including the cercozoans, the foraminiferans, the radiolarians, the Alveolates and the Stramenopiles, were derived from a common bikont ancestor that had engulfed a rhodophyte [16]. The main rationale for the Chromoalveolata monophyly was that plastid gain was thought to be much more evolutionary difficult than plastid loss [17]. Thus, it was more parsimonious to hypothesize a single secondary endosymbiotic event in a common ancestor to all Chromoalveolata, and subsequent loss of plastids in ciliates, some apicomplexans and early-diverging members of many chromalveolate lineages [14], than to propose multiple plastid acquisitions by horizontal transfer. On the other hand, tertiary endosymbiosis is observed in multiple dinoflagellate taxa that have chloroplasts of different origins [6,18]. For example, two dinoflagellate genera, *Karenia* and *Karlodinium*, have permanent haptophyte-derived plastids [19,20], while species of the *Dinophysis* obtain temporary chloroplasts from ingestion of cryptophytes [21]. Another problem with the Chromoalveolata hypothesis was that the very few phylogenies based on nuclear DNA and including all groups within the chromoavleolates were incongruent with plastid-based phylogenies [6,20,22]. Thus, it was suggested that the red algal-derived plastid in chromoalveolates was more likely acquired horizontally by tertiary endosymbiosis than by vertical inheritance from a common ancestor [15,18]. However, this alternative was recently challenged by the discovery of *Chromera velia*, a free-living photosynthetic alga closely related to apicomplexans and sharing a common plastid origin with heterokonts (Stramenopiles) [23]. Combined with the observation of a vestigial chloroplast in some apicomplexans [24], and the discovery of several plastid-targeted genes in the nuclear genome of the heterotrophic dinoflagellate *Oxyrrhis marina* [25], it now seems more likely that the common ancestor of dinoflagellates and apicomplexans was photosynthetic rather than heterotrophic.

Chloroplasts of peridinin-containing dinoflagellates also possess multiple distinctive features. They have replaced the typical form I ribulose-1,5-bisphosphate-carboxylase-

oxygenase (RuBisCO) by a form II RuBisCO [26], which is usually found in proteobacteria growing in high-CO_2, low-O_2 environments [27]. The reason for this is that form II RuBisCO has a significantly lower affinity to CO_2 than the form I enzyme [27]. However, dinoflagellates typically live in low-CO_2, high-O_2 environments, and thus, it was suggested that these organisms needed novel CO_2-concentrating mechanisms (CCM) to compensate for the imperfections of form II RuBisCO [6]. One such CCM was identified in *Lingulodinium polyedrum*, where a δ-type carbonic anhydrase (CA), which catalyzes the rapid interconversion of CO_2 and HCO_3, was found to be exclusively localized at the plasma membrane [28]. Treating the cells with acetazolamide, a non-membrane-permeable CA inhibitor, resulted in decreases in photosynthetic rates [28]. This suggested that the action of the CA at the vicinity of the cell membrane increased CO_2 uptake, leading to higher photosynthetic rates [28]. Interestingly, *Lingulodinium* also showed a circadian variation in the localization of RuBisCO within individual chloroplasts that correlated with the CO_2^- fixation rhythm [29]. During the day, where carbon fixation rates are highest, RuBisCO was sequestered near the center of the cell in the pyrenoid within the chloroplast, while the enzyme distributed evenly within the chloroplasts at night. Thus, the strategic localization of RuBisCO in day-phased cells was proposed to optimize carbon fixation by limiting access of oxygen to the active site of the enzyme, rather than increasing CO_2 concentrations within the chloroplasts [29].

Unlike most genes that are typically encoded in the plastids of photosynthetic eukaryotes, the form II RuBisCO is nuclear-encoded in peridinin dinoflagellates [26]. In fact, these organisms have the smallest known functioning plastid genomes, with only 16 genes described so far [30], in contrast to the ~100 genes typically found in chloroplasts of other photosynthetic eukaryotes [6]. This dramatic reduction is thought to be the result of massive gene transfer from the chloroplast to the nucleus in dinoflagellates [31]. The DNA structure in their plastids is also peculiar. Whereas conventional plastid genomes have their genes distributed on a single circular DNA molecule, the plastid genome of peridinin dinoflagellates has been broken down in multiple small 2- to 3-kb plasmids, termed "minicircles" [32]. Each of these minicircles encodes one to several genes and possesses a noncoding core sequence proposed to act as an origin of replication [32,33]. Transcription in the chloroplasts was suggested to occur in a "rolling circle" fashion where the minicircular DNA is transcribed

continuously to generate polycistronic transcripts larger than the minicircle itself [34]. These transcripts are then cleaved by an endonuclease to produce long RNA precursors, which are further processed into mature RNAs by processes including 3'-polyuridylylation [35].

On an evolutionary perspective, it is interesting that all the usual plastid features that were mentioned above (i.e. peridinin, form II RuBisCO, small genomes, minicircles, 3'-polyuridylylation of mRNAs) were lost in the dinoflagellates that have replaced this ancestral peridinin plastid with plastids from other algal sources [6]. The term "replacement" is used, because many nuclear-encoded genes that are targeted to the plastids of non-peridinin dinoflagellates have chimeric origins. For example, the fucoxanthin dinoflagellates *Karenia* and *Karlodinium* possess a plastid proteome derived from many genes that originated from the recent haptophyte endosymbiont, while also retaining some that are remnants of the peridinin-containing ancestor [36,37]. This suggests that the ancestors of non-peridinin dinoflagellates lived with at least two plastids of different origins in the same cell [37].

1.1.3. A unique mitochondrial genome

Similar to the plastid genome, gene content of the mitochondrial genome in dinoflagellates is highly reduced when compared to other eukaryotes. Only 3 protein-coding genes (*cob*, *cox1*, *cox3*) and 2 rRNAs sequences have been identified [38,39,40], which are the same as those reported for the apicomplexans [41,42]. However, dinoflagellates mitochondrial gene arrangements and expression are unique. In contrast to apicomplexans where the mitochondrial genome is compactly arranged on a contiguous and linear stretch of DNA [41,42], dinoflagellate mitochondrial genomes are highly fragmented, contain multiple copies of the same genes and are characterized by large amounts of inverted repeats and noncoding DNA [43]. The *cox3* gene is encoded by two genomic elements that are each transcribed and polyadenylated, and the two RNA fragments are joined by *trans*-splicing to produce a mature *cox3* mRNA[38]. *Trans*-splicing is a particular RNA process where exons of two pre-mRNAs are ligated to produce a single mature mRNA molecule. Mitochondrial transcripts also lack canonical start and stop codons [38,40,44], and they are extensively edited with a bias toward G or C [38,39,40]. While the function of mRNA editing is mostly unknown, dinoflagellates generally possess GC-rich nuclear sequences, and thus, reducing the AT content of

mitochondrial transcripts could potentially make them better suited for imported nucleus-encoded tRNAs [45].

1.1.4. Particularities of nuclear structure and biology

It is impossible to describe dinoflagellates without mentioning their nuclear biology since this is among the most divergent in the eukaryotic domain. It is so divergent that before molecular phylogenetics confirmed their membership within the Alveolates, dinoflagellates were considered mesokaryotes, an intermediate between prokaryotes and eukaryotes [46]. All core dinoflagellates possess a "dinokaryon" that is characterized by permanently condensed chromosomes attached to the nuclear envelope and lacking the nucleosomes necessary for DNA packing [47]. Instead of histones, the organization of chromatin in these organisms relies on histone-like proteins (HLP), which are structurally similar to bacterial DNA-binding proteins [48]. However, the HLP/DNA ratio in dinoflagellates is roughly one tenth of the histones/DNA ratio found in other eukaryotes, and this low level of nucleoproteins is thought to favor the liquid crystalline form of DNA that is observed in core dinoflagellates [49,50]. While histones have long been postulated to be absent in these organisms, this idea has been rejected with the finding of all core nucleosomal histones along with histone modifying enzymes and a nucleosome assembly protein in dinoflagellate transcriptomes [51,52]. However, the relevance of these histones in chromatin organization is still questioned, because no proteins have yet been detected on immunoblots [52].

In contrast to their organellar genomes, some dinoflagellate nuclear genomes are among the largest found in nature. For example, *Prorocentrum micans* contains 250 pg of DNA per haploid cell [53], which is about eighty-fold more than what is found in a haploid human cell. While regression models can predict gene content in most organisms based on their genome size [54], genes in many dinoflagellate genomes are present in several copies organised in tandem arrays [54,55,56,57]. Thus, based on sizes of known dinoflagellate genomes, the estimation of 37000 to 87000 unique genes in these organisms is bound to be an exaggeration of the actual gene content [54]. The reason why single cell eukaryotes like dinoflagellates accumulate such large amounts of DNA and how they manage to conserve and express the relevant sequences is still being investigated.

A major breakthrough in dinoflagellate biology was made by the discovery that every nuclear transcript contained an identical 22-nucleotides spliced leader (SL) sequence on the 5' end [58,59]. This SL sequence was found to be added to mature mRNAs by 5'-*trans*-splicing. The leader sequences themselves were found to be encoded in tandem gene arrays of unknown number and size [58,59]. Interestingly, the same SL sequence was found in all dinoflagellate species studied, including those of the Oxyrrhinales [60], and Syndiniales [61] orders, which suggest that 5' *trans*-splicing arose early in the evolution of dinoflagellates. Kinetoplastids, which include the trypanosome parasites, are another group that make extensive use of SL-*trans*-splicing for mRNA maturation. In these organisms, mRNAs are first transcribed as polycistrons, where *trans*-splicing of the SL sequence serves to delineate and excise individual open reading frames (ORFs) [62]. This observation led to the hypothesis that dinoflagellate mRNA could also be transcribed as polycistrons [58]. However, a recent study invalidated this hypothesis [63], and the function of SL-*trans*-splicing in dinoflagellates still needs to be clarified.

Transcriptional regulation in dinoflagellates is another particularity that sets them apart from other eukaryotes. First, the canonical eukaryotic TATA box promoter element is absent in dinoflagellate [6,64]. However, it was suggested to have been replaced by a TTTT motif, because an intermediate TATA box binding protein with a higher affinity for TTTT was identified in *Crypthecodinium cohnii* [65]. While this prediction was made more than 10 years ago, it was only recently confirmed experimentally with the analysis of *Symbiodinium kawagutii* genome, which is the first genome sequenced for dinoflagellates [66]. A global search revealed that the TTTT motif was present in the upstream regions of 94% of the predicted genes in the genome [66]. Moreover, the strategic localization of the TTTT ~30 bp upstream of potential transcriptional sites strongly suggested that it served as a *bona fide* dinoflagellate core promoter motif [66].

A second difference to typical eukaryotes, is the infrequent use of transcriptional regulation in dinoflagellates. For example, microarray analysis in *Pyrocystis lunula* revealed that only 3% of transcripts showed a circadian variation [67], while 4% responded to oxidative stress [68]. Another microarray study in *Karenia brevis* also found that 3% of genes showed circadian changes at the mRNA level [69]. Massively parallel signature sequencing in *Alexandrium* detected that 10% to 27% of transcripts were differentially expressed in various

conditions [70,71]. A likely explanation for this limited use of transcriptional control is that dinoflagellates might show a reduction in the number protein factors necessary for transcriptional regulation, when compared to other eukaryotes. This hypothesis was confirmed in *Lingulodinium* where it was found that DNA-binding proteins were greatly underrepresented when compared to diatoms, ciliates and green algae [63]. Analysis of sequences common to *Lingulodinium*, *Karenia* and *Alexandrium* also showed that DNA-binding proteins were depleted, while translational factors, protein kinases and protein phosphatases were enriched [63]. These findings support the idea that dinoflagellates favor posttranscriptional mechanisms to control their gene expression over transcriptional regulation.

1.1.5. Ecological functions

If the oddities of dinoflagellate biology inspired many cellular, molecular and evolutionary researchers, dinoflagellates have also had a tremendous impact on past and modern ecology. Dinoflagellates have one of the most extensive fossil records among microscopic eukaryotes, due to the ability of many species to form resting cysts [72]. These dormant cells can resist unfavourable conditions and remain viable for hundred of years [73]. Assemblages of cysts from different species deposit in sediments and form stratum. Changes in these dinoflagellate assemblages reflect variations in productivity [74,75], water temperature [76,77], salinity [76,78] and ice cover [79,80], and are used extensively by paleoecologists to reconstruct the history of past seas and oceans, particularly those of the Quaternary Period. Cysts of freshwater dinoflagellates were also shown to be useful indicators of productivity, temperature and pH for paleoecological reconstructions [81].

In present marine environments, dinoflagellates are major contributors to primary production, either as free-living phytoplankton or as symbionts to reef-forming corals [6,82]. Some heterotrophic and mixotrophic species are prolific grazers that can prey on multiple planktonic groups [83]. Dinoflagellates are in turn excellent prey for some protists and metazoans. Thus, dinoflagellates play diverse roles in marine food webs. However, their ecological value is often overshadowed by the propensity of some species to form harmful algal blooms (HABs), commonly described as red tides. HABs often kill fishes and other marine wildlife and microorganisms through oxygen depletion, irradiance reduction, physical

damage and/or secretion of biotoxins [84]. Some of these toxins can also accumulate within shellfish and fish, and can cause serious diseases in humans such as paralytic shellfish poisoning, neurotoxic shellfish poisoning and ciguatera fish poisoning [85]. Thus, red tides have serious negative impacts on marine ecosystems, human health and economic activities.

While the development and persistence of HABs involve multiple factors, an increase in nutrient inputs is often correlated with bloom outbreaks [86,87,88]. Nitrogen is one of these essential nutrients that is commonly found in agricultural fertilizers in the form of nitrate, ammonium or urea. Nitrogen runoffs contribute to the eutrophication of many coastal regions of the world and are sometimes directly linked to the development of HABs dominated by dinoflagellates [89]. Anthropogenic addition of nitrogen also modifies the elemental ratios that have been reported to influence the composition and abundance of phytoplankton [90,91,92]. For example, decreases in the Si:N [91,93], and increases in the N:P [92], ratios in coastal waters have globally reduced the diversity and abundance of diatoms to the benefit of flagellate species. Thus, dinoflagellates and the problems associated with HABs are becoming more prevalent in coastal ecosystems.

Figure 1.1.1. Distinctive features of dinoflagellate evolution within the Alveolata

Schematic representation of the Superphyllum Alveolata, based on molecular phylogenetic analyses [6].

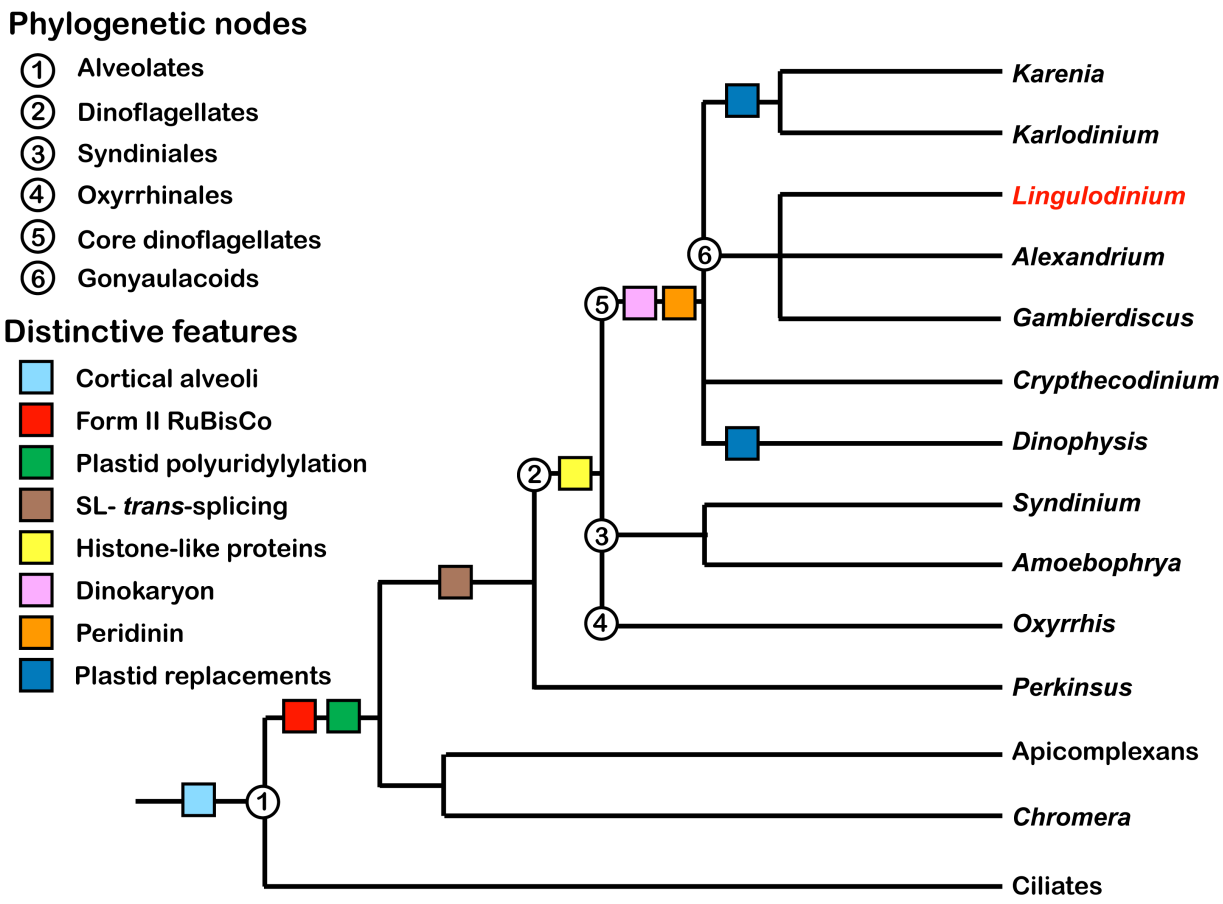
Phylogenetic nodes
1 Alveolates
2 Dinoflagellates
3 Syndiniales
4 Oxyrrhinales
5 Core dinoflagellates
6 Gonyaulacoids
Distinctive features
Cortical alveoli
Form II RuBisCo
Plastid polyuridylylation
SL- trans-splicing
Histone-like proteins
Dinokaryon
Peridinin
Plastid replacements
Karenia
Karlodinium
Lingulodinium
Alexandrium
Gambierdiscus
Crypthecodinium
Dinophysis
Syndinium
Amoebophrya
Oxyrrhis
Perkinsus
Apicomplexans
Chromera
Ciliates

1.2. Publication # 1

Putting the N in dinoflagellate

Steve Dagenais Bellefeuille, David Morse

Review article published in Frontiers in Microbiology, 2013, 4: 369
DOI:10.3389/fmicb.2013.00369

Author contributions:

S. Dagenais Bellefeuille wrote the first version of the text, which was revised and corrected by D. Morse. Figures were drafted by S. Dagenais Bellefeuille.

In this section, I review nitrogen metabolism in dinoflagellates. I present the multiple strategies that these organisms have developed to meet their nitrogen demands while competing for this resource with other phytoplankton, particularly diatoms. I also present the adaptation mechanisms dinoflagellates have evolved to cope with nitrogen stress.

1.2.1. Abstract

The cosmopolitan presence of dinoflagellates in aquatic habitats is now believed to be a direct consequence of the different trophic modes they have developed through evolution. While heterotrophs ingest food and photoautotrophs photosynthesize, mixotrophic species are able to use both strategies to harvest energy and nutrients. These different trophic modes are of particular importance when nitrogen nutrition is considered. Nitrogen is required for the synthesis of amino acids, nucleic acids, chlorophylls, and toxins, and thus changes in the concentrations of various nitrogenous compounds can strongly affect both primary and secondary metabolism. For example, high nitrogen concentration is correlated with rampant cell division resulting in the formation of the algal blooms commonly called red tides. Conversely, nitrogen starvation results in cell cycle arrest and induces a series of physiological, behavioral and transcriptomic modifications to ensure survival. This review will combine physiological, biochemical and transcriptomic data to assess the mechanism and impact of nitrogen metabolism in dinoflagellates and to compare the dinoflagellate responses with those of diatoms.

Key words: Dinoflagellates, diatoms, nitrogen metabolism, nitrogen stress, autotrophy, mixotrophy, heterotrophy

1.2.2. Introduction

Dinoflagellates are unicellular eukaryotes that appeared ~ 400 MYA and still thrive today in most marine and freshwater ecosystems [94]. They have evolved various life styles, which has enabled them to populate a great diversity of ecological niches. Many dinoflagellates are found within the phytoplankton, and are important contributors to oceanic primary production. Others, such as *Pfiesteria* or *Protoperidinium*, are predators that are known to feed on a wide array of prey. Still other dinoflagellates can be symbiotic, as exemplified by the endosymbiotic associations formed between *Symbiodinium* and some anthozoans. This mutualistic symbiosis is of immense ecological importance because many tropical reef corals live in nutrient-poor water and the photosynthetic products supplied by the zooxanthellae symbionts are essential for growth and survival of the host [82]. The order Syndiniales is comprised exclusively of parasitic species that infect tintinnid ciliates, crustaceans, dinoflagellates and fish [95,96,97,98,99,100]. Curiously, some dinoflagellate genera, such as *Gambierdiscus*, *Ostreopsis* or *Prorocentrum*, can live fixed to a substrate. They can be found both in epiphytic associations with macroalgae and in benthic sediments [101]. The benthic zone also contains dinoflagellate temporary or resting cysts. It is now believed that one explanation for the ecological versatility of dinoflagellates comes from the three trophic modes, autotrophy, mixotrophy and heterotrophy, they have evolve to harvest energy.

Traditionally, dinoflagellates have been categorized as either photoautotrophic or heterotrophic, based on the presence or absence of chloroplasts. Over the past 30 years, however, it became evident that these two trophic modes were actually the extremes of a continuum, with the middle region being composed of mixotrophic species. Mixotrophs combine photosynthesis and food ingestion to harvest both energy and nutrients, and are quite common in marine phytoplankton, with the diatoms being a noteworthy exception [102]. Mixotrophy can be found in all dinoflagellate orders, even if evidence is stronger in some taxa [103]. Most dinoflagellates have complex life cycles, and in some cases mixotrophic behavior is only apparent in some life stages. For example, *P. piscicida* lacks chloroplasts and is heterotrophic for most of its life, except in its flagellated zoospore stage where the cells contain functional kleptochloroplasts stolen from ingested cryptophytes [103,104].

Although dinoflagellate life styles are diverse, all species require carbon (C), phosphorus (P) and nitrogen (N). Of these, N nutrition is of particular interest, because high concentrations of various N sources are often correlated with the appearance of harmful algal blooms (HABs) dominated by dinoflagellates [86,89,105,106,107]. There is a general scientific consensus that HAB events have globally increased in frequency, magnitude and geographic extent over the last 40 years [105]. Concurrently, the impacts of HABs on public health, tourism, fisheries and ecosystems have also increased. Some HABs are toxic, such as those caused by the widespread *Alexandrium* genus, as they can synthesize a suite of paralytic shellfish toxins (PST) [108,109]. These toxins accumulating within filter-feeding mollusks can cause paralytic shellfish poisoning. PSTs all contain N and their concentration within *Alexandrium* cells can increase up to 76% following N-enrichment [109,110]. A better understanding of N metabolism in dinoflagellates could help to better predict the occurrence of HABs and limit their impact.

This review will cover nitrogen metabolism in dinoflagellates of various marine life styles. Unfortunately, even though some physiological and transcriptional studies are available, there is little known about the molecular components involved in N metabolism for these organisms. However, it is known that most dinoflagellates species with permanent chloroplasts can live in medium supplemented strictly with various inorganic nutrients, nitrate (NO_3^-) being the predominant N form [83]. This implies that N assimilation genes are present in these species and, because this process is remarkably well conserved in plants and algae, it is likely that parallels can be made with dinoflagellates (Fig. 1.2.1, see further sections for details). This review will first address these parallels by describing what is currently reported about the molecular components involved in N metabolism in plants and eukaryotic algae. We will then discuss the particular case of mixotrophy for the uptake of N in dinoflagellates. This nutrient being essential for synthesis of amino acids, nucleic acids, chlorophylls, and toxins, it is a major factor limiting growth. In conditions of N-stress dinoflagellate cells either die or modify their metabolism and trophic behavior to ensure their survival. We will finish by presenting the various adaptations used by dinoflagellates to cope with N stress. Throughout the text, we will compare the dinoflagellate N responses to those of diatoms to examine which environmental conditions could favor one group of organisms over the other.

1.2.3. Overview of the marine N cycle

The marine N cycle is probably the most complex of the biogeochemical cycles, as it involves various chemical forms and multiple transformations that connect all marine organisms. In this section and the following one, we will begin by giving a brief overview of the N cycle to better understand how N flux in the oceans and what chemical forms are the most relevant for dinoflagellates. We will then describe the molecular mechanisms of N transport in plants and algae. We will finish with what is currently known about physiological N uptake in dinoflagellates and how our understanding has been helped by genomic and functional studies in diatoms.

About 94% of the oceanic N inventory exists as biologically unavailable dissolved nitrogen gas (N_2) [111]. This gas can be made bioavailable through N_2- fixation, a process carried out by photoautotrophic prokaryotes, mainly cyanobacteria, using iron-dependent nitrogenases to catalyze reduction of N_2 to NH_4^+. N_2-fixation thus provides a counterbalance to the loss of bioavailable N through denitrification (NO_3^- to N_2) and anaerobic ammonium oxidation (Annamox, NH_4^+ to N_2), both of which are anaerobic reactions catalyzed by bacteria. The 6% of biologically available N exists primarily as NO_3^- (~88%) and dissolved organic nitrogen (DON, ~11.7%) [111]. The remaining 0.3% is found in other chemical forms, such as NO_2^-, NH_4^+, nitrous oxide (N_2O) and particulate organic nitrogen (PON) [111].

The distribution and composition of fixed N forms vary with depth as direct consequences of combined biological and physical processes. In the euphotic zone, C fixation by photosynthesis drives the assimilation of inorganic N in order to sustain growth. If the resulting organic N produced is released into the seawater in the euphotic zone, most can be directly reassimilated, remineralized into inorganic N or respired for energy production. However, some organic N will sink down to the aphotic zone where ammonification and nitrification will remineralize it back to inorganic N. Finally, ocean circulation and mixing can return this remineralized N to the euphotic zone where it can be used to sustain new growth. The direct consequences of this biogeochemical loop are that surface waters are generally depleted in inorganic N while the deep oceans are enriched [111]. Conversely, concentrations of PON and DON are much higher near the surface than deeper in the oceans [111]. While this scenario holds in the open ocean, anthropogenically-derived N additions have significantly

changed the nutrient states in the coastal regions of the world [112,113]. Agricultural runoffs and aquaculture industries bring sizeable amounts of new inorganic and organic N which tend to accelerate the N cycle in coastal ecosystems [107,111,112,114]. The main engine driving this accelerated N cycle is the ability of phytoplanktonic species to take up nitrogen directly from the environment using very efficient transport systems.

1.2.4. Uptake of nitrogen using transporters

The work of Epstein and Hagen on ionic transport in plant rhizodermal cells was among the first to describe the dynamics of transporters [115]. They found that the kinetics of ion uptake shared all the characteristics of classic Michaelis-Menten enzyme catalyzed reactions, although uptake of potassium (K) and rubidium was later shown to have a low K_m or a high K_m depending if the external ionic concentrations were low (μM) or high (mM), respectively [116]. In plants and eukaryotic algae, physiological import of inorganic and organic N is also generally dependent on environmental concentrations [109,117,118,119,120,121,122,123]. Expression of transport proteins in heterologous systems such as yeast and *Xenopus* oocytes has greatly helped to determine their biochemical properties [121,124]. At the molecular level, dual affinity can be explained by the presence of a group of transporters, which individually have either a high or a low affinity for their substrates. However, dual affinity can also result when an individual transporter is able to switch between the two affinities. The best example of a switching transporter is CHL1/AtNRT1.1 in *Arabidopsis*, where phosphorylation of threonine 101 (T101) changes its activity from a low-affinity to a high-affinity NO_3^- transporter [125]. Interestingly, T101 was also shown to be involved in NO_3^- sensing, as assessed by the ability of NO_3^- to induce expression of genes involved in NO_3^- metabolism. Mutants mimicking the phosphorylated form of the transporter were unable to elicit a low-affinity NO_3^- response, whereas mutants mimicking the dephosphorylated form had an increased NO_3^- response at all concentrations of N [126]. CHL1/AtNRT1.1 was thus named a "transceptor". Finally, a last group of transporters is made up of channel-like proteins such as the major intrinsic proteins (MIPs), a family which also contains aquaporins. MIPs provide facilitated diffusion of NH_4^+ and urea into plant cells and tonoplasts and have only low affinity for their substrates [127,128,129,130].

N transporters and channels are often multi-selective and differentially regulated. For example, the *Chlamydomonas reinhardtii* transporters CrNRT2.1 and CrNRT2.3 transport both NO_3^- and NO_2^- with identical or different affinities, respectively. CrNRT2.1 has a high affinity for both NO_3^- and NO_2^-, while CrNRT2.3 has a low affinity for NO_3^- and a high affinity for NO_2^- [131]. Generally, however, most transporters of the same family or subfamily share similar substrate selectivity and affinity. As for the regulation patterns, some transporters

are constitutively expressed while others are influenced by different conditions such as pH, light and level of substrates in the environment.

Facilitated diffusion such as carried out by MIPs follows down the concentration gradient and thus has no requirement for energy. However, for the majority of inorganic and organic N compounds, transport goes against a concentration gradient and thus needs a source of energy. Plants and algae produce a proton motive force (PMF) using H^+-ATPases at their plasma membranes and other cell compartments. The PMF is an electrochemical gradient exploited by transporters, such as those for NO_3^-, NO_2^-, the high-affinity system of urea, some amino acids and peptides. These transporters work either by the symport or antiport of H^+, and their activities are thus dependent on pH [121,124,131,132,133,134]. Others, such as the high-affinity NH_4^+ uniporter AMT1.1 from *Arabidopsis*, exploit the electrical gradient generated by the PMF, and thus do not require H^+ transport [120]{Ninnemann, 1994 #129}.

One problem concerning the use of a PMF in marine organisms is that seawater is typically alkaline (pH ≥ 7.8). Fortunately, seawater also contains abundant sodium (Na^+, 450-500 mM), and as in animal cells, many marine algae can exploit these Na^+ gradients for uptake of nutrients such as NO_3^-, PO_4^{3-}, glucose, amino acids and silica [135,136,137,138]. Moreover, existence of P-type Na^+-ATPases in marine algae was confirmed in *Tetraselmis viridis* and *Heterosigma akashiwo* [139]. The Na^+ versus H^+ powered-transport in, respectively, marine and freshwater/terrestrial organisms, is however not an absolute rule. For example, the freshwater chlorophyte *Ankistrodesmus braunii* requires Na^+ for the transport of PO_4^{3-} while Charales living in brackish waters typically use H^+ symporters for nutrient transport [140,141]. The strong negative membrane potential of characean cells is thought to enable H^+-symport even in alkaline environments [140]. Notably, Charales are also able to use Na^+-coupled transport for PO_4^{3-}, urea and Cl^- [142,143,144]. To date, no comparisons of the energetics of transport have been made between dinoflagellates living in freshwater and those living in seawater.

Physiological uptake of NO_3^-, NO_2^-, NH_4^+, urea and other DON by chloroplast-containing dinoflagellates has been reported in both field and laboratory studies [145,146,147,148,149,150,151,152,153,154]. Most describe the uptake kinetics in relation to cell growth, and the variability in the kinetics has emerged as an important feature. Depending

on the experimental sampling conditions, different intraspecific half-saturation constant (K_m) values for NO_3^-, NH_4^+ and urea were reported in *Lingulodinium polyedrum* and *Alexandrium catenella* [84,145,148]. In the latter species, K_m for NH_4^+ and K_m for urea varied from 0.2 to 20 μM and 0.1 to 44 μM over a 4-year period, respectively [145]. In the same study, the authors' measured K_m values range from 0.5 to 6.2 μM NH_4^+ within a 3-day interval, showing how fast transport kinetics can change within the same dinoflagellate population. Similar variations were also noted in *L. polyedrum* [147]. In a 2005 review, Collos et al. noted a linear relationship between K_m for NO_3^- and ambient NO_3^- concentrations for various freshwater and marine unicellular algae in the field [155]. They proposed that most phytoplankton possess an ability to physiologically acclimate to different NO_3^- concentrations. The variations of K_m observed for NH_4^+ and urea in dinoflagellates suggest that acclimation could be generalized to various N forms, not only NO_3^-. From a molecular perspective, these results suggest that different combinations of transporters each with particular kinetics and level of expression/activity will be found in dinoflagellates.

Generally, when growing in presence of various different N compounds, dinoflagellates (as well as plants and algae) prefer to take up NH_4^+. However, there is a concentration threshold above which NH_4^+ becomes toxic to the cells, and this threshold seems to be species-specific. For example, in *A. minutum*, NH_4^+ concentrations of 25 μM and higher lead to growth inhibition while for *A. tamarense* and *Cochlodinium polykrikoides*, this threshold was not observed until 50 μM [149,150,156]. Another tendency in dinoflagellates is inhibition of NO_3^- uptake when in the presence of NH_4^+. In *A. minutum*, this inhibition was found to be greater when the cells were in N-sufficient compared to N-deprived conditions [153]. This suggests that when N is limiting, uptake of different forms will be favored over strict assimilation of NH_4^+ which has a reduced energy cost. Curiously, different blooming populations of dinoflagellates were found to have high uptake rates for urea and/or amino acids, and these rates were always higher than the rates for NO_3^- uptake [145,146,148]. In *L. polyedrum*, the urea uptake rate was also about 2 times more than that of NH_4^+, even if environmental urea concentrations were less than NH_4^+ [148]. Taken together, these observations suggest that dinoflagellates possess a full suite of transporters for inorganic N and organic N forms, that they have the biochemical means to assimilate these N forms, and

that they show a great physiological plasticity in response to external N types and concentrations.

Dinoflagellates are able to store large amounts of inorganic and organic N forms. Comparison of N uptake and assimilation rates at various growth rates in *A. minutum* showed that most of the NO_3^- and NH_4^+ taken up in 1 h was not assimilated, and it was hypothesized that the unassimilated N was stored within the cell [153]. This species was also found to have a great storage capacity for amino acids [157], and a similar storage capability was also described in *A, catenella*, *A. tamarense*, and *Amphidinium cartarae* as well as other unicellular algae [158,159,160]. One recent study, using Nanoscale Secondary-Ion Mass Spectrometry (NanoSIMS) and transmission electron microscopy, showed that *Symbiodinium* spp. temporarily stored N in the form of uric acid crystals after sudden increases in environmental N [161]. Indeed, pulses of ^{15}N-labeled NH_4^+, NO_3^- or aspartic acid promoted accumulation of cytosolic crystalline uric acid inclusions in the zooxanthellae, which were formed in only 45 minutes in the case of NH_4^+. After 24 h of chasing with unlabeled-NH_4^+ seawater, the inclusions completely dissolved and were remobilized uniformly within the cell. These results suggest that dinoflagellates might store their N within the cytosol, in contrast to plants where up to 50 mM of NO_3^- can be stored in the vacuoles [162]. The chemical nature of the long-term storage of N in dinoflagellates is still unclear.

Another interesting feature of N transport in dinoflagellates is the ability of some species to take up substantial amounts of various N forms in the darkness (Table 1.2.1.). Dinoflagellates often display a diurnal vertical migration (DVM) in the water column and, because NO_3^- concentrations increase with depth, dark NO_3^- uptake was first described as a means to sustain uninterrupted growth by meeting their N requirements under conditions where the cells cannot photosynthesize [147]. It was further suggested that the DVM of dinoflagellates gave them a competitive advantage for N uptake over the non-motile diatoms [84,147]. Paasche et al. showed that uptake efficiency and the N form preferentially taken up in the dark were species-specific. At one end of the spectrum, *P. minimum* took up NH_4^+ and NO_3^- at similar rates in the light or in the dark, while at the other end, *Gyrodinium aureolum* in the dark had smaller rates of uptake for NH_4^+ and did not take up NO_3^- in N-sufficient conditions [163]. Recently, dark uptake of NO_3^-, NH_4^+ and urea was confirmed in *A. tamarense* [151].

In contrast to dinoflagellates where molecular characteristics of transporters are mainly based on predictions from physiological studies, the three presently available diatom genomes have helped considerably to better appreciate the full extent of N transport and assimilation in these organisms [164,165,166]. Consistent with their fast growth rate and high productivity, diatom genomes were found to contain multiple transporters for NO_3^-, NH_4^+, urea and other organic N forms [164,167]. Analysis of genomes and studies in *Cylindrotheca fusiformis* revealed that diatoms seemed to possess twice as many transporters for NH_4^+ compared to NO_3^- [168,169,170]. It was suggested that these numbers reflect the fact that marine phytoplankton generally face low concentrations of NH_4^+, while NO_3^- concentrations are higher [168]. Amino acid sequence analysis of five NH_4^+ transporters of *C. fusiformis* showed that they shared 40% similarity with the vascular plant NH_4^+ transporters AMT1 and AMT2 [169]. Furthermore, rescue by functional complementation of a yeast strain missing all three of its native NH_4^+ transporters not only confirmed the functionality of the identified transporters, but also showed that AMT1 in diatoms were much more efficient transporters than AMT2 [169]. Identification and characterization of NO_3^- transporter sequences were also made in C. *fusiformis* [170]. As a general rule, genomic data and functional characterization showed that marine N transporters share sequence homology with N transporters of terrestrial and freshwater organisms, and that these tools can be used to better understand the responses of an organism to different N forms and concentrations. In dinoflagellates, the immense sizes of their genomes and the high gene copy number have long hindered sequencing projects. However, efforts are now being made to sequence the smallest of dinoflagellate genome, *Symbiodinium* [171]. There is no doubt that the presently available transcriptomic data for *Alexandrium*, *Karenia*, *Lingulodinium* and *Symbiodinium*, as well as the upcoming genome sequences will help in unraveling the complexity of N transport and assimilation in dinoflagellates [63,172,173,174].

1.2.5. Uptake of nitrogen by feeding

Because “food” comes from whole organisms (or parts of them), it contains a large spectrum of inorganic and organic matter, in which each individual compound is not ingested differently. For this reason, the following section will begin by describing general feeding mechanisms measured in mixotrophic studies of dinoflagellates, taking for granted that N is not ingested differentially than from other nutrients. Following this, we will discuss some specific examples of the N contribution obtained from feeding and of the inorganic N influence on the mixotrophic behavior of different dinoflagellates. We will finish with a model proposed by Jeong et al., where mixotrophy explains the outbreak and persistence of HABs in aquatic ecosystems limited in inorganic nutrients [175].

Mixotrophic dinoflagellates (MTDs) and heterotrophic dinoflagellates (HTDs) have similar feeding strategies. These strategies include 1) raptorial feeding, where the predator actively searches for its prey, 2) filter/interception, where the predator generates feeding currents to drag the prey into proximity of its feeding parts, and 3) diffusion feeding, where the predator passively wait until the prey comes close [175,176]. Raptorial feeding uses 3 mechanisms for ingestion of preys, 1) direct engulfment (phagocytosis), 2) pallium feeding, where a feeding veil is deployed around the prey, and 3) peduncle feeding, in which a straw-like structure is used to siphon out the prey’s cytoplasm [175,177]. Pallium feeding has still not been observed in MTDs, and thus seems to be unique to HTDs. HTDs are also able to engulf bigger preys than MTDs. In fact, the upper size limit of prey is generally proportional to the size of MTDs, while this correlation is not observed for HTDs [178]. It was suggested that morphological adaptations to the sulcus, the “mouth” of most HTDs, as well as a stronger pulling force for ingestion of prey, could enable them to ingest larger prey [175]. In general, the prey upper size limits are greater when using pallium and peduncle feeding than when using engulfment. Spectacularly, some pallium and peduncle feeders are able to ingest prey up to 10 times their size [177]. As for prey types, MTDs and HTDs feed on a wide array of taxa. They were shown to ingest cryptophytes, haptophytes, chlorophytes, prasiophytes, raphidophytes, diatoms, heterotrophic nanoflagellates, ciliates and other dinoflagellates [179,180,181,182,183,184,185,186,187,188,189]. However, while some HTDs can feed on

blood, flesh, eggs and early naupliar stages and adults forms of metazoans, no MTDs have been shown to do so [190,191,192].

In 1998, Stocker has proposed three physiological types of mixotrophic protists [193]. Type III contains "photosynthetic" protozoa that require prey for growth and survival. In the same manner as HTDs, type III MTDs take the majority of their nutrients from feeding. Type I is made of "ideal" mixotrophs, which grow equally well either using light and inorganic nutrients or when they consume food. Very few MTDs with permanent chloroplasts are of this type. In fact, only 3 out of 36 reported species grew in the dark when prey was provided [83]. Most mixotrophs belong to type II, which was defined as "phagotrophic" algae that primarily photosynthesize and can assimilate inorganic nutrients. In this group, different proportions of N can be taken up either by transporters or through feeding. Estimations of these proportions have been made using *in situ* grazing experiments in *Ceratium furca* and *Akashiwo sanguinea* [194,195]. In *C. furca*, hourly ingestion rates (I) of the fluorescently labeled prey *Strobilidium* spp., were measured by dividing the mean number of food vacuoles in the predator with the incubation time of prey and predator. The % body N was then estimated as daily ingestion relative to cellular N content of *C. furca* (100 x 24h x I x (cellular N of prey/cellular N *C. furca)*). On average, the % N obtained through feeding was 6.5 % with a maximal value of 51 % [195]. Similarly in *A. sanguinea*, a gut clearance/gut fullness approach estimated an average of 4 % N obtained through feeding with a maximal value of 18.5 % [194]. Both of these species have low averages, which signifies that under low light and with inorganic nutrient concentrations normally found in the environment, uptake of N by transporters is dominant over feeding. Interestingly, *C. furca* and *A. sanguinea* show only a marginal increase in growth rate with increasing prey concentrations [83]. However, in another 6 out of 36 chloroplast-containing species, a large increase in growth rates with increasing prey concentrations was observed [83]. Although the % body N in these species was not estimated, it could be argued that a larger proportion of N was obtained through feeding compared to *C. furca* or *A. sanguinea*. An extreme case of mixotrophy is observed in some dinoflagellates such as the *Dinophysis* genera that may contain chloroplasts of cryptophyte, haptophyte or cyanobacterial origin [196]. All the species studied in this genus cannot grow on an inorganic medium alone, as all require both light and prey for growth and survival [83,197,198,199,200,201]. *Dinophysis* spp. are thus considered obligate mixotrophs. It is still

unclear what are the proportions of N obtained by feeding and by transporters in these organisms.

The grazing behavior of some MTDs was shown to be under the influence of light and inorganic nutrient concentrations. In laboratory cultures of *Gyrodinium galatheanum* and *C. furca*, the incidence of feeding was negatively correlated with the amount of inorganic N present in the medium [202,203]. In *C. furca*, cells only started to ingest food after 11 to 16 days in NO_3^--depleted medium [203]. Similarly in *P. minimum*, additions of NO_3^- inhibited feeding [204]. Curiously, this organism followed a diel pattern of prey ingestion with peaks in the afternoon and evening, and a trough in the morning. Moreover, the number of food vacuoles observed within *P. minimum* cells did not change between surface populations and the ones deeper in the water column. Because of these spatio-temporal evidences, the authors suggested that feeding in this organism was primarily a means for obtaining limiting nutrients, and not a mechanism to supplement C nutrition during light limitation [204]. In contrast to the above-mentioned species, prey ingestion rates in *Fragilidium cf. mexicanum* was shown to be independent of inorganic N concentrations [205]. Also, most of the chloroplast-containing MTDs were reported to ingest prey in N-replete conditions [83]. Thus, the effects of inorganic N on grazing behavior must be species-specific.

It was long believed that bacteria were too small to be ingested by dinoflagellates. In the last few years, however, fluorescence and transmission electron microscopy observations revealed that multiple HTDs and MTDs were able to feed on heterotrophic bacteria and cyanobacteria [184,185,206,207]. In particular, feeding on the N_2-fixing *Synechococcus* spp. was seen in 18 species reported to form HABs [184,206,207]. Generally, when prey concentration was high (10^6 cells/ml), the ingestion rates increased with increasing size of the dinoflagellate predators [184]. Moreover, ingestion rates of *Synechococcus* were comparable to those observed in heterotrophic nanoflagellates [207]. A mixture of *P. mininum* and *P. donghaiense* was able to remove up to 98% of the *Synechococcus* population within 1 h, showing that grazing by these species on bacteria could be very substantial [184]. Thus, bacterivory in dinoflagellates was suggested to be a cause of HABs outbreaks and persistence in nutrient-limited waters [175,206]. A model was further proposed where MTDs would supply their N requirement by ingesting cyanobacteria, while meeting their P requirement by

ingesting heterotrophic bacteria, which are reported to generally have a high P:N ratio [175]. This model as yet to be tested in the environment.

1.2.6. Nitrogen assimilation and metabolism

Once inorganic N has entered the cells, phototrophic and mixotrophic dinoflagellates can either store it or assimilate it in the form of amino acids. Whether organic N is taken up by means of transport or by ingestion of food, all dinoflagellates must metabolize it for further use using enzymes such as ureases, hydrolases, peptidases and aminotransferases (also known as transaminases). In this section, we will start by giving a brief description of the enzymes involved in inorganic N assimilation, based on the available knowledge from plants and algae. We will follow with different evidence on the presence of these enzymes in dinoflagellates, particularly the NR of *L. polyedrum*, which was found to be under the control of a circadian clock. We will finish with a description of N assimilation in diatoms with emphasis on the newly discovered ornithine-urea cycle.

There are two structurally different types of NR, dissimilatory and assimilatory. The first type is found mainly in anaerobic prokaryotes, but is also present in some eukaryotes, such as the benthic foraminiferans and some fungi [208,209,210]. These organisms use their dissimilatory NR to respire NO_3^- instead of O_2. Direct reduction of NO_3^- to NH_4^+ is a process named dissimilatory NO_3^- reduction to ammonium (DNRA), and is well documented in prokaryotes such as large sulfur bacteria [211]. Surprisingly, DNRA was also identified in the benthic diatom *Amphora coffeaeformis* [212]. The authors suggested that this organism respired NO_3^- as a means to survive dark and anoxic conditions. Considering that some dinoflagellates can form resting cysts that will sink in the benthic zone, and that others are also living there, dinoflagellates might also rely on the energy produced by dissimilatory NRs for excystment and for survival. However, the second type, assimilatory NR (usually just called NR) is the most common form in both eukaryotes and prokaryotes and is the type that was implied until now in this review. It catalyzes the reduction of NO_3^- to NO_2^- for assimilation. NRs usually form homodimers, but homotetramers have been reported in organisms such as the green algae *Chlorella* [213]. Each monomer contains an electron transport chain made of three prosthetic groups: a flavine adenine dinucleotide (FAD), a cytochrome b557 and a molybdenum cofactor [214,215]. These groups are ubiquitous in all reported NR and are necessary for the stepwise transfer of 2 electrons from NAD(P)H to NO_3^- in eukaryotes. In contrast, prokaryotes use ferredoxins (Fd) or NADH for reduction of NO_3^- and their NR is

generally membrane-bound whereas the eukaryotic one is soluble [214,216]. Eukaryotic NRs are generally localized to the cytoplasm.

In photosynthetic eukaryotes, once NO_3^- has been reduced, the resulting NO_2^- is imported into the chloroplasts where it will be further reduced. There are two types of assimilatory NiR. The first one uses reduced-Fd from the photosynthetic transport chain as an electron donor, while the second one, usually found in non-photosynthetic organisms, uses NAD(P)H [214]. Both types require 6 electrons to catalyze the reduction of NO_2^- to NH_4^+. Similarly to NR, Fd-NiRs contain three prosthetic groups: an iron-sulfur center, a FAD and a siroheme [214,215]. Most of NiRs are soluble and work as individual enzymes. Generally, NiRs have a greater affinity for NO_2^- than NRs have for NO_3^- [214]. As a consequence, NO_2^- is completely reduced to NH_4^+ and does not accumulate within the cells. In plants and algae, there are GS localized to the chloroplast and the cytosol [131,217,218]. GS adds NH_4^+ to Glu using ATP to produce 1 molecule of Gln. Gln is a central metabolite, which acts as a precursor for the biosynthesis of purines, pyrimidines, proteins and ureides [218]. GOGATs are found exclusively in the chloroplasts/plastids in plants and algae [131,218]. They combine Gln to 2-oxoglutarate using 2 electrons from either reduced-Fd or NAD(P)H and produce 2 molecules of Glu. The α-amino group of Glu can then be transferred by amidotransferases to a wide variety of 2-oxo acid acceptors to form amino acids, and back to form Glu, when amino acids and 2-oxoglutatare are abundant. GDH present in the mitochondria can also use NH_4^+ and 2-oxoglutarate to produce Glu. Thus, Glu and Gln are at the crossroads of amino acid metabolism where they act both as N acceptors and N donors.

The presence of all inorganic N assimilation enzymes was tested indirectly or directly in some MTDs. In *Symbiodinium*, analysis of transcriptomic data revealed sequences for NR and NiR [172,219]. Moreover, NanoSIMS observations showed that after pulses of ^{15}N-labeled NO_3^-, zooxanthellae assimilated this N form before translocation to the coral host [161]. Because the host does not encode any NR or NiR genes, it was concluded that the dinoflagellate symbionts were responsible for the assimilation. In dinoflagellates, it is believed that N is principally assimilated by the GS-GOGAT pathway. In fact, GS activities were directly measured in *S. microadriaticum* and the use of the GS inhibitor L-methionine sulfoximine (MSX) strongly reduced the uptake of NH_4^+ [220]. Use of the GOGAT inhibitor azaserine also led to inhibition of NH_4^+ uptake [221]. Moreover, 1 h pulses in NH_4^+-enriched

seawater led to a relative ~2 fold increase in levels of Gln and Glu, followed by a decrease back to control levels after a 3 h chase with normal seawater [154]. Increases in levels of Gln and Glu were also reported when pulses of ^{15}N-labeled NH_4^+, NO_3^- or urea were applied [222]. In *Karenia brevis*, a microarray-analysis of N-depleted cultures revealed that sequences for GS and transporters of NO_3^- and NH_4^+ were upregulated compared to N-replete cultures [174]. In *L. polyedrum*, a NR was purified by affinity chromatography and its activity was measured using NO_3^- as substrate [223]. Antibodies were then raised against the protein in order to measure the daily level of expression. Interestingly, it was found that both NR activity and the amount of the protein oscillated under light-dark and constant light conditions, the latter being a hallmark of circadian rhythms [223]. Furthermore, it was reported in this organism that NO_3^- deficiency shortened the period of the circadian rhythms of bioluminescence and photosynthesis. MSX added to cultures containing a saturating amount of NO_3^- mimicked the effects of NO_3^- deficiency on circadian period, arguing for the existence of GS. Altogether, these experiments strongly suggest MTDs possess the full suite of enzymes required for N assimilation and that these enzymes are homologous to those of other photosynthetic eukaryotes.

Circadian clocks confer a selective advantage to organisms by preparing their internal biochemistry for upcoming rhythmic environmental cues, the most typical of these being light and darkness produced the succession of days and nights. These rhythmic cues are called *zeitgebers* (time givers), because an organism's circadian clock can entrain or synchronize to it. The fact that NO_3^--deficiency or NO_3^- pulses act on the phase and the period of the endogenous clock of *L. polyedrum* means that NO_3^- acts as a nonphotic *zeitgeber* [224]. It also indicates that the internal clock can react adaptively to changes in NO_3^- concentration. Usually the greatest responses of a *zeitgeber* happen during the times when the organism is least likely to receive a cue, for example by light during the night. *L. polyedrum* swims at the surface during the day, but in the late afternoon sinks in the water column to where NO_3^- concentrations are higher. Thus, the effects of NO_3^- pulses are greatest early at dawn where the organisms must optimize between taking and assimilating more NO_3^- or photosynthesize. However, these effects on the clock must be interpreted carefully since the greatest uptake rates of NO_3^- or NH_4^+ in all dinoflagellate species tested, including *L. polyedrum*, were obtained during the middle of the light period rather than the night [147,163,225]. This

suggests that the C skeletons and electrons provided by photosynthesis are more important factors affecting the efficiency of uptake than is the N abundance alone. Furthermore, because the circadian clock also controls the activity and expression of the NR *in L. polyedrum*, it means the N metabolism in this species is both involved in the inputs and the outputs of the clock. Circadian-control of the NiR activity in *C. reinhardtii* and on the expression of the NR gene, *NIA2*, in *Arabidopsis thaliana* has also been reported [226,227]. Thus, circadian regulation of the N metabolism in MTDs might be more common than what is currently appreciated.

All the enzymes needed for N assimilation have been identified in diatoms by analysis of their genome sequence [164,165,166]. Surprisingly, the genome also encoded all enzymes required for the ornithine-urea cycle (OUC), present in metazoans but absent in plants and green algae [164,228]. This cycle seems to be fully integrated within diatom metabolism, principally through ornithine and arginine intermediates. Ornithine is a precursor for the synthesis of polyamines, which, among other functions, are necessary for the precipitation of silica during frustule formation, in a reaction catalyzed by ornithine decarboxylase [164]. Ornithine can also be directly converted to proline by ornithine cyclodeaminase, making this intermediate an entry point into amino acid metabolism. As for arginine, it is used by nitric oxide synthase to synthesize nitric oxide, an important signaling molecule in plants and animals [229]. A pathway leading to the formation of the energy-storage molecule creatine-phosphate, was also found to originate from arginine [164]. Integration of the OUC with the TCA cycle and the GS-GOGAT pathway (see next section) were also shown in *Phaeodactylum tricornutum* [228]. In order to check if dinoflagellates could also possess all the genes necessary for the OUC, BLAST searches against dinoflagellate nucleotide databases were performed using the protein sequences of *T. pseudonana* and *P. tricornutum* as queries. In fact, *Alexandrium tamarense* had candidates for all OUC enzymes (Fig. 1.2.2, Table 1.2.2.). This suggests dinoflagellates could also possess a complete ornithine-urea cycle. In diatoms, OUC was recognized as an important N remobilization hub, and it has been suggested that it might give a general advantage when urea concentrations are high or any form of N are abundant in the environment. This was thought to perhaps explain the success and prevalence of diatoms over other phytoplankton species in eutrophic waters [228], but this idea may have to be revisited if dinoflagellates are also able to catalyze the same reactions.

1.2.7. Adaptations to nitrogen stress

Generally, dinoflagellates and diatoms need to cope with varying concentrations of N, particularly in the open ocean where it is often limiting. Thus, each group has developed various strategies, some of which are used by both, to respond and survive to oligotrophic environments (Table 1.2.1.). In this section, we will present these responses based on environmental and laboratory experiments. We will discuss symbiosis and various physiological, behavioral and transcriptomic responses, with an emphasis on dinoflagellates.

Symbiosis with diazotrophs is an example of a strategy that is shared by some diatom and dinoflagellate species. The diatom genera *Hemiaulus* and *Rhizosolenia* both form endosymbiotic associations with the cyanobacteria *Richelia intracellularis* [230,231]. Both the hosts and the symbionts were observed to bloom together in the oligotrophic waters of the North Pacific Central Gyre and South West Atlantic Ocean. N_2-fixation by *Richelia* introduced an amount of "new N" to the ecosystems that could even exceed the N_2 fixed by non-blooming *Trichodesmium*. Carpenter and colleagues suggested that the silicate- and iron-enriched water of the Amazon River could have been factors in initiating and sustaining the blooms in the SW Atlantic Ocean [230]. Silicate is required for the formation of the diatom frustule, while iron is necessary for the action of the diazotroph nitrogenases.

In N-limited conditions, endo- and ectosymbiosis with cyanobacteria were exclusively identified within the dinoflagellate order Dinophysiales [232]. In the genera *Amphisolenia* and *Triposolenia*, the symbionts were found inside the host, while the genera *Ornithocercus*, *Histioneis*, *Parahistioneis* and *Citharistes* appeared to "farm" cultures of cyanobacteria outside the cells in an enlarged cingulum or in special cavities [83,232]. Further microscopic observations of *Ornithocercus* spp. suggested that they could also ingest their symbionts, depending on the size, shape, and color of the prey and on the presence of peduncle in the dinoflagellates. However, it is not clear if these species take up the majority of the external N fixed by the cyanobacteria using transporters and ingest the bacteria only occasionally, or if they "farm" the symbionts exclusively to feed on them. While it was not directly shown that *Symbiodinium* formed symbiotic association with cyanobacteria, the coral host was found to do so. In fact, whole communities of beneficial bacteria including N_2-fixers and chitin decomposers were identified in all coral structures, including the surface mucous layer, tissue

layers and the skeleton [233,234]. Interestingly, amplification of the nitrogenase gene *nifH* in tissues of 3 different coral species revealed that 71% of the sequences came from a bacterial group closely related to rhizobia, the N_2-fixers symbiotic with legumes [235]. The products of N_2-fixation were initially assimilated by the zooxanthellae, then translocated to the animal host, as determined by $\delta^{15}N$ analysis [236]. Moreover, *Symbiodinium* population density was positively correlated with *nifH* sequence copy number, suggesting that growth and division of the zooxanthellae might be dependent upon the product of N_2-fixation [237]. Taken together, these examples suggest that the cyanobacteria barter their N_2-fixing ability for protection and nutrients from their hosts, thus providing a selective advantage to the hosts in N-limited environments.

For the majority of diatom and dinoflagellate species, unable to form any symbiotic associations with diazotrophs, N-limitation sets in motion a series of physiological and behavioral modifications to avoid cell death. Generally, in both groups, N-limitation results in a decrease in the levels of proteins and chlorophylls [238,239,240]. Toxin content in *Alexandrium* sp. and *Ostreopsis ovata* was also shown to diminish when N-stressed [110,241,242,243]. Furthermore, N-limitation or complete N-starvation induces a reduction or an arrest of the cell cycle in both groups [174,238,239,242]. The phase at which arrest occurs was shown to vary in different dinoflagellate species. For example, when completely N deprived, *A. cartarae* cells stop in G1, while *P. piscicida* cells stall at both G1 and G2/M phases [244,245]. Of course, independent of the phase of cell cycle arrest, the resulting consequence is the same: cells cease dividing. At this point, organisms reach a state of stasis where the cells will either form cysts or store/remobilize their internal metabolites until N becomes available again. In photosynthetic eukaryotes, photosynthesis still occurs when N is limiting and C skeletons can accumulate. These were shown to be stored in the form of starch and/or as lipids in plants and green algae [246,247]. In dinoflagellates, accumulation of lipids in the form of triacylglycerol was found to be ~200% higher in N-limited conditions compared to control [248]. In contrast, N-limitation in the HTD *Crypthecodinium cohnii* did not have any significant effects on the rates of lipid production [240]. Thus, N stress may have different effects on the regulation of the enzymes involved in C storage between dinoflagellate groups.

Diatoms can also accumulate lipids, but only when cultured under very low N concentrations [164,238,249,250]. At the early stages of N-stress, when the intracellular

concentrations of NO_3^-, amino acids and proteins were about half the amount measured in N-replete cultures, no changes in C stores such as starch or lipids were detected in *T. pseudonana* [238]. It was proposed that diatoms had a greater tendency to remobilize rather than to store C compounds, because their OUC gives them the potential to increase the efficiency of N reassimilation from catabolic processes [251]. An augmentation of reassimilation would lead to a greater use of C skeletons compared to organisms lacking a urea cycle [238]. This N remobilization hypothesis was suggested by the finding that recovery from N-stress in *P. tricornutum* was impaired in a RNA interference (RNAi) line having a reduced level of carbamoyl phosphate synthase, the enzyme catalyzing the first committed step of the OUC [228]. Indeed, compared to wild type, this mutant accumulates less of most metabolites in the tricarboxylic acid (TCA) cycle and OUC. There are also reduced levels of Gln and other amino acids in the RNAi line, indicating that the OUC acts to link the TCA cycle and the GS-GOGAT pathway together. Thus, the OUC, being at the crossroad of catabolic and anabolic metabolism, was described as a distribution and repackaging hub for C and N compounds, which could have contributed to the success of diatoms in the modern oceans [228].

In some dinoflagellates, such as the MTD species *G. galatheanum*, *C. furca* and *P. minimum*, N-limitation elicits a change in their N nutritional strategy, which switches from a primarily inorganic N uptake by transporters to uptake relying on both transporters and feeding mechanisms. A similar change in behavior was also recently shown to occur in free-living *Symbiodinium* spp. [252], as while the cells ingested prey in both N-replete and N-limited conditions, the feeding rates were higher in the latter. In these experiments, ingestion of the raphidophyte *H. akashiwo* in NO_3^--limited conditions contributed up to 229% of *Symbiodinium* spp. daily body N compared to 105% in NO_3^--replete conditions. In other dinoflagellates, such as the type III MTD *P. piscicida,* when the amount of prey was reduced to ~ 1% of the predator population in the presence of high concentrations of DIN and DON (principally NO_3^-), uptake rates by transporters increased to levels similar to those cited for phytoplankton [253]. Indeed, the highest rates of N uptake by transporters were comparable to the rates of N uptake by ingestion in *P. piscicida* cultures containing high amounts of prey [253]. Clearly, some MTDs adapt to the N status of the environment by modifying their feeding behavior and altering the expression or activity of N transporters.

Transcriptional regulation of N metabolism is widespread in plants and algae [119,254,255]. In diatoms, comparative analysis of expressed sequence tags (ESTs) libraries under N stress in *T. pseudonana* and *P. tricornutum* revealed altered expression of numerous genes involved in N transport and assimilation [256]. In this study, an NH_4^+ transporter was among the most up-regulated genes in N-depleted *P. tricornutum* cells. Similarly, in *C. fusiformis*, AMT1 and AMT2 transcript levels were highest in N-starved conditions [169]. Curiously, other transcripts, such as the one encoding NR in *C. fusiformis*, do not respond to variations in NO_3^- concentrations, although its expression is inhibited by NH_4^+ [257]. These examples highlight the complex regulation of different N metabolism genes in diatoms.

Interestingly, in dinoflagellates, different high-throughput analysis of transcriptomes under N-stressed conditions revealed that transcriptional control also seems to occur in these organisms. Massively parallel signature sequencing (MPSS) in *Alexandrium fundyense* revealed that ~10% of the signatures were differentially expressed between N-stressed and P-stressed cells [70]. This does not mean that 10% of the transcripts varied, however, as rapid amplification of cDNA ends (RACE) sequencing and mapping to known dinoflagellate genes showed that multiple signatures arose from sequence variants of individual genes. This redundancy was ascribed to the gene duplication events commonly described in dinoflagellate genomes [70]. MPSS of *Alexandrium tamarense* cultures grown under various stresses was also performed, but in this study most of the differentially expressed genes were observed in comparisons between xenic and axenic cultures, rather than the N-limited ones [71]. In *Karenia brevis*, a microarray comparison of N-limited and N-replete cells showed that ~11% of the probes differ between the two conditions [174]. Interestingly, an NH_4^+ transporter, NO_3^- /NO_2^- transporters and type III GSs were among the sequences up regulated under N-limitation. These experiments show that stress can induce transcriptional responses in dinoflagellates, which presumably act to fine tune dinoflagellate N metabolism in relation to environmental N status.

1.2.8. Conclusion

Dinoflagellates use various strategies to acquire and assimilate N, depending on their trophic preferences and life styles. Some make an extensive use of transporters, others preferentially ingest prey and still others exploit both strategies equally. Enzymes for uptake and assimilation of N seem to share homology and kinetic properties with those reported in other photosynthetic eukaryotes. A remarkable feature both found in diatoms and dinoflagellates is their adaptability to changes in environmental N concentrations, particularly under stress conditions. Some mechanisms are common, such as symbiosis and transcriptional control; others are particular to dinoflagellates, like mixotrophy and vertical migration. With the advent of next-generation sequencing technologies, transcriptomic and even genomic tools will soon help in identifying and characterizing the molecular components involved in dinoflagellate N metabolism. Understanding how N is put in dinoflagellates will certainly help to better predict their behavior into our future anthropogenically-altered aquatic ecosystems.

Table 1.2.1. Comparison of adaptation mechanisms to N stress between dinoflagellates and diatoms

Mechanism	Dinoflagellates	Diatoms
Encystment	✓	✓
C storage	✓	✓
High-affinity transporters	✓	✓
Decreased Internal N pool	✓	✓
Ornithine-urea cycle	✓	✓
Symbiosis	✓	✓
Transcriptional control	✓	✓
Circadian control	✓	✗
Mixotrophy	✓	✗
Vertical migration/ Dark nitrate uptake	✓	✗

Table 1.2.2. Nitrogen Metabolizing Enzymes similar to those in diatoms in the Transcriptome of *Alexandrium tamarense*

Enzyme	E-value	Query length (AA)	Coverage	Accession
Carbamoyl phosphate synthase	0	1485	95%	GAJB01000224
Ornithine carbamoyltransferase	e^{-56}	352	90%	GAIT01092113
Argininosuccinate synthase	e^{-62}	418	95%	GAIT01061622
Argininosuccinate lyase	e^{-43}	469	78%	GAJG01001449
Arginase	e^{-18}	223	96%	GAJB01022416
Urease	0	807	99%	GAJB01002972

Figure 1.2.1. Nitrogen metabolism in dinoflagellates.

In this schematic overview of N metabolism, transporters and channels are depicted as individual proteins that transport a range of N forms, even though transporters/channels are normally selective for particular N forms. A (?) signifies that the pathways or proteins have not been reported in dinoflagellates, but can be present in other photosynthetic eukaryotes. The (NR ?) indicates that while this enzyme is usually localized to the cytoplasm, a study in *L. polyedrum* indicated it was found to the chloroplast (Fritz et al., 1996). AA, amino acids; DIN, dissolved inorganic nitrogen; DON, dissolved organic nitrogen; GS, glutamine synthetases; GOGAT, glutamine 2-oxoglutarate amidotransferase; NH_4^+, ammonium; NO_3^-, nitrate; NO_2^-; nitrite; NiR; nitrite reductase; NR, nitrate reductase; NT, nucleotides.

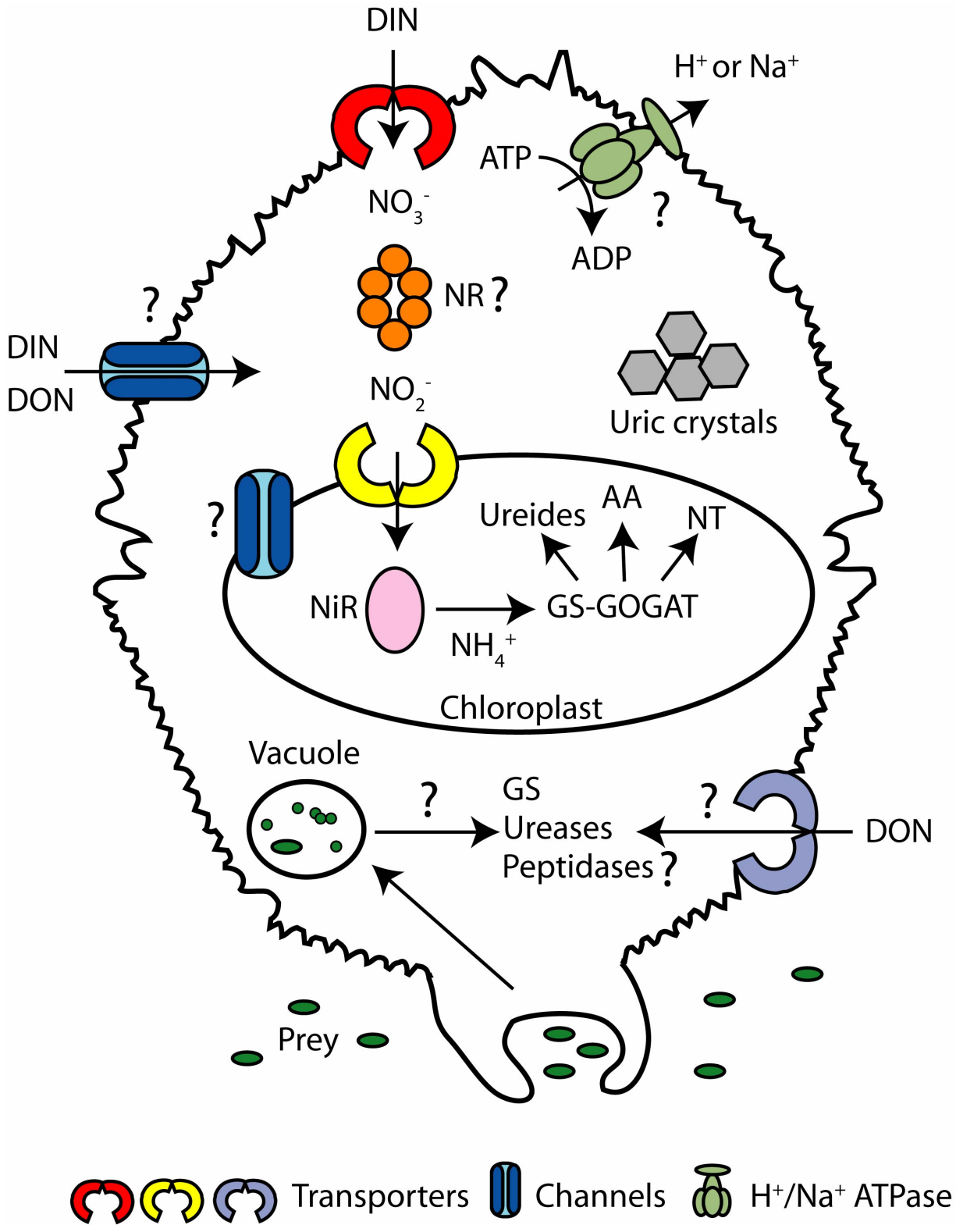
DIN
H+ or Na+
ATP
ADP
?
NO3-
NR ?
?
DIN
DON
NO2-
Uric crystals
?
Ureides
AA
NT
NiR
GS-GOGAT
NH4+
Chloroplast
Vacuole
?
GS
Ureases
Peptidases ?
?
DON
Prey
Transporters
Channels
H+/Na+ ATPase

Figure 1.2.2. Ornithine-urea cycle.

This pathway is derived from that identified in diatoms. CPS, Carbamoyl phosphate synthase; OTC, ornithine carbamoyltransferase; AsuS, argininosuccinate synthase; AsL, argininosuccinate lyase; Arg, arginase (depicted twice, because it produces both ornithine and urea); Ure, urease.

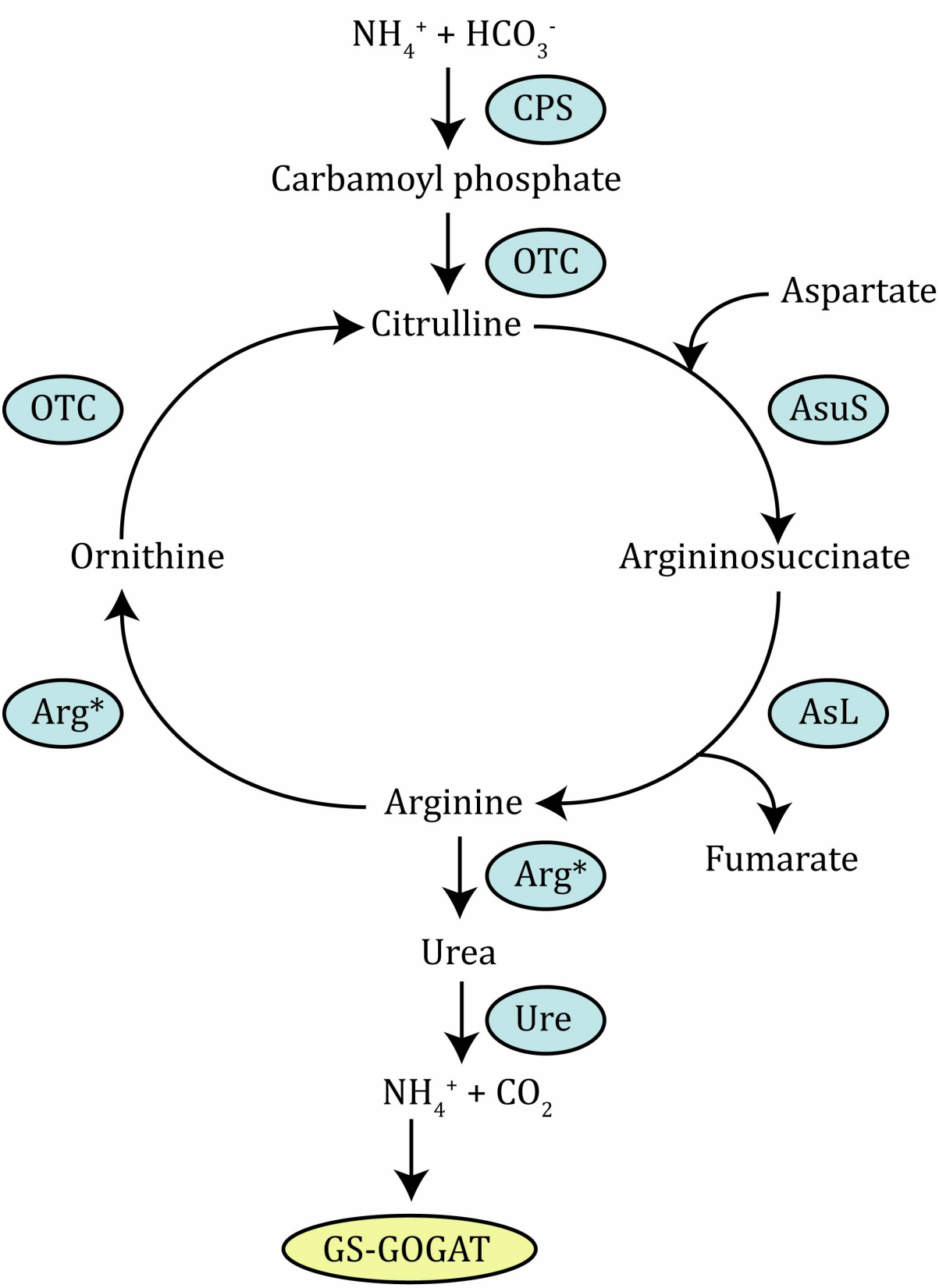
$NH_4^+ + HCO_3^-$
CPS
Carbamoyl phosphate
OTC
Aspartate
Citrulline
OTC
AsuS
Ornithine
Argininosuccinate
Arg*
AsL
Arginine
Fumarate
Arg*
Urea
Ure
$NH_4^+ + CO_2$
GS-GOGAT

1.2.9. Acknowledgments

Funding by the National Science and Engineering Research Council of Canada (NSERC) in the form of a student fellowship (SDB) and a research grant (DM, Grant number 171382-03) is gratefully acknowledged.

1.3. *Lingulodinium polyedrum* and the circadian clock

Lingulodinium polyedrum is a marine, bioluminescent and armored (thecate) dinoflagellate (Fig. 1.3.1, 1.3.2), found in various regions of the world [258] but commonly seen along the Southern California coast, where it typically blooms during late spring and early summer [148]. This species belongs to the gonyaulacoids, which is a rare core dinoflagellate group that is monophyletic [6]. While the gonyaulacoids include important toxic genera such as *Alexandrium,* and *Gambierdiscus*, *L. polyedrum* is generally described as non-toxic. In fact, some studies have identified yessotoxin in *Lingulodinium* [259], but their levels were so low, that blooms dominated this species are considered harmful mainly because they cause anoxia and reduce irradiance in the water column. Morphologically, *Lingulodinium* is approximately 35 by 45 μm in size [260], and has a C-shaped nucleus with about 200 pg of DNA distributed over roughly 200 chromosomes [261]. It also possesses a triple-membrane bound, peridinin-chloroplast with all the features described in section 1.1.2, and relies principally on photosynthesis for its living, even though evidence of mixotrophy has been reported [178]. For about 60 years, *L. polyedrum* has been recognized as a useful model in chronobiology, because many physiological activities in this species show daily rhythms that are independent of external cues and thus controlled by a circadian clock [262].

Circadian clocks are endogenous, self-sustained oscillators that living organisms have developed in response to daily variations in environmental conditions, such as light, temperature and nutrients. The adaptive importance of circadian clocks has been illustrated in multiple models, from bacteria to mammals [263,264,265,266]. In a notable experiment, a co-culture competition with two strains of the cyanobacterium *Synechococcus elongatus*, each having different internal clock periods (often called free-running periods), showed that the strain having the period most closely matching the external light/dark cycle clearly outcompeted the other strain [263]. In contrast to rhythms simply responding to environmental cues, biological rhythms that are circadian-regulated continue to oscillate with a period of ~24 h in constant conditions and are temperature-compensated [267]. The circadian clock can also synchronize to the environment using cues such as changes in light or temperature. External stimuli are detected by the internal clock, which in turn conveys timing signals to the organism to regulate cellular physiology [267]. The clock circuitry can thus be thought as being

composed of three interlocking parts: the input pathway; the central oscillator; and the output pathway [268].

With the exception of cyanobacteria, whose central oscillator can run using posttranslational modifications alone [269], the core clock mechanisms in eukaryotic circadian systems appears to be based on transcriptional/translational feedback loops (TTFL) [270,271]. These TTFL involve rhythmic expression of "clock genes", which give rise to oscillating levels of RNA and proteins. After a lag, the proteins feedback to repress their own expression by interfering with their transcriptional activators, thereby closing the loop [270]. Rhythmic expression of clock genes drives the expression of output genes that manifest in the form of physiological rhythms. However, while the TTFL mechanism is conserved among diverse eukaryotic phyla, the clock genes are not, which is indicative of convergent evolution. For this reason, homology searches could not be used to identify clock genes in dinoflagellates, and the central oscillator components in these organisms are still unknown. Studies of *L. polyedrum* in chronobiology have thus been related to understanding the biochemical basis of clock control on output rhythms, rather than working of the clock itself. In this regard, *Lingulodinium* has proven to be an interesting model, because the clock in this organism was found to prefer translational control over transcriptional regulation for gene expression [262].

Bioluminescence is one of the rhythmic output in *L. polyedrum* that has received particular attention. Not only is bioluminescence easy to measure, but light emission appears to require only a substrate (luciferin), and two proteins: the luciferin-binding protein (LBP) and luciferase (LCF). All three components are localized in distinct spherical organelles called scintillons, that protrude into the acidic vacuole and are in fact almost completely surrounded by the vacuolar membrane [272]. The bioluminescent reaction involves the catalysed oxidation of luciferin by LCF. However, in *Lingulodinium*, luciferin is sequestered by LBP at cytoplasmic pH of ~7.5 and prevents this reaction [273]. Upon mechanical or temperature stimulation, a voltage-gated proton channel in the vacuolar membrane is activated and decreases the cytoplasmic pH around the scintillons to ~6.5 [274]. This acidic pH releases LBP from luciferin and activates LCF [273], which produces light in the form of brief (~100 msec) [275] and bright (~10^9 photons/cell) flashes [274]. The number of scintillons at night is roughly tenfold higher than during the day [276] (Fig. 1.3.2), which correlates with the protein levels of LBP and LCF [277,278,279]. Both proteins were shown to be circadian-regulated

[277,278,279] at the translational level, based on the observation that levels in LBP and LCF mRNA did not vary during a daily cycle [277,280].

In contrast to bioluminescence, photosynthesis in *Lingulodinium* is a circadian output that does not seem to rely on changes in abundance of key proteins. Both oxygen evolution [281] and carbon fixation [282] are rhythmic and peak during the day, but levels of the main proteins associated with these rhythms, the peridinin-chlorophyll *a*-protein (PCP) [283], and RuBisCO [29,284], respectively, do not change appreciably over the daily cycle. While the mechanism behind the oxygen evolution rhythm is still unknown, circadian control over carbon fixation was shown to correlate with the sub-cellular distribution of RuBisCO (see section 1.1.2.) [29]. The chloroplasts in *Lingulodinium* also experience daily changes in shape and position in the cell. Plastids of day phase cells are 50% longer and seem to radiate from the center toward the cell periphery, while night phase chloroplasts are more centrally localized and are characterized by the presence of widely separated thylakoid stacks [285] (Fig. 1.3.2). Studies of both the bioluminescent and photosynthesis rhythms in *Lingulodinium* has showed that circadian control of cell physiology does not involve regulation at the transcriptional level and that various translational and posttranslational mechanisms can control different rhythms in the same cell.

Figure 1.3.1. Illustration of a *Lingulodinium polyedrum* cell.

Artistic representation of *Lingulodinium polyedrum* obtained by modifying a scanning electron microscopy photograph of a single cell. The picture was taken with a FEI Quanta 200 3D (Dualbeam) microscope and modifications were made using Adobe Photoshop 8.0.

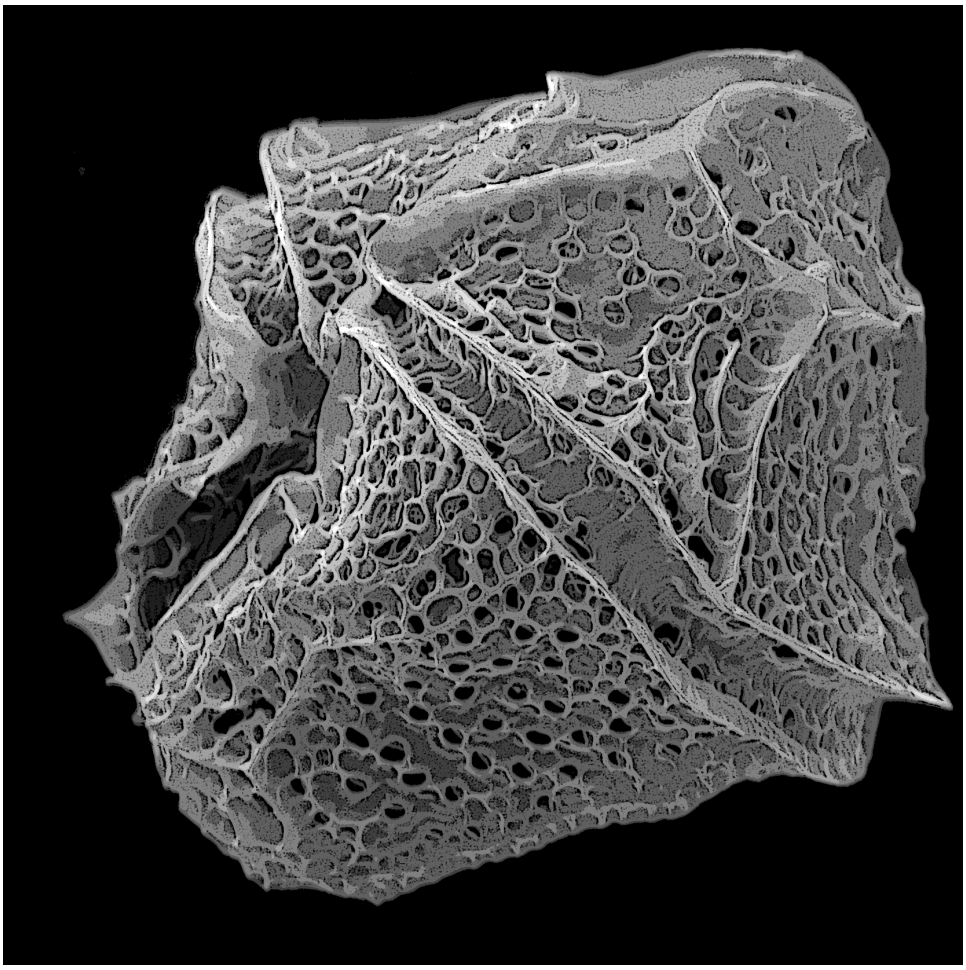

Figure 1.3.2. Circadian rhythms of bioluminescence and photosynthesis in *Lingulodinium polyedrum*.

Scintillons (blue) and chloroplasts (orange) of A), day phase and B), night phase *Lingulodinium* cells. Images were taken on a LSM 5 Duo confocal microscope (Zeiss). A 405 nm argon laser was used for excitation, and emitted light was passed through a beam splitter for simultaneous observation of scintillons (420-480 nm band pass filter) and chloroplasts (575 nm long pass filter). Images were reconstructed from z-stacks using Imaris. Bars are 10 μm.

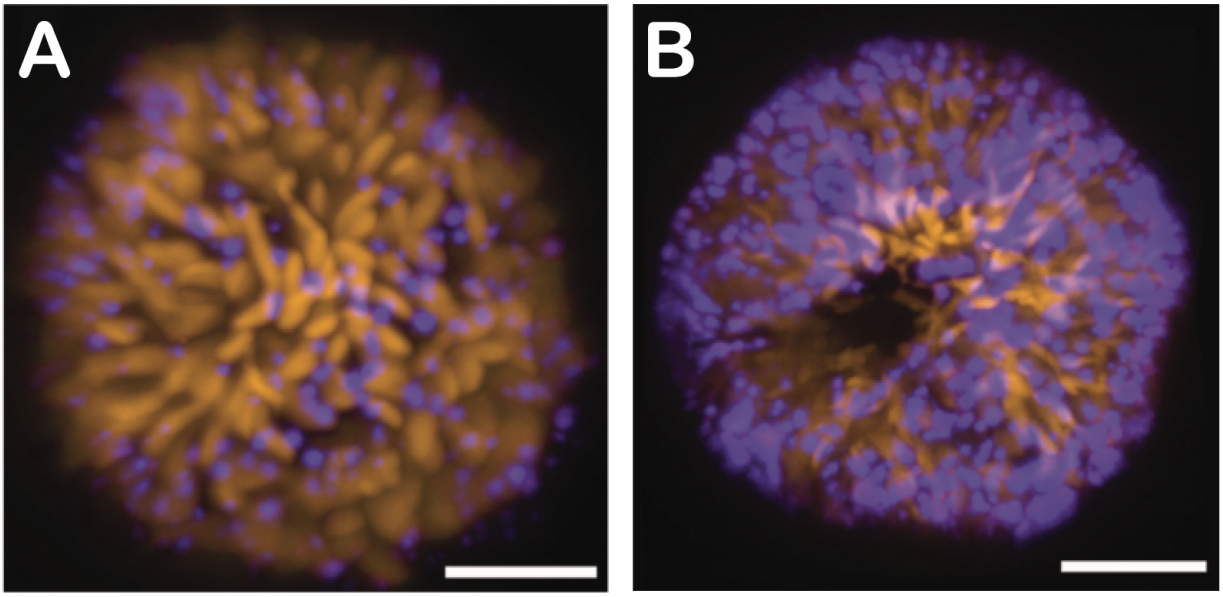
A
B

1.4. *Lingulodinium polyedrum*: a circadian model for the study of nitrate metabolism

Another important circadian rhythm of *Lingulodinium* and the topic of this thesis, is the nitrate metabolism. Interestingly, nitrate is not only an essential nutrient for the survival of this dinoflagellate, it also acts both as an input to and an output from the circadian clock; an input, because nitrate influences fundamental clock properties (period, amplitude and phase) [224,286], and an output because assimilation is circadian-regulated at the NR level [223]. Studying nitrate metabolism in *Lingulodinium* could potentially answer important ecological questions, such as how dinoflagellates respond to their environmental nitrogen status, and what are the conditions required for nitrogen pollution to trigger the formation of HABs. Identification and characterization of molecular components involved in the nitrate metabolism of *Lingulodinium* could also reveal important players of the clock input pathway and give a better appreciation of the regulation mechanisms used by the circadian system to optimize a primary metabolic pathway. These broad ideas were used as guidelines to define the specific goals of my thesis. Each of these goals is presented in the following three chapters.

My first objective was to describe the physiological responses of *Lingulodinium* to nitrogen stress and to explain why HABs are sometime observed in conditions of nitrogen limitation [287]. Secondly, I aimed to identify and characterize nitrate transporters, because it was previously suggested that nitrate transport was circadian-regulated in *Lingulodinium* [224], and it is known that these transporters are sometimes also used as nitrate sensors [126]. Finally, I used a high-throughput RNA sequencing method to verify if any molecular component of the nitrate metabolism in *Lingulodinium* was circadian-regulated at the transcriptional level.

Chapter 2- Publication # 2

The dinoflagellate *Lingulodinium polyedrum* responds to N depletion by a polarized deposition of starch and lipid bodies

Steve Dagenais Bellefeuille, Sonia Dorion, Jean Rivoal, David Morse

Published in PLoS One, 2014, 9 (11) : e111067

Author contributions:

S. Dagenais Bellefeuille and D. Morse designed the project. Experiments were performed by S. Dagenais Bellefeuille and S. Dorion. Data was analyzed by S. Dagenais Bellefeuille, J. Rivoal and D. Morse. The first version of the manuscript was written by S. Dagenais Bellefeuille and the text was revised and corrected by S. Dorion, J. Rivoal and D. Morse.

As an explanation for the occurrence and sustenance of HABs in oligotrophic environments, Vargo and colleagues suggested that mixotrophic dinoflagellates could meet their daily N demands by feeding on fishes killed by blooms [287]. In this chapter, I wanted to offer an alternative to this suggestion by showing the particular resilience of photosynthetic dinoflagellates to N stress. I present the physiological responses of *Lingulodinium* to N starvation with an emphasis on amino acid and carbon metabolisms. I also show that N stress triggers acclimation mechanisms in this dinoflagellate.

2.1. Abstract

Dinoflagellates are important contributors to the marine phytoplankton and global carbon fixation, but are also infamous for their ability to form the spectacular harmful algal blooms called red tides. While blooms are often associated with high available nitrogen, there are instances where they are observed in oligotrophic environments. In order to maintain their massive population in conditions of nitrogen limitation, dinoflagellates must have evolved efficient adaptive mechanisms. Here we report the physiological responses to nitrogen deprivation in *Lingulodinium polyedrum*. We find that this species reacts to nitrogen stress, as do most plants and microalgae, by stopping cell growth and diminishing levels of internal nitrogen, in particular in the form of protein and chlorophyll. Photosynthesis is maintained at high levels for roughly a week following nitrate depletion, resulting in accumulated photosynthetic products in the form of starch. During the second week, photosynthesis rates decrease due to a reduction in the number of chloroplasts and the accumulation of neutral lipid droplets. Surprisingly, the starch granules and lipid droplets are seen to accumulate at opposite poles of the cell. Lastly, we observe that cells acclimated to nitrogen-depleted conditions resume normal growth after addition of inorganic nitrogen, but are able to maintain high cell densities far longer than cells grown continuously in nitrogen-replete conditions.

Keywords: Dinoflagellate, harmful algal bloom, acclimation, nitrogen limitation, proteins, photosynthesis, carbon, starch, triacylglycerol

2.2. Introduction

Nitrogen (N) is an essential nutrient for all living organisms as it is required for biosynthesis of proteins and nucleic acids. While N is highly abundant in the atmosphere as dinitrogen gas (N_2), this chemical form is inaccessible to most organisms, which thus depend on diazotrophs, prokaryotes able to transform N_2 to bioavailable N forms. As a result, demand for N often exceeds its supply, which limits growth in many ecosystems. This is particularly severe in the open oceans where diverse phytoplanktonic species must compete for small amounts of bioavailable N and be able to survive periods of natural N depletion [288].

Dinoflagellates are important members of the phytoplankton that have developed a variety of strategies to cope with N stress [289]. These strategies have a particular importance for those dinoflagellate species able to form harmful algal blooms (HAB), or "red tides". Some HAB can produce toxins, which can have a strong negative impact on other parts of the ecosystem and on human health. Strategies allowing blooms to deal with N stress might appear counterintuitive, as natural and anthropogenic N addition rather than N deprivation is a factor often associated with HAB [86,105]. However, in some cases dense blooms can form and persist in oligotrophic environments where the measured inorganic N supply would seem to be insufficient to support their biomass, as was observed for *Karenia brevis* in the West Florida Shelf [287]. In this particular example it was proposed that organic N coming from decaying fish killed by the HAB explained the persistence of the dinoflagellate populations [287,290]. However, another possibility is that acclimation mechanisms triggered by N deprivation during a bloom could allow the dinoflagellates to maintain bloom-density population levels until new N becomes available. Unfortunately, testing this hypothesis in the environment would be difficult, because of the complex interplay between biotic and abiotic factors involved in bloom dynamics [105].

Lingulodinium polyedrum is a marine dinoflagellate usually studied as a model system in circadian biology, but is known to form HAB in various regions of the world, particularly along the coast of Southern California [148,262,291]. Laboratory cultures of this species can be readily transferred to media of different composition after filtration, which makes it a good candidate to test the effects of controlled nutrient conditions on its biochemistry and physiology. Interestingly, *L. polyedrum* grown in N-deprived artificial sea water was reported

to survive up to 4 times longer than when grown in the normal nitrate (NO_3^-) enriched f/2-medium [224]. These findings implied that this species was able to acclimate to N limitation, but the underlying mechanisms were not evaluated. In this study, we have addressed this issue by monitoring the physiological responses of *L. polyedrum* to N stress. In particular, we note that cells acclimated to N limitation rose to high cell densities when new inorganic N was supplied and these for durations normally observed in *L. polyedrum* blooming populations in the environment. This is in sharp contrast to the behavior of non acclimated cells, which abruptly die after reaching their maximum cell density. We also note an accumulation of reduced carbon (C) in the form of starch granules and lipid bodies in N-limited cells. Curiously, these two forms accumulated in different regions of the cell.

2.3. Material and methods

2.3.1. Cell culture

Unialgal but not axenic *Lingulodinium polyedrum* (CCMP 1936, previously *Gonyaulax polyedra*) was obtained from the Provasoli-Guillard National Center for Marine Algae and Microbiota (East Boothbay, ME, USA). Cell cultures were either grown in normal f/2 medium prepared using Instant Ocean (termed day 0) or in f/2 lacking added N (f/2-N) for one or two weeks (termed day 7 or day 14). Day 0 cells acted as control during all experiments. To transfer cells to f/2-N (N-depleted medium), cultures grown in f/2 were filtered on Whatman 541 paper and washed with 200 ml of f/2-N medium before resuspension in f/2-N medium. Normal f/2 medium is made from Instant Ocean supplemented with 0.88 mM NO_3, and Instant Ocean alone contains 1 µM NO_3, 10 µM NH_3 and 3 µM dissolved organic N [292]. All cultures were grown under a 12 h light (40 µmol photons m^{-2} s^{-1} cool white fluorescent light) and 12 h darkness at a temperature of 18 ± 1 °C. This light/dark regime is termed LD, with LD 0 corresponding to lights on and LD 12 to lights off. Cells used for elemental analysis, the quantification of total proteins, amino acids, starch and neutral lipids were harvested by filtration and stored at -80 ºC until use.

2.3.2. Cell density measurements

Cells in multiple 10 µl aliquots of f/2 and f/2-N cultures were placed on microscope slides and were counted every 3 or 4 days using a Leica Wild M3B stereo microscope. After 17 days, a time when the cultures had typically reached their maximum cell density, 880 µM of $NaNO_3$ was added to each culture. Counts were continued every 3 or 4 days until the cultures did not contained anymore cells swimming in the medium.

2.3.3. Elemental analysis

Measurements of total C and N contents were performed using a Carlo Erba NC2500 Elemental Analyzer (at Geotop-UQAM, Montreal, PQ, Canada). The analytical step was preceded by a preparative step, where cells were harvested, lyophilized, weighed and inserted into tin capsules. Results are reported as percent of total dry weight.

2.3.4. Protein and amino acid quantification

For total protein quantification, cultures grown in f/2 were split into f/2 and f/2-N cultures, and samples were taken before, as well as 3, 7, 10 and 14 days after the split. Protein from 30 mg wet weight of cells was extracted following a slightly modified Trizol (Life technologies) protocol as described previously [293]. Protein pellets were resuspended in 7 M urea, 2 M thiourea, 4% CHAPS and 20 mM dithiotreitol, and incubated overnight to completely solubilize the pellets. Protein concentrations were measured using Bio-Rad (Bradford) Protein Assay following the manufacturer's protocol.

Amino acid quantification was performed by HPLC using a protocol previously optimized for plant tissues [294]. Samples were lysed mechanically in 80% (v/v) ethanol for 2 min at 4°C in a bead beater (BioSpec products). They were then extracted at 70°C in 80% (v/v) ethanol and fractionated into neutral, anionic and cationic fractions by preparative ion exchange purification [295]. The cationic fractions were aliquoted and evaporated to dryness before derivatization with the AccQ Fluor reagent kit (Waters). The amino acids in the aliquots were analyzed on a Waters HPLC system controlled by the Empower Pro software and equipped with a 600 controller, a 717 Plus refrigerated automatic sample injector, a 2996 Diode Array Detector and an AccQ·Tag Amino Acid Analysis Column (Waters). HPLC parameters were set according to manufacturer's recommendations. Quantification was done using standard curves from commercial amino acids.

2.3.5. Photosynthetic measurements

Chlorophyll *a* content was measured after extraction of 50 mg wet weight of cells in 100% acetone. The pigment-containing supernatants were collected after centrifugation and cell residues were re-extracted with small volumes of acetone until colorless. Supernatants were combined and chlorophyll optical densities were measured using a Cary 100 Spectrophotometer (Varian). Concentrations were calculated using the equations presented by [296].

Photosynthetic C fixation rates in normal and N-depleted cultures were calculated from incorporation of ^{14}C to an acid-soluble form. For each assay, 1.48 kBq (= 0.04 µCi) of radiolabelled bicarbonate ($NaH^{14}CO_{3(aq)}$, ICN, 310 MBq $mmol^{-1}$) was added to 5 mL of cell culture with dissolved inorganic carbon ≈ 2 mM [297] and the culture incubated for 90 min

under normal lighting (40 μmol photons m^{-2} s^{-1} cool white fluorescent light). The ^{14}C labeling was quenched by adding HCl to a final concentration of 1 N and gaseous radioactivity was allowed to escape from unsealed samples vials during an overnight incubation in a fume hood. Samples were transferred into scintillation vials with 2 mL Scintiverse (Fisher Scientific) then counted in a TriCarb 2800TR scintillation counter (Perkin Elmer). Values were reported as the number of disintegrations per minute (DPM) from light-induced C fixation after subtraction of the number of DPM for identical subcultures incubated in the dark. Samples were normalized to cell number.

2.3.6. Starch quantification

For starch analysis, cells from all cultures were harvested at both LD 0 and at LD 12 and were lysed mechanically in 80% (v/v) ethanol for 2 min at 4°C in a bead beater (BioSpec products). Starch was assayed enzymatically as described [298]. Briefly, the procedure included the removal of soluble sugars with 80% (v/v) ethanol washes at 70°C, the solubilization of starch in 1M KOH and its conversion into glucose by amyloglucosidase. The glucose concentration was determined using hexokinase (HK) to phosphorylate the glucose and glucose-6-phosphate dehydrogenase (G6PDH) to convert the glucose-6-phosphate to 6-phosphogluconolactone and simultaneously reduce NAD^+ to NADH. This reduction was monitored spectrophotometrically at 340 nm with the amount of NADH produced proportional to the amount of glucose in the samples.

2.3.7. Nile red quantification of neutral lipid

Neutral lipids were quantified with Nile red using a fluorometric assay previously optimized for various microalgae [299]. Two mg wet weight cell pellets were resuspended in 25% dimethyl sulfoxide (DMSO) in 1.5 mL tubes with glass beads (0.5 mm, BioSpec products) and were lysed mechanically for 2 min at 4°C in a bead beater (BioSpec products). Small aliquots of these cell solutions were added to a black 96-microplate and the volume was adjusted to 297 μL with 25% DMSO. Fluorescence was recorded using a SpectraMax M5 Microplate Reader (Molecular Devices) under high scan control and high PMT detector voltage mode, using emission and excitation wavelengths of 530 nm and 575 nm, respectively. These wavelengths were selected based on the emission/excitation spectra of the triolein

standard used for quantification. Three µL of a 50 µg mL^{-1} Nile red solution was added to each well to a final concentration of 0.75 µg mL^{-1} and the plate was incubated at 37ºC for 10 min. Fluorescence values after Nile red-staining were recorded and, after subtraction of the pre-stain fluorescence values, were used for quantification using a triolein standard curve.

2.3.8. Microscopy

Starch was observed in cells from the a culture taken at both LD 0 or LD 12, after fixation in 70% (w/v) ethanol, and staining using a solution containing 0.5 % (w/v) I_2 and 1 % (w/v) KI. Stained cells were visualized with a bright-field Axio Imager M1 microscope (Zeiss).

The contrast of all images was adjusted with Adobe Photoshop 8.0 using the same tonal curve to provide better contrast between the black-stained starch and the dark brown cell background.

Chloroplasts and lipid bodies of day phase living cells were visualized with a LSM 5 Duo confocal microscope (Zeiss). Chlorophyll autofluorescence was observed using a UV-diode (405 nm) excitation and a long pass filter (> 575 nm) emission. For lipid bodies, 1 mL aliquots were incubated at 18°C in the dark for 20 minutes with Nile red at a final concentration of 10 µg mL^{-1}. Stained lipid bodies were observed using an argon laser (excitation at 514 nm) and emissions at 575 and 615 nm. Differential interference contrast (DIC) images were taken at the same time as the fluorescent images. Cells with the ventral side up were selected for imaging so that the optical slices would have a similar appearance with respect to the location of the C-shaped nucleus and the pyrenoids. All microscope parameters used were the same between samples. Nile red images were modified for contrast only using Adobe Photoshop 8.0.

For transmission electron microscopy, cells were harvested at LD 0, fixed with 2% glutaraldehyde in 0.4 M NaCl, 0.05 M PBS (pH 7.2) for 2 h and then washed 3 times in 0.4 M NaCl, 0.05 M PBS (pH 7.2). Fixed cells were dehydrated following standard procedures and embedded in Spurr's resin as recommended by the manufacturer. Thin sections were contrasted with a saturated solution of uranyl acetate in 50% (w/v) ethanol and immediately observed with a JEOL JEM-1010 electron microscope operating at a voltage of 80 keV.

2.3.9. Statistical analyses

All experiments were run in triplicate (n=3) and results were presented as means ± SE. Analysis of variance or Student's t-tests were used for all data. Statistical tests were performed using the JMP software (SAS).

2.4. Results

To examine the acclimation mechanisms of *Lingulodinium* to N stress, we first determined the physiological responses after transferring N-replete cultures (in standard f/2 medium) to a medium lacking added nitrate (f/2-N). Cultures grown in f/2 medium generally show robust growth for 10-14 days after which the cell densities remain high for several days then drop precipitously (Fig. 2.1). In some cases, where average growth rates decrease at earlier times, the cultures can survive for slightly longer (Fig. 2.1B). In contrast, cell growth in f/2-N medium stalled immediately after transfer (Fig. 2.1A). This inhibition of cell growth is a direct consequence of N depletion, as the addition of nitrate to f/2-N cultures on the 17^{th} day restarted cell growth (Fig. 2.1B). Interestingly, some cultures acclimated to N depletion demonstrated an ability to survive at high cell densities far longer than cells grown in the N-replete f/2 medium (Fig. 2.1B). A similar robustness in culture lifetime was also observed for cases where cell densities declined to intermediate values. The cultures acclimated to low N thus appear able to avoid the precipitous collapse of cell densities typically observed for cultures grown in N replete conditions.

Elemental analysis revealed that proportion of cell dry weight as N for cultures grown in f/2-N decreased to almost half their original value after 7 or 14 days (Fig. 2.2A), while the proportion of cell dry weight as C remained unchanged (Fig. 2.2B). As these values represent the fractional dry weight allocated to a particular element rather than the absolute amount of that element, the smaller percentage of N observed in f/2-N-grown cells implies that the absolute amounts of other elements are increasing while absolute cellular N levels remain constant.

The bulk of cellular N is normally sequestered in proteins, and so a reduction in the proportion of N should be accompanied by a reduction in the proportion of protein. To test this, protein levels were measured as a function of time for cultures growing in f/2 and f/2-N media. After 7 days in f/2-N, the protein concentration declined to half the value of the f/2-cultures and remained roughly constant for the following days (Fig. 2.3A), consistent with the decrease observed for elemental N. The decrease in protein observed for cells grown in normal f/2 medium after 14 days may involve a decrease in protein synthesis rates such as observed in stationary phase cells of *Escherichia coli* [300]. A consequence of this, should protein

degradation rates remain unchanged, would be a decrease in protein levels. However, we do not know what signals or environmental factors cause the transition to stationary phase in *Lingulodinium*.

To test if the changes in protein levels observed for f/2-N cultures were also reflected in the free amino acid (FAA) pools, we next characterized the FAA profile of N-depleted cultures using a previously described HPLC-based protocol (Fig. 2.3B)[294]. Of the 14 FAAs that were quantified by this method, only Gln and Arg levels were found to decrease after N deprivation consistent with the requirement of NH_4^+ for their biosynthesis. Most of the FAAs measured, in particular the most highly abundant ones, did not vary significantly during N stress. However, levels of several of the less abundant FAAs, including Tyr, Met, Ile and Leu, were observed to increase after 7 or 14 days in f/2-N. When the FAA data are considered as a whole, the total N in FAA shows no significant change between f/2 and f/2-N cultures (Fig. 2.S1A, 2.S1B). However, the calculated Gln/Glu ratio, considered a useful indicator of N assimilation rates [301] was ~ 4 times lower in N-deplete than in N-replete cells (Fig. 2.S1C). Thus, despite a constant total FAA pool, N-depleted cultures show the effect of a severe decrease in N assimilation.

When compared to the f/2-cultures, chlorophyll *a* concentrations gradually diminished by two- and six-fold by 7 and 14 days of incubation in f/2-N, respectively (Fig. 2.4A). However, a concomitant decrease in the rate of photosynthesis, as measured by ^{14}C-incorporation in acid-soluble compounds, was only observed after 14 days in N deprivation (Fig. 2.4B), with CO_2 fixation rates actually showing an increase after 7 days N deprivation. One possible explanation for this is that the initial decrease in chlorophyll aids C fixation by decreasing O_2 evolution rates [29], but by 14 days the ability of the cells to produce photosynthetic reductant is no longer sufficient to maintain high CO_2 fixation rates. Interestingly, observation of chlorophyll autofluorescence in living cells by confocal microscopy (Fig. 2.4C-K) supports the steady decrease in chlorophyll levels during N- stress from 7 (Fig. 2.4G) to 14 days (Fig. 2.4J). Cells observed after 14 days also show a decreased number of chloroplasts (Fig. 2.4J).

The ability of the cells to maintain high levels of C fixation for at least one week in N-deplete conditions suggested that reduced C might accumulate in these cells. To test this, we

assessed the levels of starch and neutral lipids, two C pools previously reported to increase during N stress in other dinoflagellates and microalgae [240,302,303,304]. *L. polyedrum* cultures show a clear increase in starch levels after 7 and 14 days of N depletion (Fig. 2.5A). In the leaves of higher plants, starch is synthesized during the day and degraded at night [305], and the data show that a similar rhythm is found in *L. polyedrum* grown in the presence of N. In these cells, starch levels were substantial at dusk (LD 12) yet almost undetectable at dawn (LD 0). However, this daily variation was abolished in N-deplete cells after 14 days, suggesting the reduced C stores are not being used for metabolism. Curiously, a higher variation in starch levels was repeatedly observed in cells grown for 7 days in f/2-N and measured at LD 0 indicative of a greater heterogeneity in starch metabolism at that stage. Starch accumulation can also be visualized microscopically using iodine to stain the starch granules (Fig. 2.5B-G). Most of the cells at day 0 did not contain starch at the end of the night (LD 0), but contained substantial amounts at the end of the day (LD 12) (Fig. 2.5B, 2.5C). In addition, higher levels of starch accumulate in N-deplete cultures (Fig. 2.5D-G). Intriguingly, starch granules always accumulated at the posterior end of the cells. This suggests that starch is not localized within chloroplasts, as these organelles are distributed over the entire cell. A cytosolic localization of starch granules has been reported in other dinoflagellates, in contrast to the plastidic localization seen in land plants and green algae [306,307,308].

Neutral lipids, particularly triacylglycerols (TAGs), also accumulate in N-deplete *Lingulodinium* (Fig. 2.6). TAG levels in cell extracts, measured using Nile red, were ~ 2 times and ~ 10 times higher than in cells at day 0 after 7 and 14 days in f/2-N, respectively (Fig. 2.6A). Again, this form of C storage can be visualized in cells microscopically (Fig. 2.6B-J). Abundance and size of lipid bodies clearly increased with the duration of N stress (Fig. 2.6C, 2.6F, 2.6I). However, in sharp contrast to the starch granules, TAGs accumulated preferentially at the anterior end of the cell (Fig. 2.6D, 2.6G, 2.6J).

To confirm the asymmetrical distribution of TAGs and starch granules, cells were examined using transmission electron microscopy to visualize both types of C stores in the same cell (Fig 7). Cells at day 0 and day 14 cells were fixed at LD 0, a time at which neither lipid bodies nor starch were observed in the day 0 cell (Fig. 2.7A). However, the two types of C stores have clearly accumulated at opposite ends of the cell by 14 days in f/2-N medium (Fig. 2.7B). Lipid bodies are located at the anterior end and appear dark due to the lipophilic

nature of the osmium tetroxide stain used to contrast the sections (Fig. 2.7C) while starch granules appear white and are located at the posterior end of the cell (Fig. 2.7D). The white striations observed in the lipid droplets are likely due to a sectioning artifact, as their orientation is the same for all cells in a section independent of how the individual cells are orientated in the section. Lastly, we also note that chloroplasts appear smaller and are less abundant in the day 14 cell when compared to the day 0 cell, in agreement with the confocal images (Fig. 2.4D, 2.4G, 2.4J).

2.5. Discussion

In this study, we show that *Lingulodinium polyedrum* cultures with cell densities similar to those observed in blooming populations in the field (~10^7 cells L^{-1}), are able to survive and maintain these elevated cell densities for more than 2 weeks if previously acclimated to N-deplete conditions (Fig. 2.1) [309]. The cells cease cell division upon transfer to the N-depleted medium, a response to N limitation commonly observed in other dinoflagellates, plants and algae [174,239,242,244,245,310]. The arrest of growth in f/2-N was immediate, not gradual, and suggests that *L. polyedrum* grown in a NO_3^--replete medium does not store N in a form that could have sustained growth and division under N stress. This differs from the N storage observed in *Symbiodinium* spp. where uric acid crystals accumulate following increases in environmental N [161]. The crystalline inclusions rapidly dissolve, but it has been suggested that the resulting N is remobilized for long-term storage in other forms within the cytosol. Either *L. polyedrum* does not share this long-term storage ability with *Symbiodinium* or its storage capacity is insufficient to support cell division under N limitation. Another possibility is that sensors at the *Lingulodinium* plasma membrane, similar to the CHL1 nitrate transporter in *Arabidopsis*, detected an absence of extracellular NO_3^- and signaled a stress response, which included an early arrest of the cell cycle [126].

C and N metabolism are normally coupled because synthesis of amino acids and nucleotides is dependent upon C skeletons and energy provided by photosynthesis [310]. During N depletion, *L. polyedrum* was restricted in its ability to assimilate N, while its photosynthetic machinery was, for at least a week, still fully functional. This is indicated by the ^{14}C fixation rates, which only showed a significant decrease after 14 days of N deprivation (Fig. 2.4B). We propose that during their first week of N-limitation, the cells divert their excess C toward the synthesis of starch and neutral lipids (Fig. 2.5, 2.6). Because neither of these storage compounds contain N, this would result in the decrease in the proportion of N in these N-limited cells that we have observed (Fig. 2.2A). Furthermore, as the proportion of C in sugar and TAG is roughly 40% C and 75% C, respectively, it seems reasonable that a mixture of both could provide a means of increasing the mass of the cell through new C fixation while at the same time maintaining a constant proportion of C. However, the situation after 14 days in N-limited condition differs. Importantly, the rates of C fixation have decreased markedly

(Fig. 2.4B), in agreement with the small increase in starch observed (Fig. 2.5A). Despite this, we observe a pronounced increase in TAG (Fig. 2.6A). We suggest that the accumulation of TAG may result from a recycling of the membranes associated with the chloroplast, whose size and numbers have both decreased in 14 days N-limited-cells (Fig. 2.4J). Therefore, the acclimation of cells to N-limited conditions appears to show a biphasic metabolic response, with an initial maintenance of photosynthesis producing primarily starch as accumulated C, and a subsequent recycling of chloroplast membranes resulting in an increased TAG accumulation.

The proportional reduction in elemental N content is mirrored by the decrease in cellular protein (Fig. 2.3A) since protein is the most important pool of cellular N in the cell. In contrast, the total FAA levels remained unchanged (Fig. 2.S1A). Thus, since the mass of the cells increases as a result of ongoing photosynthesis, this implies that the absolute amount of FAA in the culture increases during N limitation in order to maintain the same levels relative to the cell mass. One possibility is that the extra FAA result from protein degradation. However, it seems unlikely that degradation of proteins would change the relative abundance of the FAA pools, suggesting that some of the variations may reflect other causes. For example, the lack of available N for ammonium synthesis seems the likely explanation for the decrease observed in Gln and Arg levels (Fig. 2.3B). In addition, the levels of some FAA, in particular those derived from pyruvate (such as Leu and Ile) or phospho*enol*pyruvate (such as Tyr or Phe) might be augmented using excess C skeletons originating from glycolysis (Fig. 2.3B). An increase in the levels of these glycolytic intermediates might in turn result from a decreased activity of the tricarboxylic acid cycle under N limitation where energy requirements are likely to be lower than in actively dividing cells. However, additional studies investigating levels of both glycolytic and TCA cycle intermediates would be required to test these possibilities.

N limitation in *L. polyedrum* causes a gradual decrease in chlorophyll *a*, in agreement to what is observed in other photosynthetic eukaryotes [310,311]. It is unlikely that the dinoflagellate had difficulties in synthesizing new chlorophyll molecules in N-deplete conditions, since glutamate, the precursor for the porphyrin moiety in chlorophyll, remained stable under N stress (Fig. 2.3B). However, many different N-limited algal cells are shown to be more susceptible to photoinhibition in normal light conditions than N-replete cells [312]. In

fact, levels of the D1 protein are markedly lower when the cells are N-limited than when N-replete. D1 is a component of the photosynthetic reaction center in PSII and is proposed to be the site of photodamage. It has been suggested that photoinhibition occurred at lower irradiance in N-limited cells, because the lower rates of protein synthesis are unable to keep pace with degradation of damaged D1 [312]. In our study, it is likely that *L. polyedrum* diminishes its chlorophyll content during N depletion to prevent photooxidative damage, because a similar susceptibility to photoinhibition has been previously reported for this species [313].

The reduction in chlorophyll levels, and the resulting protection against oxidative stress, thus appears distinct from the reduction in the size and number of the chloroplasts observed by 14 days in N limiting conditions (Fig. 2.4J). The decrease in chloroplast number and size during N stress is suggestive of autophagy, the process by which an organism degrades its own cellular components in order to recycle nutrients or eliminate damaged material. Interestingly, autophagy is important for the survival of *Arabidopsis* and *Chlamydomonas* in conditions of N limitation [314,315]. In the latter organism, N stress causes the polar lipids of plastid membranes to be recycled for the production of TAGs [316,317]. We propose that initially, neutral lipids could be produced *de novo*, fueled by C fixation, while at latter stages during N-limitation, TAG accumulation reflects autophagy of chloroplast membranes.

Interestingly, a recycling of plastid membranes might also explain the polarized distribution of lipid bodies in *L. polyedrum*. This species typically contains a single PAS (Periodic acid-Schiff) body, thought to be a dinoflagellate lysosome, in the posterior end of the cell where the lipid droplets are rare [318]. Thus, if the PAS body was involved in neutral lipid degradation, this might favor an anterior location for the accumulation of lipid droplets. TEM observations show small lipid bodies surrounding the cell center in addition to the larger droplets that accumulate predominantly at the anterior end (Fig. 2.7B). It is possible that the smaller droplets are associated with lipid bodies that have recently budded off from the ER membranes, centrally localized in this dinoflagellate [319]. This would agree with the ER membranes being the site for the last reactions of TAG biosynthesis. The restricted cellular location of the large lipid droplets could result from the fusion of smaller lipid bodies that would, because of the PAS body, strictly accumulate at the anterior end of the cell. Another

intriguing possibility could be that enzymes for TAG biosynthesis are polarized within the cell. Independent of the mechanism for localizing the lipid body, however, their location may be functionally important, as lipids were shown to contribute to cell buoyancy in various planktonic species [320,321]. For example, an accumulation of lipid droplets at the anterior pole at the beginning of the day could help *L. polyedrum* migration to the water surface.

Starch accumulation is a common response to N limitation, both in plants and green algae, as well as in *L. polyedrum*. However, it is unlikely that these different organisms share a common regulatory pathway, because they synthesize starch in different cellular compartments. In the plastids of plants and green algae, glucose-1-phosphate is activated to ADP-glucose using an ADP-glucose pyrophosphorylase before being transferred by starch synthase to a terminal glucose residue for elongation of a glucan chain [322]. The ADP-glucose pyrophosphorylase is inhibited by inorganic phosphate and activated by the Calvin cycle intermediate, 3-phosphoglycerate [322]. Cytosolic P_i is produced by sucrose synthesis and is exchanged with chloroplastic triose-phosphate by the triose phosphate-phosphate translocator [322]. In contrast, if starch is synthesized in the cytosol of dinoflagellates, then no exchange of metabolites across the plastid membranes is required. Furthermore, multiple soluble starch synthases and one granule-bound starch synthase of the heterotrophic dinoflagellate *Crypthecodinium cohnii,* display a marked substrate preference for UDP-glucose rather than ADP-glucose [308]. A similar preference is observed in all organisms storing starch in the cytosol, such as the rhodophytes, glaucophytes and cryptophytes [323,324,325]. Thus, starch synthesis in dinoflagellates might proceed through a cytosolic UDP-glucose pyrophosphorylase, but characterization of this enzyme and its regulators will be required to validate this suggestion.

Localization of the enzymes involved in *L. polyedrum* starch biosynthesis is of particular interest, considering the observation that starch granule accumulation is polarized in these cells (Fig. 2.5B-G, Fig. 2.7B). The asymmetrical distribution is not simply a result of N limitation, because N-replete cells at LD12 accumulate granules at the same position as in N-limited cells. It also seems unlikely that starch could be transported to the posterior end by motor-proteins traveling on cytoskeletal filaments, because we were unable to detect any membrane surrounding the granules (Fig. 2.7D), in agreement with a previous TEM study of this species [319]. We suggest that starch synthases and starch branching enzymes might be

tethered to membranes at the posterior end of *L. polyedrum* and these localized enzymes might provide a scaffold for polarized starch synthesis. Protein immunolocalization could assess this hypothesis, particularly now that sequences of starch metabolic enzymes are likely to be found in the complete transcriptome of *L. polyedrum* [63].

The adaptation to N-deplete conditions allow *L. polyedrum* cells that are re-exposed to N to survive at high cell densities for up to a month instead of the few days that N-replete cultures normally tolerate (Fig. 2.1B). Thus, during the period of N depletion, the cells have acquired a capacity to resist N stress that N-replete cells do not have. Interestingly, conditions of N stress are more likely to be encountered by this species in the field than continuous exposure to high N such as is the case for usual laboratory culture conditions. This increased endurance could help blooming populations survive and maintain their density for long periods of N stress in the environment. Further studies will be required to determine which molecular adaptations accompany this physiological adaptation.

Figure 2.1. Growth of N-replete and N stressed cultures.

The cell density in 6 independent cultures, 3 supplemented with 880 μM $NaNO_3$ (f/2) and 3 without added N (f/2-N), was assessed until no swimming cells remained in the culture flasks. The first 14 days are shown on an expanded time scale (A) or over the 100 days of the experiment. The time at which 880 μM $NaNO_3$ was added to all cultures is shown by a black arrow. Results are mean ± SE of 3 technical replicates made on cell counts.

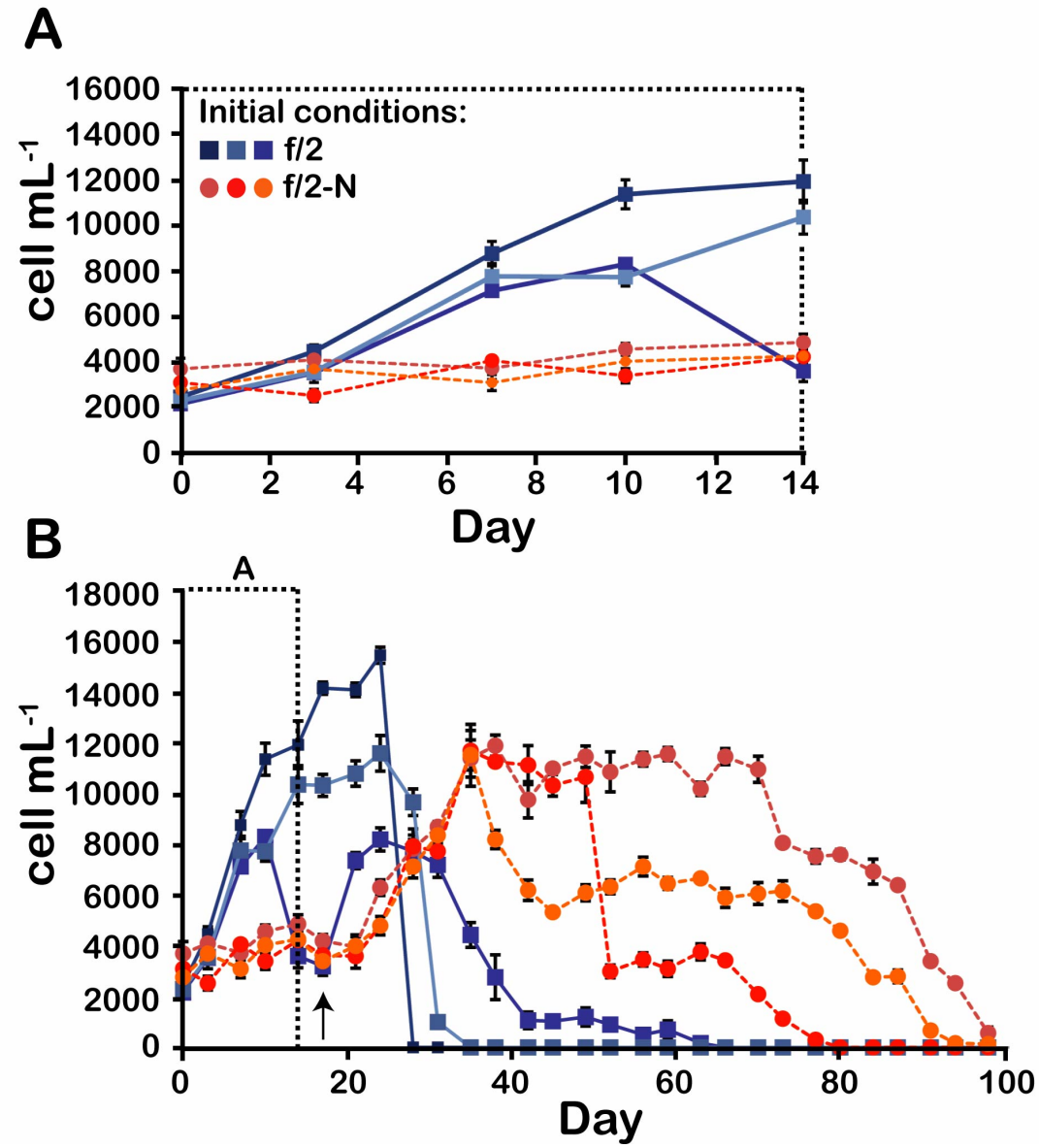
A
Initial conditions:
f/2
f/2-N
cell mL-1
Day
B
A
cell mL-1
Day

Figure 2.2. Elemental analysis shows a decreased N content in N stressed cells without a change in their C content.

(A) Dry weight percent of total N and B) total C. Results are mean ± SE (n=3). Statistically different results ($p < 0.05$) are marked with a different letter (Analysis of variance). DW; Dry weight

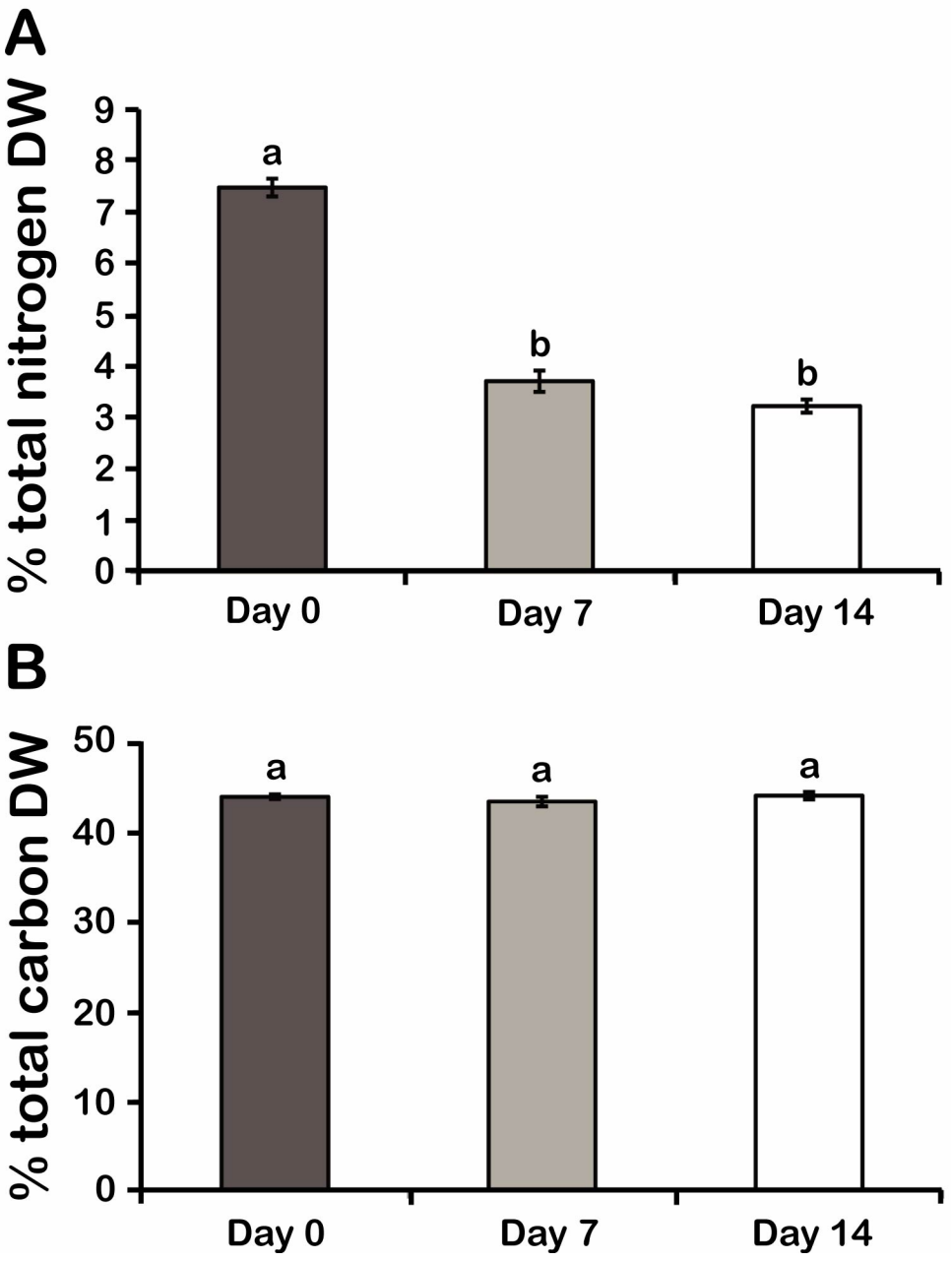
A
% total nitrogen DW
9
8
7
6
5
4
3
2
1
0
a
b
b
Day 0
Day 7
Day 14
B
% total carbon DW
50
40
30
20
10
0
a
a
a
Day 0
Day 7
Day 14

Figure 2.3. Changes in the total protein content and free amino acid profile in N stressed cells are consistent with a decrease in N assimilation.

A) Total protein content. B) Free amino acids, classified into three groups based on their relative abundance. Results are mean ± SE (n=3). Statistically different results ($p < 0.05$) are marked using either a different letter (Analysis of variance) or an asterisk (Student's t-test). FW; Fresh weight

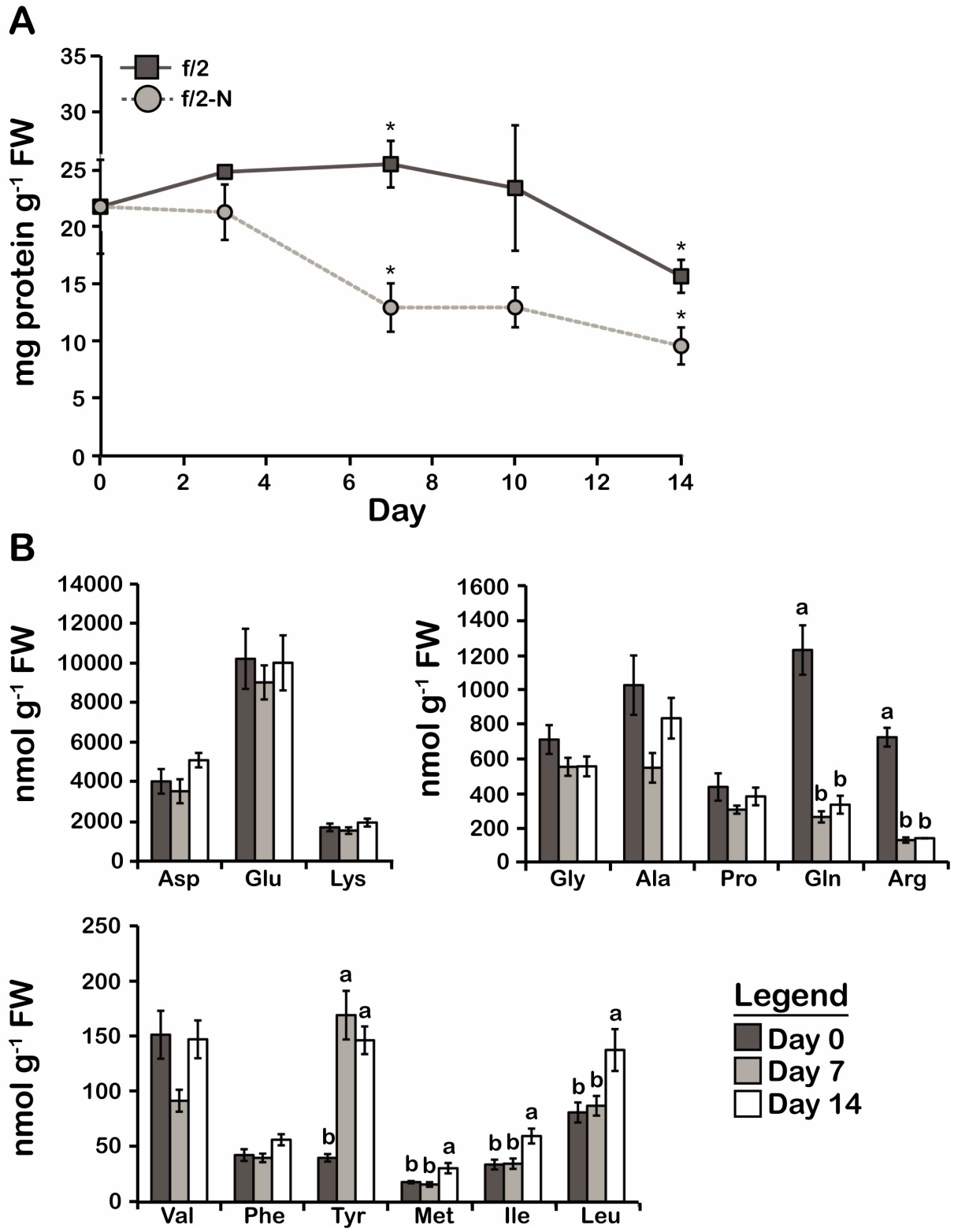
A
f/2
f/2-N
mg protein g-1 FW
Day
B
nmol g-1 FW
Asp
Glu
Lys
Gly
Ala
Pro
Gln
Arg
Val
Phe
Tyr
Met
Ile
Leu
Legend
Day 0
Day 7
Day 14

Figure 2.4. Photosynthesis decreases in N stressed cells.

A) Chlorophyll *a* levels. FW; Fresh weight. B) Photosynthetic rates of ^{14}C fixation. Results are mean ± SE (n=3). Statistically different results ($p < 0.05$) are marked with a different letter (Analysis of variance). (C-K) DIC, chlorophyll autofluorescence and merged images of day phase cells at day 0 (C-E), day 7 (F-H) and day 14 (I-K). Chlorophyll intensity is highest in the periphery of day phase cells cells (white arrows) due to a separation of RuBisCO and the light harvesting peridinin-chlorophyll *a*-protein within individual chloroplasts [29]. All cells were pictured from a ventral view. In this orientation, two ends of the C-shaped nucleus (n) surround the centrally located ER and Golgi membranes (m). Scale bars are 10 μm.

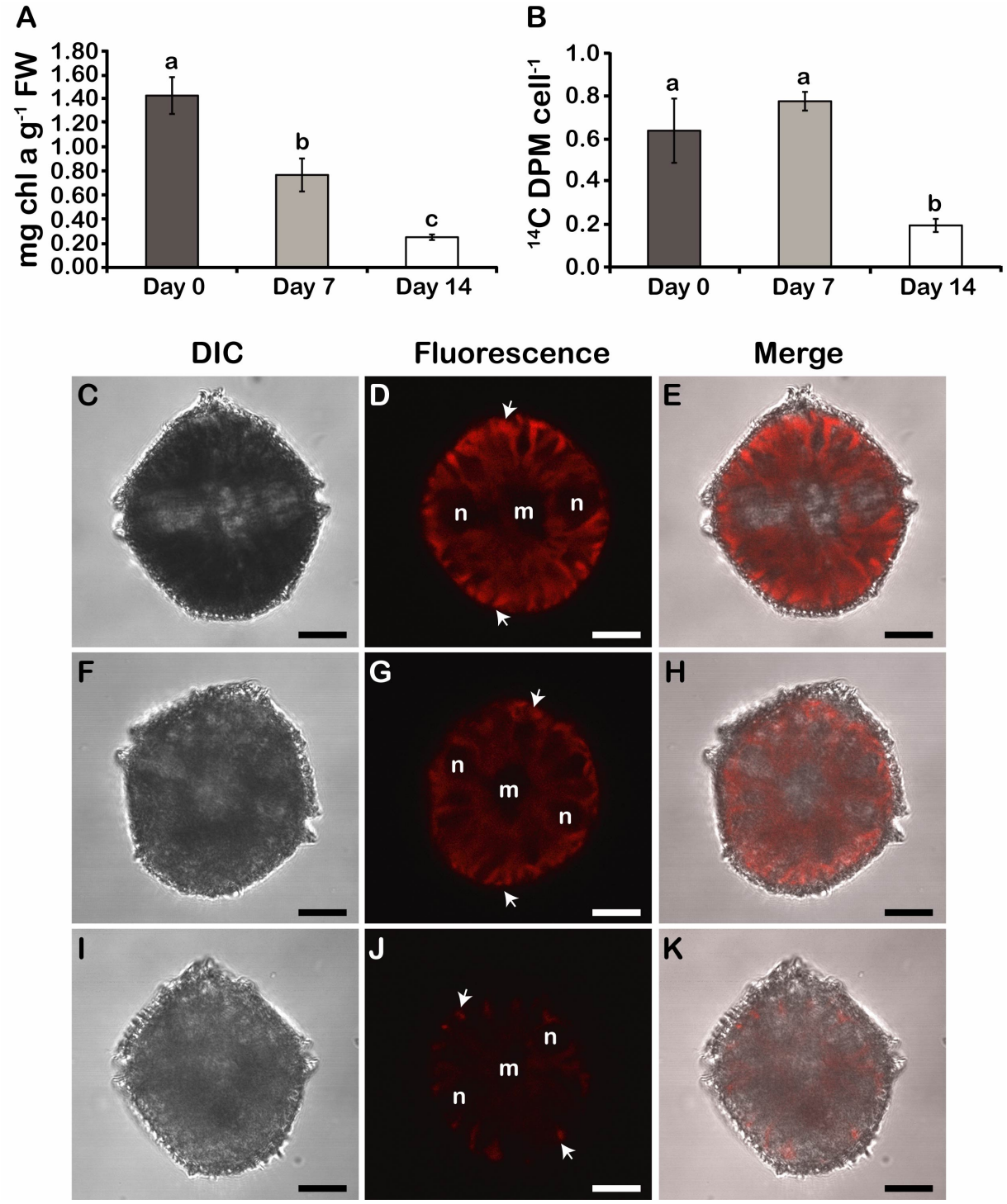
A
mg chl a g-1 FW
1.80
1.60
1.40
1.20
1.00
0.80
0.60
0.40
0.20
0.00
a
b
c
Day 0
Day 7
Day 14
B
14C DPM cell-1
1.0
0.8
0.6
0.4
0.2
0.0
a
a
b
Day 0
Day 7
Day 14
DIC
Fluorescence
Merge
C
D
E
F
G
H
I
J
K
n
m
n

Figure 2.5. Starch accumulates in N stressed cells.

A) Starch levels in cells harvested at LD 0 and LD 12. Results are mean ± SE (n=3). Statistically different results ($p < 0.05$) are marked using either a different letter (Analysis of variance) or an asterisk (Student's t-test). FW; Fresh weight. Bright-field microscopy of iodine-stained starch granules at day 0 (B-C), day 7 (D-E) and day 14-cells (F-G) at either LD 0 (B, D, F) or LD 12 (C, E, G). Starch is localized at the posterior part of the cells.

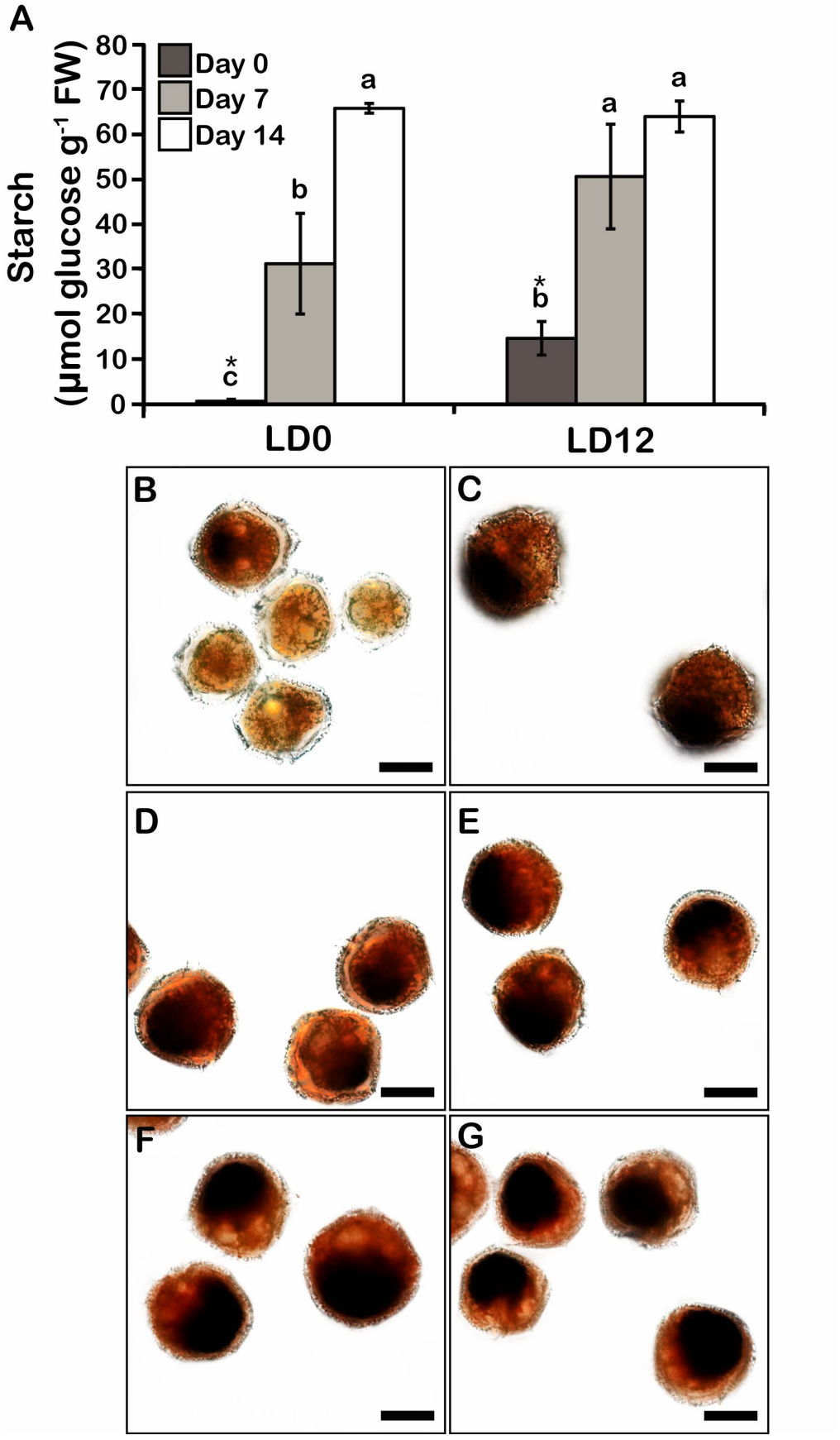
A
Starch
(µmol glucose g-1 FW)
80
70
60
50
40
30
20
10
0
Day 0
Day 7
Day 14
a
b
*
c
a
a
*
b
LD0
LD12
B
C
D
E
F
G

Figure 2.6. TAGs accumulate in N stressed cells.

A) Neutral lipid levels. Results are mean ± SE (n=3). Statistically different results ($p < 0.05$) are marked with a different letter (Analysis of variance). FW; Fresh weight. DIC, Nile red-stained lipid bodies and merged images of day 0 (B-D), day 7 (E-G) and day 14 cells (H-J). All cells were pictured from a ventral view. Lipid bodies were most predominant in the anterior part of the cells.

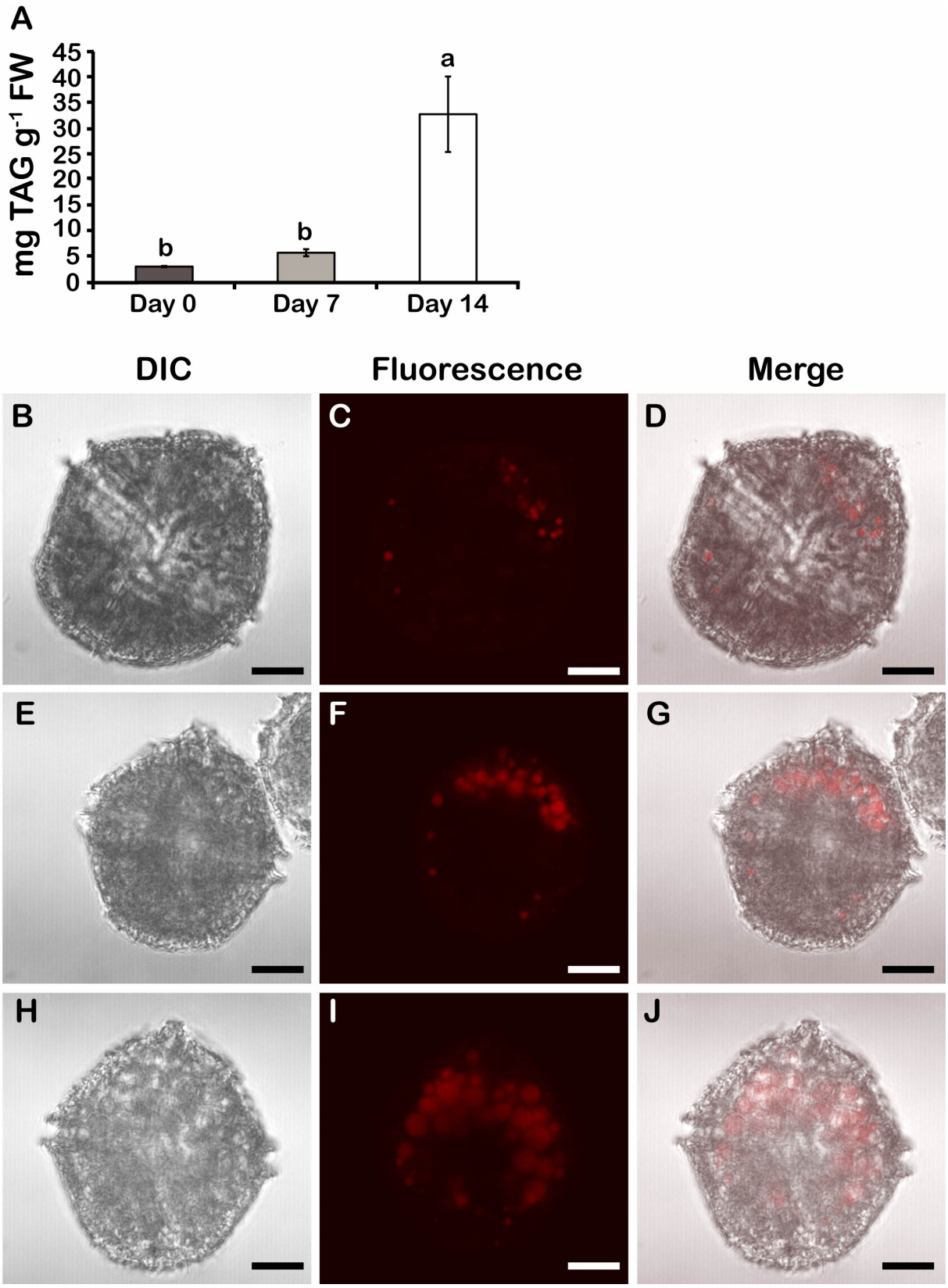
A
mg TAG g-1 FW
45
40
35
30
25
20
15
10
5
0
b
b
a
Day 0
Day 7
Day 14
DIC
Fluorescence
Merge
B
C
D
E
F
G
H
I
J

Figure 2.7. Polarized localization of lipid bodies and starch granules visualized by transmission electron microscopy.

Cross-sections of a cell at day 0 (A) and at day 14 in f/2-N medium (B). Both are in a ventral orientation and scale bars are 10 μm. Lipid bodies (l) are located predominantly at the anterior (a) end of the cell, while starch granules (s) are localized at the posterior (p) end. The ends of the C-shaped nucleus (n) surround a central Golgi/ER membrane region (m). Chloroplasts (c) are less abundant in day 14 cells. Higher magnification images of lipid bodies (C) and starch granules (D) in a cell at day 14. Scale bars are 1 μm.

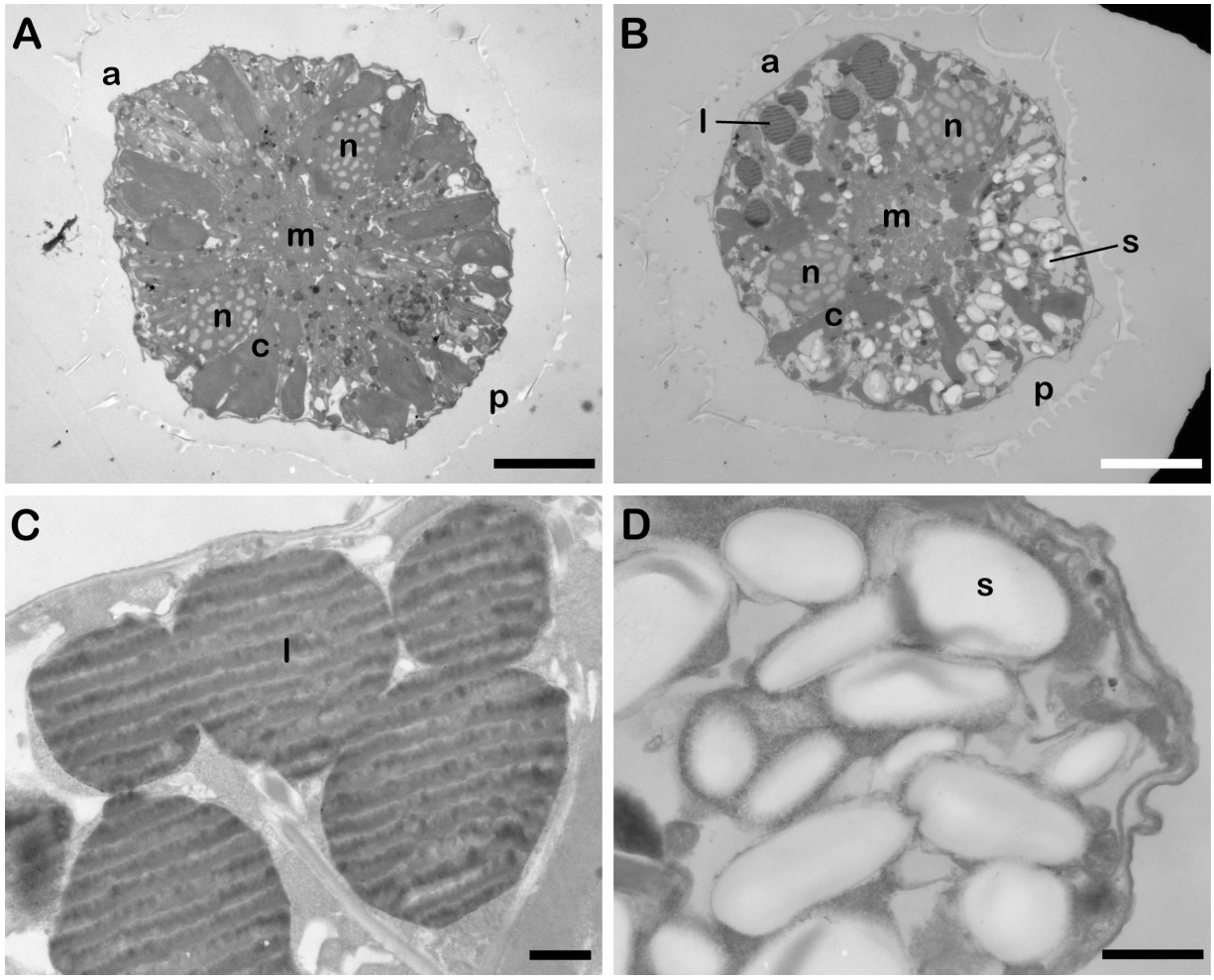
A
a
n
m
n
c
p
B
a
l
n
m
s
n
c
p
C
l
D
s

Supplementary Figure legend
Figure 2.S1.

A) Sum of all free amino acids. B) Sum of N in amino acids. C) Gln/Glu ratio. The amino acid data were compiled from Fig. 2.3B.

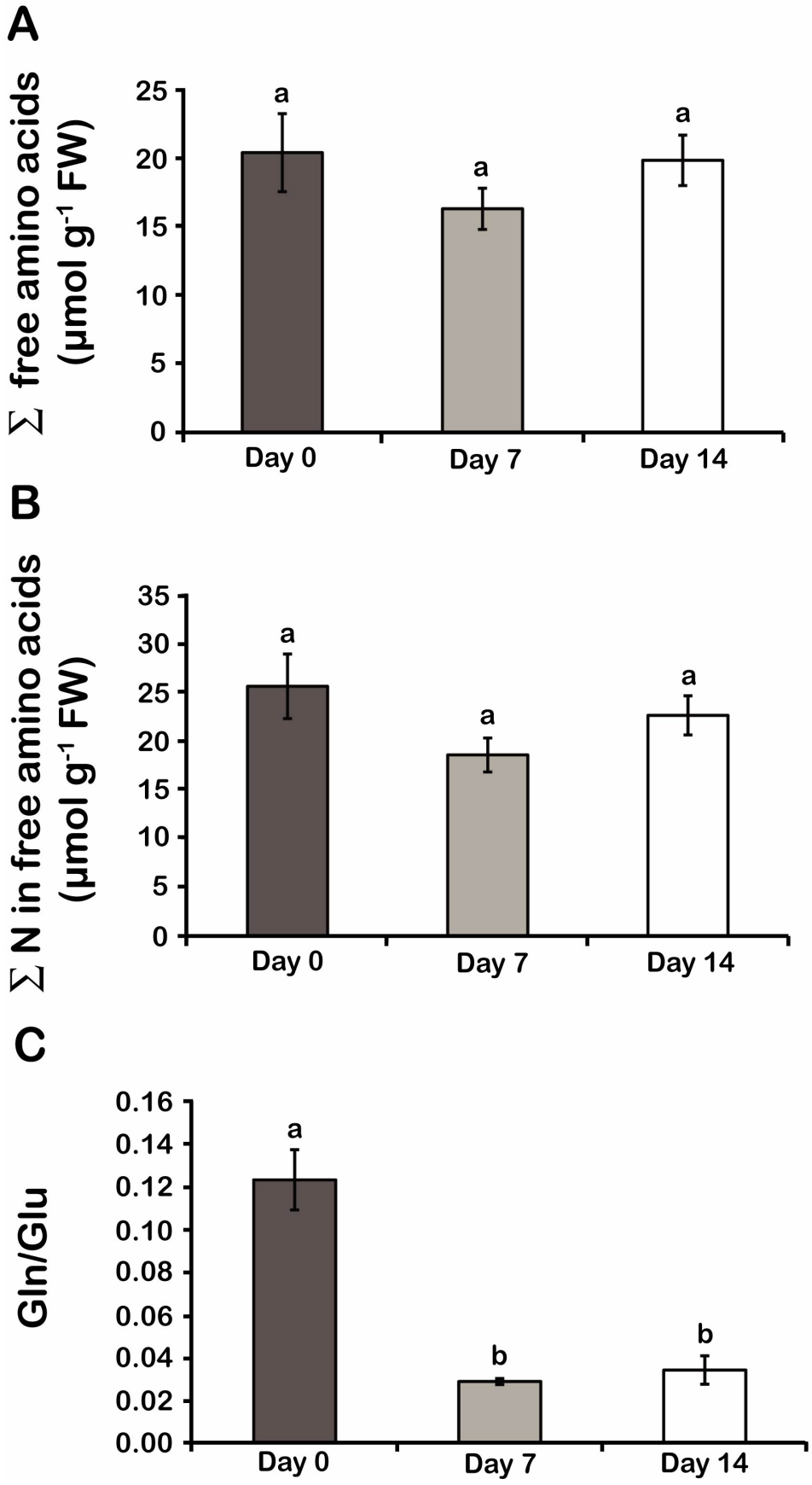
A
∑ free amino acids (µmol g-1 FW)
25
20
15
10
5
0
a
a
a
Day 0
Day 7
Day 14
B
∑ N in free amino acids (µmol g-1 FW)
35
30
25
20
15
10
5
0
a
a
a
Day 0
Day 7
Day 14
C
Gln/Glu
0.16
0.14
0.12
0.10
0.08
0.06
0.04
0.02
0.00
a
b
b
Day 0
Day 7
Day 14

2.6. Acknowledgments

We thank L. Pelletier for technical assistance. We also gratefully acknowledge the financial support of the Natural Sciences and Engineering Research Council of Canada (NSERC) for discovery grants to DM and JR and of the Fond de Recherche du Québec-Nature et Technologies (FQRNT) for a studentship (SDB).

Chapter 3- Publication # 3

The main nitrate transporter of the dinoflagellate *Lingulodinium polyedrum* is constitutively expressed and not responsible for daily variations in nitrate uptake rates

Steve Dagenais Bellefeuille and David Morse

This article was submitted to Harmful Algae, reference: HARALG_2015_94

Author contributions:

S. Dagenais Bellefeuille and D. Morse designed the project. S. Dagenais Bellefeuille performed all experiments and data was analyzed by S. Dagenais Bellefeuille and D. Morse. The first version of the manuscript was written by S. Dagenais Bellefeuille and the text was revised and corrected by D. Morse.

In this section of my thesis, I aimed at identifying and characterizing nitrate transporters in *Lingulodinium* to better understand the molecular mechanisms of nitrate uptake in dinoflagellates. I was particularly interested in nitrate transporters, because nitrate uptake was suggested to be under circadian control in *Lingulodinium*, but this idea had not been tested experimentally.

3.1. Abstract

Dinoflagellates are unicellular eukaryotes capable of forming spectacular harmful algal blooms (HABs). Eutrophication of coastal waters by fertilizer runoff, nitrate in particular, has contributed to recent increases in the frequency, magnitude and geographic extent of HABs. However, while physiological nitrate uptake and assimilation in dinoflagellates have often been measured in the field and in the laboratory, no molecular components involved in nitrate transport have yet been reported. We report here the first identification and characterization of dinoflagellate nitrate transporters, found in the transcriptome of the bloom-forming *Lingulodinium polyedrum*. Of the 23 putative transporters found by BLAST searches, only members of the nitrate transporter 2 (NRT2) family contained all key amino acids known to be essential for nitrate transport. The dinoflagellate NRT2 sequences have 12 predicted transmembrane domains, as do the NRT2 sequences of bacteria, plants and fungi. NRT2 in *Lingulodinium* also appear to have two different evolutionary origins, as determined by phylogenetic analyses. LpNRT2.1 was the most expressed transcript of all putative nitrate transporters as determined by RNA-Seq. An antibody raised against LpNRT2.1 showed that the same amount of protein was found at different times over the light dark cycle and with different sources of N. Finally, global nitrate uptake was measured using a ^{15}N tracer, which showed that the process was not under circadian-control, as previously suggested in *Lingulodinium*, but simply light-regulated. Protein expression profiles of LpNRT2.1 are discussed in relation to the obtained nitrate uptake curves.

Key Words: *Lingulodinium polyedrum*, nitrate transporters, NRT2, nitrate uptake, diurnal rhythm, circadian clock

3.2. Introduction

Dinoflagellates are unicellular eukaryotes found in most marine and freshwater ecosystems. While members of this group contains important primary producers and, in the case of the genus *Symbiodinium*, are essential for the survival of tropical reef corals [82], dinoflagellates are also infamous because some species can form harmful algal blooms (HABs). HABs can cause illness or death to aquatic wildlife, damaging ecosystems and negatively impacting tourism and fish industries. Public health is also threatened by toxic blooms, because human consumption of toxin-contaminated seafood can result in intoxication or even death in extreme cases. Some HAB species, such as *Karenia brevis* in the Gulf of Mexico, secrete neurotoxins that have an airborne component and can mix with marine aerosols [326]. When driven by winds, people onshore inhaling the toxic sea spray can suffer severe respiratory irritations. Thus, it is a growing concern that HAB events have globally increased in frequency, magnitude and geographic extent over the last 40 years [105]. It also justifies the heightened attention scientific and governmental authorities are giving to research on bloom dynamics and the causes leading to HAB expansions [105].

While bloom formation and its persistence involve a complex interplay of biotic and abiotic factors [105], increases in nutrients, particularly phosphorus (P) and nitrogen (N), has often been positively correlated with HABs in various coastal regions of the world [86,87,88]. A recent example is the Changjiang River in China where agricultural runoffs have contributed to a dramatic ~ 400% increase in nitrate concentration between 1960s and 2004, while phosphate concentration increased by ~ 30% between 1980s and 2004 [89]. As a result, in a 20 year-period there was a ~ 4-fold augmentation in phytoplankton standing stocks. Also during the same period, the initially diatom-dominated communities started to shift toward dinoflagellates, which is consistent with the observation that diatoms are poor competitors to flagellates when the N: P ratio is high [92]. The most striking consequence of the Changjiang eutrophication was the difference in number of reported HABs in the adjacent coastal waters of the East China Sea, that passed from 2 events before 1980s to ~ 30-80 HABs per year between 2001 and 2005 [89]. Because these recent HABs are mainly caused by photosynthetic dinoflagellates [89], these organisms must have very efficient ways in utilizing nitrate for rapid proliferation.

Since nitrate is the most abundant form of bioavailable N in most aerobic soils and marine environments [111,327], its uptake is expected to control the majority of N that can be assimilated for most organisms. This explains the intensive effort over the past several decades to isolate and characterize the genes responsible for nitrate transport in many phylogenetic groups, including bacteria [328], fungi [329,330], and green plants [331,332]. The alveolates, among which are found the dinoflagellates, are a noteworthy exception. The rationale for the molecular characterizations is that nutrient uptake results from the combined action of multiple transporters each with particular enzymatic kinetics, regulation patterns and crosstalk, and that once transporter properties are defined, an overall system can be developed to help in the predictions of an organism's behaviour under fluctuating nutrient conditions. Thus, characterization of dinoflagellate nitrate transporters could complement physiological and field studies in understanding how N uptake influences HABs.

Four gene families have been shown to possess nitrate transport activity in eukaryotes: the nitrate transporter 1/ peptide transporter (NPF) (previously NRT1/PTR), the nitrate transporter 2 (NRT2) of the major facilitator superfamily (MFS), the chloride channels (CLCs) and the slow anion channel-associated 1 homologues (SLAC1/SLAH) [331]. Although not working as a transporter alone, nitrate assimilation related (NAR2) is a small protein that directly interacts with several NRT2 [333,334]. NAR2 stimulates nitrate uptake of all seven *Arabidopsis* NRT2 [333], and interaction is mandatory for NRT2.1 of the green alga *Chlamydomonas reinhardtii* where nitrate-elicited current are only detected when both proteins are co-expressed in *Xenopus* oocytes [335]. However, another well characterized NRT2, NrtA (previously CrnA) from the fungus *Aspergillus nidulans*, functions without NAR2 [336]. Members of the NPF and NRT2 families can be found in all kingdoms of life [337], except for animals that lack NRT2 proteins [338]. CLCs are also ubiquitous in nature [339], but nitrate transport has only been demonstrated in two members, both in *Arabidopsis* [132,340]. AtCLC-a was shown to be a nitrate/proton antiporter involved in the accumulation of nitrate into the plant tonoplast [132], while AtCLC-b showed a similar activity after heterologous expression in *Xenopus* oocytes [340]. AtSLAC1 and AtSLAH3 proteins also displayed nitrate transport activity when expressed in oocytes [341,342], but they are the only members of the SLAC1/SLAH family that were shown to possess this function. These

observations suggest that dinoflagellate nitrate transporters are more likely to belong to the NPF and NRT2 families than to the CLCs or SLAC1/SLAH.

Lingulodinium polyedrum is a non-toxic marine dinoflagellate reported to form HABs along the Southern California coast [148,258]. Success of this organism during the upwelling season was attributed in part to its ability to migrate into nitrate-rich subsurface waters at night and assimilate nitrate in the dark [147]. However, nitrate uptake was also found to have a strong diel rhythmicity, with the peak observed in the middle of the day [147]. Furthermore, a circadian peak in nitrate reductase (NR) activity was also found during the day [223]. It has been suggested that nitrate uptake could be controlled by an endogenous clock in *Lingulodinium* [224], but experimental data supporting this hypothesis has not yet been reported. Thus, the first aim of this study was to test for circadian nitrate uptake for *Lingulodinium* grown in constant light. The second aim was to identify putative dinoflagellate nitrate transporters from a recently published *Lingulodinium* transcriptome database [63], and to characterize the most promising candidates. The final aim was to test the hypothesis that changes in nitrate uptake rates resulted from changes in transporter levels.

3.3. Material and methods

3.3.1. Cell culture

3.3.1.1. Initial conditions

Unialgal but not axenic *Lingulodinium polyedrum* (CCMP 1936, previously *Gonyaulax polyedra*) was obtained from the Provasoli-Guillard National Center for Marine Algae and Microbiota (East Boothbay, ME, USA). For all experiments, cell cultures were initially grown in normal f/2 medium prepared using Instant Ocean under 12 h light (40 µmol photons m^{-2} s^{-1} cool white fluorescent light) and 12 h darkness at a temperature of 18 ± 1 °C. Cells were harvested by filtration on Whatman 541 paper and stored at -80 ºC until use.

3.3.1.2. Daily and circadian nitrate uptake measurements

Nitrate uptake was monitored using a stable isotope analysis. Culture aliquots were spiked with ^{15}N-labeled $NaNO_3^-$ ($Na^{15}NO_3^-$) at different times during a light dark cycle (ZT; Zeitgeber times) or during constant light (CT; Circadian times) for 1 h durations. In the first experiment (ZT), cultures were grown under a 12:12 light/dark regime, with ZT0 corresponding to lights on and ZT12 to lights off. In the second experiment (CT), cultures were grown in continuous light for two days, with $Na^{15}NO_3^-$ incubations and cell harvests made on the second day. For both experiments, cell cultures were filtered on Whatman 541 filters and transferred to an f/2 medium supplemented with half the amount of $NaNO_3^-$ normally included in this medium (normal concentration = 880 µM). These ~ 1.5 L cultures were divided into multiple 150 ml aliquots and incubated under light dark or constant light conditions. $Na^{15}NO_3^-$ was added to the cultures to a final concentration of 440 µM at different times and cells were harvested 1 h later. Data are reported as $\delta\ ^{15}N$, which represent the ^{15}N: ^{14}N ratio found within the cells after one hour of ^{15}N accumulation.

3.3.1.3. Expression of LpNRT2.1 protein

Different cell cultures were either grown in normal f/2 medium supplemented with 880 µM $NaNO_3$ (f/2+NO_3^-), in f/2 with 10 µM $NaNO_2$ (f/2+NO_2^-), in f/2 with 40 µM NH_4Cl (f/2+NH4) or in f/2 lacking added N (f/2-N). To alter the source of N in the cultures, normal

f/2 cultures were filtered on Whatman 541 paper, washed with 200 ml of f/2-N medium and resuspended in f/2-N. After resuspension, the 1.5 L flasks were divided into multiple 200 ml aliquots and $NaNO_3$, $NaNO_2$ and NH_4Cl was added to the final concentrations listed above. All cultures were harvested after 2 h or 24 h hour of growth in their respective medium.

3.3.2. Stable isotope analysis

Measurement of $\delta\ ^{15}N$ was performed using a continuous flow Isoprime 100 TM coupled to a Vario Micro CubeTM elemental analyzer (at Geotop-UQAM, Montreal, PQ, Canada). The analytical step was preceded by a preparative step, where harvested cells were lyophilized, weighed and inserted into tin capsules.

3.3.3. BLAST searches, phylogeny and bioinformatic analyses

Protein sequences encoding putative nitrate transporters in *Lingulodinium* were selected based on their homology to reported nitrate transporters in *Arabidopsis thaliana*: AtNRT2.1; AEE28241, AtNAR2.1; CAC36292, AtNPF6.3 (CHL1); AEE28838, AtCLC-a; AED94612, and AtSLAC1; NP_563909 [331]. TBLASTN analyses were performed against the Transcriptome Shotgun Assembly (TSA) database of *Lingulodinium polyedrum* (taxid: 160621) using default parameters. Hits with e-values $\leq$ -20 were selected and a second BLAST search was made using these hits against the *Lingulodinium* TSA database to eliminate redundant sequences. Presence of complete open reading frames (ORF) for the NRT2 sequences was confirmed by PCR-amplifications of a Rapid Amplification of cDNA Ends (RACE) (Clontech) library, insertion in pUCm-t vectors (Bio Basic), and Sanger sequencing. Stop codons in frame with the longest ORF were found in both the 5'- and 3'-UTRs for all NRT2 sequences.

Phylogenetic analysis was performed using RAxML [343], which is available online at the CIPRES science gateway (Miller et al., 2010). NRT2 sequences were aligned with ClustalW, imported in PHYLIP format into CIPRES and analysed with RAxML-HPC Blackbox using default parameters. The tree was visualized using dendroscope [344]. Major taxonomic groups used for classification are reported in the Tree of Life Web Project (ToL).

Analysis of amino acids essential for NRT2 activity was based on site-directed mutagenesis studies using the NrtA of *Aspergillus nidulans* [345,346,347]. The NrtA sequence

was compared using ClustalW-alignment to all NRT2 sequences from *Lingulodinium* and one sequence for each group of organisms presented in the phylogeny. The nitrate signature (NS) motif has been previously described by [347] and [348].

Transmembrane domains (TM) and topologies were predicted using TMHMM [349], TMPred [350] and TopPred [351,352]. TMHMM version 1 and TMPred were run on default parameters, while TopPred version 1.10 was run with all parameters at default settings except for the organism type, which was set to "eukaryot" instead of "prokaryot" and the wedge window size (-q), which was set to 3 instead of 5.

3.3.4. Relative transcript abundance of Lingulodinium NRT2 sequences

Reads Per Kilobase per Million mapped reads (RPKM) values for putative nitrate transporters were obtained from a recently published transcriptomic study in *Lingulodinium polyedrum* [353]. RPKM data were generated after mapping raw reads from two different RNA-Seq experiments onto a Trinity [354] or Velvet [63] assembly. RPKM data from eight samples were combined for each sequence, because it was shown that there was no difference in expression between each sample [353]. Thus, the eight samples were considered as replicates and were used to compare the relative transcript abundance of the putative nitrate transporters.

3.3.5. Electrophoretic analyses

Samples for 1D electrophoresis were prepared from 10 mg of cells mechanically lysed 2 min in a bead beater (BioSpec products) at 4°C with 10 mM Tris, pH 8.0; 1 mM EDTA and 1 mM PMSF. SDS sample buffer (final concentration: 50 mM Tris-HCl pH 6.8; 2% SDS; 100 mM DTT; 10 % glycerol) was added to the cell lysates and boiled 10 min at 95°C. 10 µL of each sample was electrophoresed on 10% polyacrylamide gels.

Samples for 2D electrophoresis were prepared from 200 mg of cells mechanically lysed 2 min in a bead beater at 4°C with 7M urea and 2M thiourea. 4% CHAPS was added after lysis and cell solutions were desalted on Bio-Rad Econo-Pac® 10DG columns following the manufacturer's instructions. 200 µg of proteins were resuspended in 125 µl of rehydration buffer (7M urea; 2M thiourea; 4% CHAPS; 20 mM DTT; 0.2% Bio-Rad's Bio-Lyte Ampholyte pH 4-7) and applied to 7 cm ReadyStrip ™ IPG isoelectric focusing (IEF) strips

from Bio-Rad. Strips were allowed to rehydrate passively for 14 h before IEF, which was performed at 4000 V for 150 min with Rapid Ramp at 20°C. After IEF, strips were equilibrated 10 min in 2.5 ml of SDS equilibration buffer I (6M urea; 0.375 M Tris-HCl, pH 8.8; 2% SDS; 20% glycerol; 2% DTT), and 10 min in 2.5 ml of SDS equilibration buffer II (6M urea; 0.375 M Tris-HCl, pH 8.8; 2% SDS; 20% glycerol; 2.5% iodoacetamide). Second-dimension electrophoresis was carried on 10% polyacrylamide gels.

For Western analysis, 1D and 2D gels were transferred to nitrocellulose using a wet electroblotting system. The protein blots were blocked with 2.5% powdered milk and 2.5% BSA in Tris-buffered saline containing 0.05% Tween 20. Membranes were incubated overnight at 4°C with either a 1:1000 dilution of mouse anti-NRT2.1 or a 1:10000 dilution of rabbit anti-RuBisCO to control for protein loading [29]. The anti-NRT2.1 is a monoclonal antibody against the epitope GKNDADSPTD produced in mice ascites by Abmart (NJ, USA). This peptide was unique to the NRT2.1 sequence when tested with BLAST against the *Lingulodinium* TSA database. The epitope is in a predicted soluble domain near the N-terminal. Protein bands or spots had a size and pI similar to the theoretical values, 60 kD and 6.4 respectively, calculated for LpNRT2.1 using the Compute pI/Mw tool available on the ExPASy portal [355]. Antibody binding was visualized by using a 1:10000 dilution of commercial peroxidase-linked secondary antibodies against mouse (GenScript) or rabbit (Amersham Pharmacia Biotech) and chemiluminescence (HyGLO, Denville Scientific Inc). An ImageQuant LAS 4000 was used for imagery and pictures were modified for contrast only using Adobe Photoshop 8.0.

3.3.6. Statistical analysis

Results in figure 3.1 (n=3) and figure 3.2 (n=8) are presented as means ± SE. An analysis of variance was used to test for statistical significance using the JMP software (SAS).

3.4. Results

To establish the patterns of nitrate uptake by *Lingulodinium* in light dark and constant light conditions, a stable isotope analysis was performed using a ^{15}N tracer. While *Lingulodinium* was still capable of taking nitrate in the dark, all $\delta\ ^{15}N$ values measured during the day were consistently higher than those measured during the night (Fig. 3.1A). Rates of nitrate uptake were highest at the beginning of the day followed by a gradual decline during the rest of the day (Fig. 3.1A). However, the marked changes in rates observed between the transitions between light and dark phases argued that nitrate uptake was more likely to be light dependent than circadian-regulated. To test this, the ^{15}N experiment was repeated under constant light (Fig. 3.1B). No significant changes in $\delta\ ^{15}N$ could be observed during an entire CT cycle (Fig. 3.1B) indicating the process is light dependent. Interestingly, the total amount of $\delta\ ^{15}N$ taken up during a 24-h period in light dark and constant light conditions is similar (Fig. 3.S1). This may suggest the presence of an intracellular nitrate pool in *Lingulodinium* that allows N metabolism to continue unabated despite poor N uptake in the dark.

We next generated a list of putative nitrate transporters in *Lingulodinium* by searching the transcriptome with reported nitrate transporters in *Arabidopsis thaliana* (Table 1) [331]. In contrast to *Arabidopsis*, where 53 members of the NPF protein family were identified [332], only one NPF sequence was found in *Lingulodinium* and its transcripts were only expressed in cysts [354]. Because all ^{15}N experiments were performed on swimming (nonencysted) cells, it is unlikely that this NPF contributed to the nitrate uptake presented in figure 3.1. *Lingulodinium* has 17 sequences with homology to AtCLC-a, but again it seems unlikely that these are specialized for nitrate uptake, because in 15 of them a proline residue, P^{160}, necessary for nitrate selectivity in AtCLC-a and AtCLC-b [356,357], was replaced by a serine (Fig. 3.S2), a modification also observed in mammalian CLC isoforms [356,357]. Of the 2 remaining sequences, one had a glycine instead of a serine and the other sequence was incomplete and could not be aligned in the region encompassing the selectivity filter. Unsurprisingly, no homologous sequences to the plant guard cell protein SLAC1 were found in *Lingulodinium*. NAR2 sequences were also missing.

Lastly, *Lingulodinium* also expresses 5 sequences encoding putative nitrate transporters of the NRT2 family (Table 1). All of these transcripts were found in ZT and CT, again without

significant variation in either light condition [353] (Fig. 3.2, 3.S3). The mRNA levels of one NRT2, named LpNRT2.1, were much greater than all the other putative nitrate transporters in table 1, when using either a Trinity (Fig. 3.2) or a Velvet (Fig. 3.S3) assembly. Thus, NRT2 sequences, in particular LpNRT2.1, were judged the most likely candidates to be involved in nitrate transport. Two NRT2s, JO716588 and JO704794, were omitted in the following analyses, because their sequences were incomplete in the transcriptome and multiple attempts to amplify their cDNA ends failed.

To assess the evolutionary history of dinoflagellate NRT2, sequences from taxa that rely on this transporter family for nitrate uptake were used for molecular phylogenetic reconstructions (Fig. 3.3). While distant relationships were poorly supported, monophyly of the major ToL taxonomic groups were respected except for the Hacrobia (cryptophytes and haptophytes). Interestingly, *Lingulodinium* LpNRT2.3 and the NRT2 of the haptophyte (Hacrobia) *Emiliania huxleyi* both clustered together with the green plants and not with their respective groups. Thus, there are at least two different origins for the NRT2 family members in *Lingulodinium*.

Aspergillus nidulans NrtA was the first characterized NRT2 [329] and site-directed mutagenesis studies of this transporter have determined a number of residues required for nitrate/nitrite transport [345,346,347]. All these essential NrtA residues were found in *Lingulodinium* NRT2 members and a representative from each of the taxonomic groups used in figure 3.3 (Fig. 3.4). Furthermore, *Lingulodinium* NRT2s also contain the two characteristic nitrate signature (NS) motifs. Lastly, the predicted membrane topology and the placement of the essential residues and conserved motifs (F47 in TM1, R87 in TM2, R368 in TM8, NS1 after TM4 and NS2 close to TM11) within this topology [346], was also conserved for the dinoflagellate sequences (Fig. 3.5). Predictions of membrane topology for the LpNRT2s showed that the $N_{cytosolic}$: $C_{cytosolic}$ organisation, with generally 12 TMs, was also predicted in *Aspergillus*, *Arabidopsis* and other dinoflagellates (Fig. 3.5). These predictions were in agreement with previous reported models of membrane topologies for NRT2 in fungi, plants and bacteria [345,348,358]. Taken together, these results thus support the identification of *Lingulodinium* NRT2s as *bona fide* NRT2 involved in nitrate/nitrite transport.

Because the transcript abundance of LpNRT2.1 suggested it may be the most highly expressed member of the NRT2 family, a monoclonal antibody was prepared to assess

expression of the protein under different conditions (Fig. 3.6). Protein expression was first measured at regular intervals during a light dark cycle, which showed no difference at any ZT (Fig. 3.6A). Thus, changes in protein abundance of LpNRT2.1 cannot account for the difference in nitrate uptake observed between day and night in ZT (Fig. 3.1A). The possibility that post-translational modifications (PTM) such as phosphorylation could modify LpNRT2.1 and change its activity between day and night was next tested using two-dimensional gel electrophoresis (Fig. 3.6B). While multiple isoforms were detected, similar to many other dinoflagellate proteins, no difference in the number, intensity or the position of these spots was observed between ZT6 and ZT18 (Fig. 3.6B). Thus, it seems unlikely that PTM of LpNRT2.1 or/and a particular isoform of the transporter were responsible for the variation in nitrate uptake rates observed in figure 3.1A.

In addition to being important nutrients, nitrate, nitrite and ammonium have been shown to serve as signalling molecules capable of regulating expression of multiple nitrate transporters and nitrate assimilation enzymes [331,359,360]. Thus, the nutrients themselves are used as signals to control their own uptake and assimilation by the cells. Responses to these nutrients were reported to be extremely rapid (within minutes) in certain cases, and for many proteins, the changes were also transient [331,359]. For these reasons, the amount of LpNRT2.1 in *Lingulodinium* cells was assayed over a short (2 h) or a longer (24 h) duration in cultures exposed to different sources of N. No variation in protein abundance was detected under any treatments, including N deprivation, at either time (Fig. 3.6C). Taken together, these results indicated that LpNRT2.1 was the main component of a constitutive nitrate uptake system.

3.5. Discussion

This study has measured nitrate uptake rates and identified potential nitrate transporters in *Lingulodinium polyedrum*. Of the 5 classes of putative nitrate transporters found in the *Lingulodinium* transcriptome (Table 1), only proteins of the NRT2 family appear likely to be genuinely involved in nitrate transport (Fig. 3.4, 3.5, 3.S2). We have found five NRT2 sequences in the *Lingulodinium* transcriptome, a number similar to the 6 NRT2s reported in the genome of *Chlamydomonas* [131] and the 7 NRT2s in *Arabidopsis* [331]. *Lingulodinium* did not contain any NAR2 sequences, in contrast to plants and green algae (Table 1). It is possible that the NRT2/NAR2 interaction is a particularity of the green lineage, and thus, as is the case with *Aspergillus* NrtA [336], the NRT2s in *Lingulodinium* may function alone. However, it is also possible that a *Lingulodinium* NAR2 was not detected by BLAST searches because of low sequence homology. For example, NAR2 in the green algae *Chlamydomonas* shares only 28% identities and 56% coverage (e-value of 0.17) with its homolog in the higher plant *Arabidopsis* NAR2.1. *Lingulodinium* did contain a single NPF family member, although this was expressed only in cyst and not in motile dinoflagellate cells (Fig. 3.2). This is a major difference to the abundant and widely distributed NPF sequences found in plants [337]. However, the green algae *C. reinhardtii* and *Ostreococcus tauri* have only a single uncharacterized NPF each [131,361], so expansion of the NPF family may be specific to higher plants.

In general, the NRT2 phylogeny supported the monophyly of the major taxonomic groups (Fig. 3.3), and is consistent with another NRT2 phylogeny, which, although more exhaustive, did not contain sequences from the Hacrobia and Alveolates [338]. Interestingly, the NRT2.3 of *Lingulodinium* clustered with the green plants instead of with the other dinoflagellate NRT2 sequences (Fig. 3.3). This difference is also reflected in the structure, as unlike the other dinoflagellate NRT2s, LpNRT2.3 lacked the long extension between TM1 and TM2, and was thus structurally more similar to *Arabidopsis* NRT2.5 (Fig. 3.5). Lastly, the expression level of LpNRT2.3 was ~10-fold and ~100-fold less than LpNRT2.2 and LpNRT2.1, respectively (Fig. 3.2). We suggest LpNRT2.3 may have been acquired by horizontal gene transfer.

Comparison of *Lingulodinium* NRT2s with *Aspergillus* NrtA confirmed that the dinoflagellate transporters analysed contained all amino acid residues known to be essential for nitrate/nitrite transport (Fig. 3.4). Functionally, Arg^{87} and Arg^{368} were shown to be the substrate-binding sites in NrtA [347], and 3D modelling of this transporter predicted that Asn^{459} and Asn^{168} would also be involved in nitrate transport. Indeed, the Asn residues were observed to lie on opposite sides of the probable substrate translocation pore in close proximity to Arg^{87} for Asn^{459} and Arg^{368} for Asn^{168} [346]. Six conserved glycine residues, mostly localized within the two repeated motifs NS1 and NS2 (boxed in Fig. 3.4), were found to be essential for structural positioning of helices as well as for close helix packing and flexibility [346]. Phe^{47}, together with other aromatic residues in TM1, were suggested to either close the translocation pore following substrate binding or alternatively, constrain the flexibility of the long side chains of Arg^{87} and Arg^{368} [345]. In addition, all of these residues and motifs in dinoflagellate NRT2s were localized in regions with the same topology as those of *Aspergillus* NrtA or *Arabidopsis* NRT2.5 (Fig. 3.5). This suggests positioning of helixes and of the substrate translocation pore in dinoflagellate NRT2s will be similar to that of fungi or plants.

Transit of membrane proteins through the ER in dinoflagellates is not a guarantee that their final destination will be at the plasma membrane. Indeed, nuclear-encoded plastid proteins in *Lingulodinium polyedrum* were shown to reach the triple-membrane bound chloroplasts via Golgi-derived vesicles and used a leader sequence different from what is typically observed in plants and green algae [362]. This leader sequence contained two distinct hydrophobic domains flanking a region rich in hydroxylated amino acids (S/T). The first hydrophobic region acted as a signal peptide and was always followed by an AXA signal peptidase site. The S/T- rich region was a transit sequence capable of targeting a luciferase reporter into chloroplasts of transgenic plants expressing the construct. Finally, the second hydrophobic domain acted as a stop-transfer signal that anchored plastid proteins in vesicles en route through the Golgi to the chloroplasts. The NRT2 N-terminus does thus not possess the characteristics expected for a plastid-targeted protein. An alternative destination accessible from the Golgi is the vacuole, but no vacuolar targeting signals are known in the dinoflagellates. A last possible destination is the plasma membrane, and only one protein, called p43, has been localized to this location biochemically [363]. Interestingly, the N

terminus of p43 and LpNRT2 do show some elements of similarity, notably a hydrophobic region about 50 residues downstream from the N-terminus and numerous charged and hydroxylated amino acids preceding the hydrophobic region. Thus while plausible, confirmation of a plasma membrane location for the transporter will require immunulocalization. It is unfortunate that our monoclonal antibody did not detect its epitope on cell sections.

LpNRT2.1 transcripts were found to be the most abundant of all putative nitrate transporters identified in this study (Fig. 3.2) thus motivating our choice of this protein for antibody production (Fig. 3.6). Although LpNRT2.1 was constitutively expressed throughout a daily cycle (Fig. 3.6A) or under different N treatments (Fig. 3.6C), this mode of expression is not unusual for nitrate transporters, and constitutive nitrate uptake systems have long been postulated in plants and green algae [131,332]. Interestingly, *Arabidopsis* NRT2.5, which was reported as the major contributor to the constitutive nitrate uptake system in roots [364], is also the closest *Arabidopsis* homologue to *Lingulodinium* LpNRT2.1. However, AtNRT2.5 was induced by severe nitrate starvation [365], while this induction was not observed for LpNRT2.1 in N-free media (Fig. 3.6C). Ammonium is usually preferred to nitrate by most photosynthetic organisms, because its assimilation requires less energy than nitrate. Thus, ammonium is reported to repress multiple proteins of the nitrate metabolism, including NRT2s [131,332]. In contrast, LpNRT2.1 was unresponsive to ammonium treatment, and a similar resilience was also observed for the *Lingulodinium* NR [147]. Thus, nitrate uptake in *Lingulodinium* appears to rely mainly on a constitutively expressed protein.

Daily changes in nitrate uptake, as observed for *Lingulodinium polyedrum* in this study (Fig. 3.1A) and previously [147] are also well documented in plants [366,367,368]. In *Arabidopsis*, tobacco and tomato, mRNA expression of NRT2s show a diurnal pattern that correlated with the diurnal uptake of nitrate [369,370,371]. It is clear, however, that no such correlation was found for *Lingulodinium* NRT2.1, where protein levels remained constant for the daily cycle (Fig. 3.6A). Moreover, no difference in the 2D gel pattern of LpNRT2.1 was detected between day and night (Fig. 3.6B), suggesting that changes in phosphorylation were also not responsible for the diel variation observed in nitrate uptake. Several explanations can be advanced to account for this uptake rate variation. First, LpNRT2.1 may not be the only nitrate transporter in *Lingulodinium* contributing to nitrate uptake. A constitutively expressed

LpNRT2.1 could be the main contributor to basal nitrate uptake at day and night, while other transporters, such as LpNRT2.2 and LpNRT2.3 could be induced by light. Second, an unknown interaction partner may be present and capable of stimulating LpNRT2.1 activity during the day, but not at night. Lastly, it was recently discovered that dinoflagellates have acquired by horizontal gene transfer from bacteria a suite of rhodopsins, including the light-driven proton pump proteorhodopsin [372]. All characterized NRT2s are reported to be secondary active transporters coupling the transport of nitrate with that of protons, the H^+ gradient being generated by H^+-ATPase pumps [131,331]. An intriguing possibility in *Lingulodinium* could be that proteorhodopsins are used as alternative to H^+-ATPases to generate the proton motive force necessary for nitrate transport by NRT2s. In this context, *Lingulodinium* NRT2 activity would merely follow the light-regulated activity of proteorhodopsins, explaining the increased nitrate uptake observed during the day (Fig. 3.1A).

Circadian clocks are molecular systems that enable organisms to optimize their internal biochemistry in response to anticipated modifications in their environment. In *Lingulodinium*, there is circadian control of nitrate assimilation because the amount of NR in the cell is clock regulated with a maximum during the day [223]. Maximum rates of nitrate reduction thus agree well with maximum rates of uptake measured here. It can be argued that light-dependent uptake is indirectly clock-controlled, as light intensity is higher at the surface and the diurnal vertical migration, which places *Lingulodinium* at the surface during the day, is a *bona fide* circadian rhythm [373]. However, it is clear from our results that nitrate uptake is distinct from nitrate assimilation, as while nitrate reductase remains rhythmic in constant light, nitrate uptake does not.

3.6. Conclusion

This study provided a first glimpse of nitrate transporters in dinoflagellates and showed that global nitrate uptake in *Lingulodinium polyedrum* was a light-regulated, not circadian-regulated, rhythm. We have identified LpNRT2 transporters as the best candidates for nitrate uptake on the basis of sequence analysis, although their functional characterization in heterologous systems such as *Xenopus* oocytes will be necessary to confirm the role proposed here and to establish their kinetic properties. The approach presented here offers great promises for the identification of other transporters in dinoflagellates. Foremost amongst these are the ammonium, urea and phosphate transporters, which are all related to the formation and persistence of HABs.

Table 3.1. BLAST searches for putative nitrate transporters in *Lingulodinium polyedrum*

Query name	Hits ≤ e^{-20}	Unique sequences	Accession
AtNRT2.1	11	5	GABP01091661; JO755411; GABP01019652; JO716588; JO704794
AtNAR2.1	0	0	-
AtNPF6.3 (CHL1)	1	1	GABP01017364
AtCLC-a	36	17	GABP01007646; GABP01067085; GABP01030193; GABP01023136; GABP01020755; GABP01013780; GABP01037384; GABP01029549; GABP01035949; GABP01073801; GABP01068566; GABP01106673; GABP01044984; GABP01064559; GABP01053663; JO745918; GABP01000849
AtSLAC1	0	0	-

Figure 3.1. Nitrate uptake in *Lingulodinium* is light dependent.

A) Daily and B) circadian uptake measured as δ ^{15}N. Results are mean ± SE (n=3). Statistically different results ($p < 0.05$) are marked with a different letter (Analysis of variance). Data presented in B) are not statistically different. ZT; Zeitgeber time, CT; Circadian time

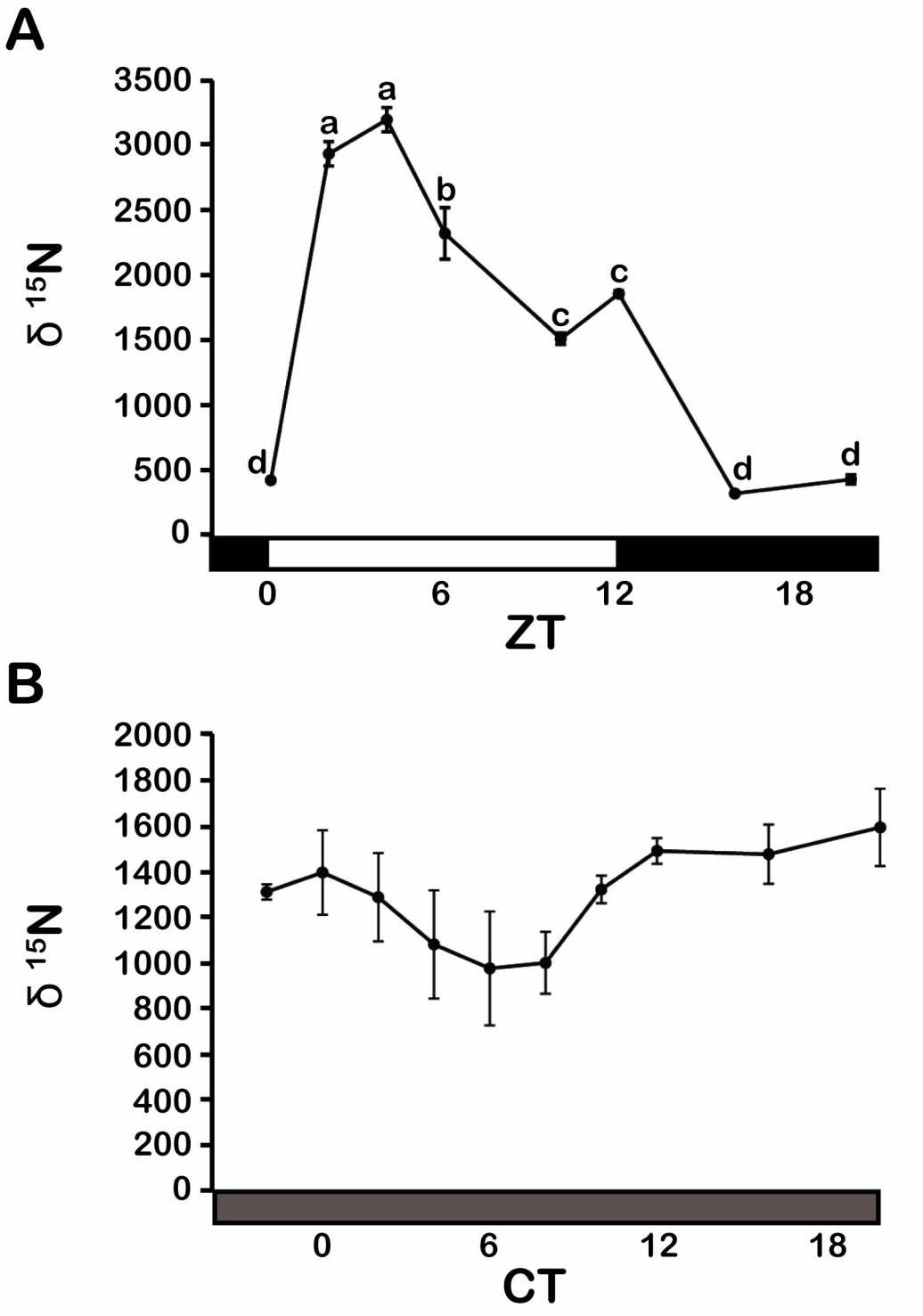
A
3500
3000
2500
2000
1500
1000
500
0
δ 15N
a
a
b
c
c
d
d
d
0
6
12
18
ZT
B
2000
1800
1600
1400
1200
1000
800
600
400
200
0
δ 15N
0
6
12
18
CT

Figure 3.2. Transcripts of NRT2.1 are the most abundant, relative to all of *Lingulodinium* putative nitrate transporter sequences.

RPKM data for putative nitrate transporters from table 1 (A to W) were generated after mapping raw reads onto a Trinity assembly. Bars are: A; LpNRT2.1 (GABP01091661), B; LpNRT2.2 (JO755411), C; LpNRT2.3 (GABP01019652), D; JO716588, E; JO704794, F; GABP01017364, G; GABP01007646, H; GABP01067085, I; GABP01030193, J; GABP01023136, K; GABP01020755, L; GABP01013780, M; GABP01037384, N; GABP01029549, O; GABP01035949, P; GABP01073801, Q; GABP01068566, R; GABP01106673, S; GABP01044984, T; GABP01064559, U; GABP01053663, V; JO745918, W; GABP01000849. Results are mean ± SE (n=8). Statistically different results ($p < 0.05$) are marked over the bars with a different lower case letter (Analysis of variance). RPKM; Reads Per Kilobase per Million.

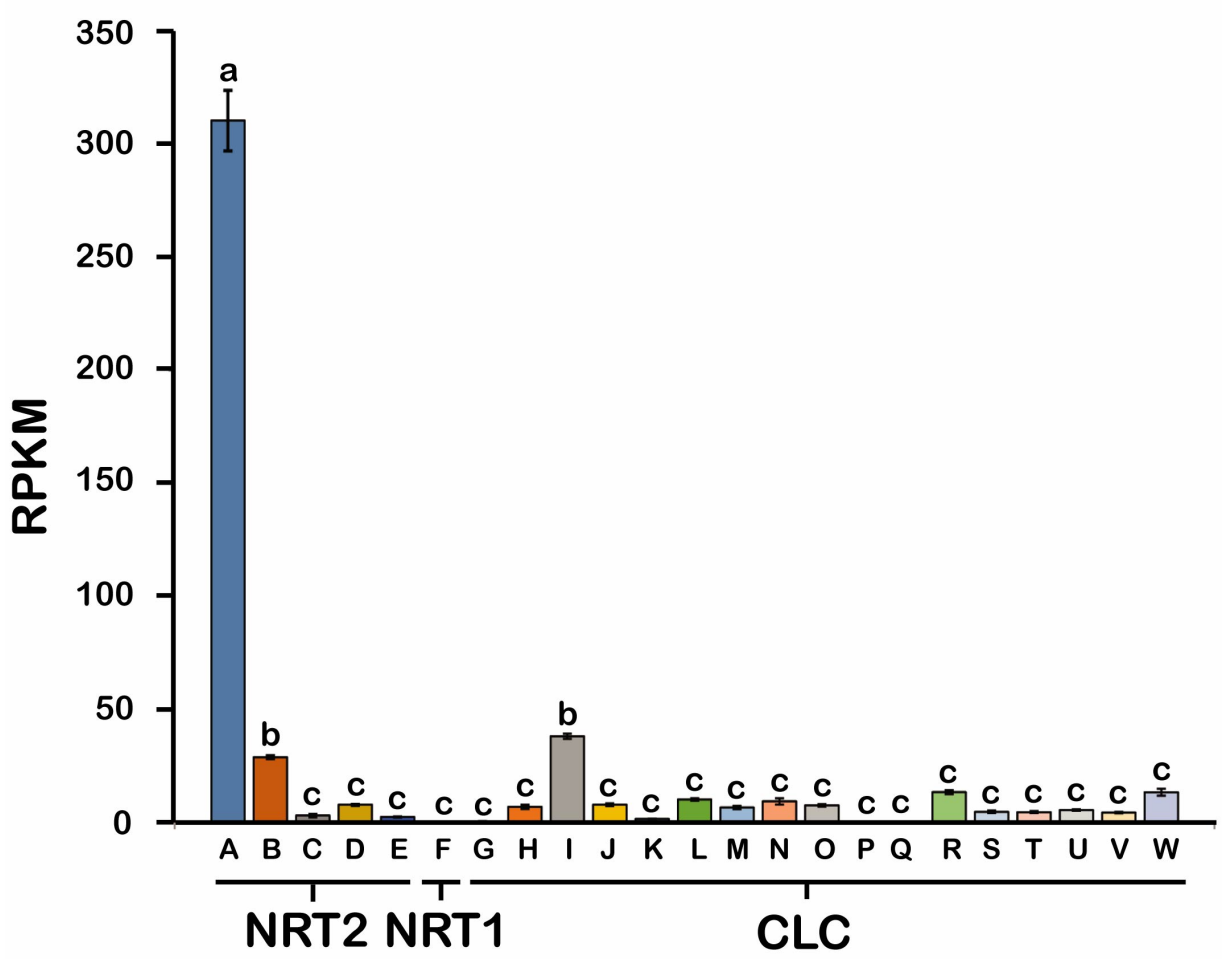
RPKM
350
300
250
200
150
100
50
0
a
b
c
c
c
c
c
c
b
c
c
c
c
c
c
c
c
c
c
c
c
c
c
c
A B C D E F G H I J K L M N O P Q R S T U V W
NRT2
NRT1
CLC

Figure 3.3. *Lingulodinium* NRT2 sequences are found in two different clades.

Maximum-likelihood tree of NRT2 sequences as reconstructed by RAxML. *Lingulodinium* sequences, coloured in red, are found in a well-supported dinoflagellate-specific clade as well as in a clade formed primarily of green algal sequences.

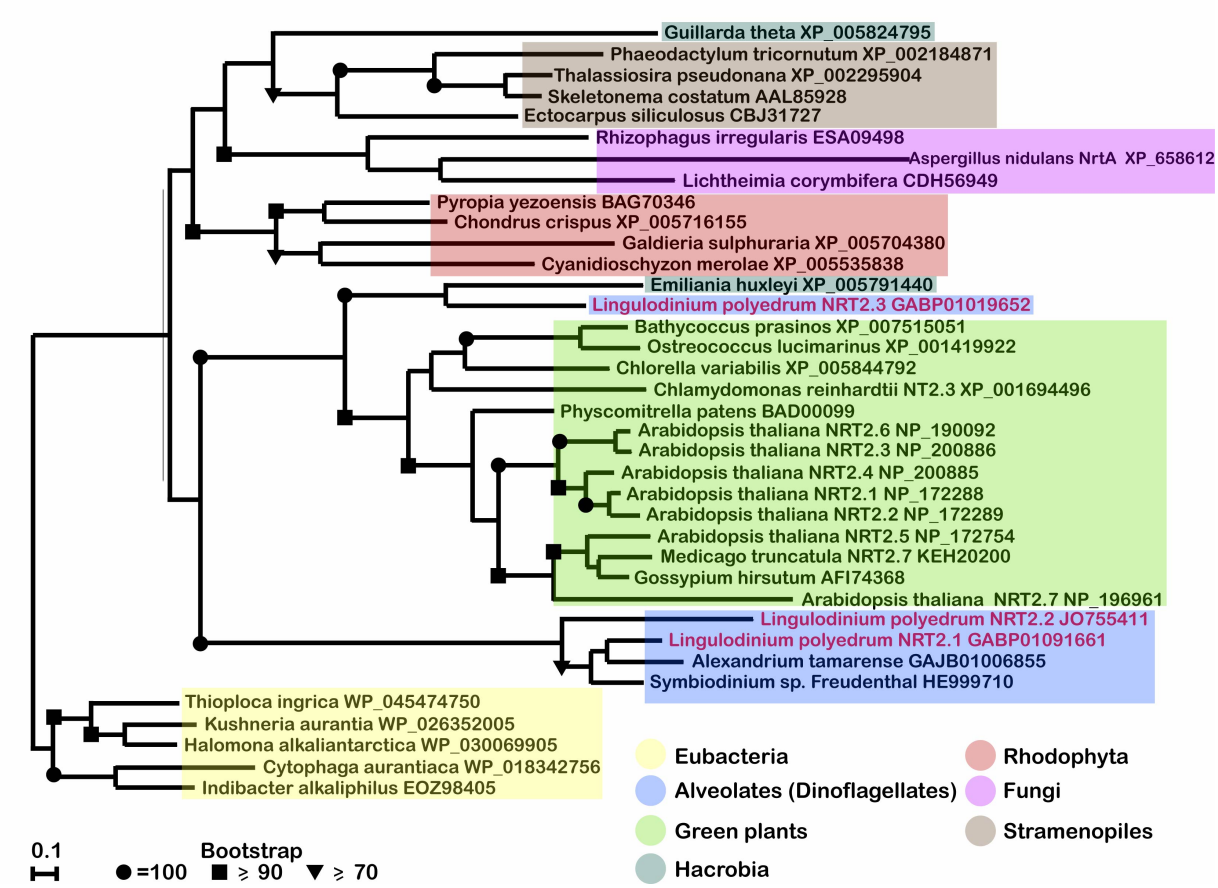
Guillarda theta XP_005824795
Phaeodactylum tricornutum XP_002184871
Thalassiosira pseudonana XP_002295904
Skeletonema costatum AAL85928
Ectocarpus siliculosus CBJ31727
Rhizophagus irregularis ESA09498
Aspergillus nidulans NrtA XP_658612
Lichtheimia corymbifera CDH56949
Pyropia yezoensis BAG70346
Chondrus crispus XP_005716155
Galdieria sulphuraria XP_005704380
Cyanidioschyzon merolae XP_005535838
Emiliania huxleyi XP_005791440
Lingulodinium polyedrum NRT2.3 GABP01019652
Bathycoccus prasinos XP_007515051
Ostreococcus lucimarinus XP_001419922
Chlorella variabilis XP_005844792
Chlamydomonas reinhardtii NT2.3 XP_001694496
Physcomitrella patens BAD00099
Arabidopsis thaliana NRT2.6 NP_190092
Arabidopsis thaliana NRT2.3 NP_200886
Arabidopsis thaliana NRT2.4 NP_200885
Arabidopsis thaliana NRT2.1 NP_172288
Arabidopsis thaliana NRT2.2 NP_172289
Arabidopsis thaliana NRT2.5 NP_172754
Medicago truncatula NRT2.7 KEH20200
Gossypium hirsutum AFI74368
Arabidopsis thaliana NRT2.7 NP_196961
Lingulodinium polyedrum NRT2.2 JO755411
Lingulodinium polyedrum NRT2.1 GABP01091661
Alexandrium tamarense GAJB01006855
Symbiodinium sp. Freudenthal HE999710
Thioploca ingrica WP_045474750
Kushneria aurantia WP_026352005
Halomona alkaliantarctica WP_030069905
Cytophaga aurantiaca WP_018342756
Indibacter alkaliphilus EOZ98405
0.1
Bootstrap
●=100 ■ ≥ 90 ▼ ≥ 70
Eubacteria
Alveolates (Dinoflagellates)
Green plants
Hacrobia
Rhodophyta
Fungi
Stramenopiles

Figure 3.4. All sites essential for nitrate transport are conserved in *Lingulodinium* NRT2 sequences.

NRT2 sequences were aligned and compared to the NrtA of *Aspergillus nidulans*, in which mutagenesis studies have defined the residues required for nitrate transport. Only the regions where these sites (boxes) are localized are presented in the alignment. Two nitrate signature regions, NS1 and NS2, were further marked because they each contained the NRT2 specific motif. There are two and four mismatches to the canonical motif in NS1 and NS2, respectively. The G after the dashed line in NS1 was not included in the motif, but is essential for nitrate transport. F47; Phe^{47} of *A. nidulans* NrtA, R87 and R368; Arg^{87} and Arg^{368} of *A. nidulans* NrtA, N168 and N459; Asn^{168} and Asn^{459} of *Aspergillus* NrtA.

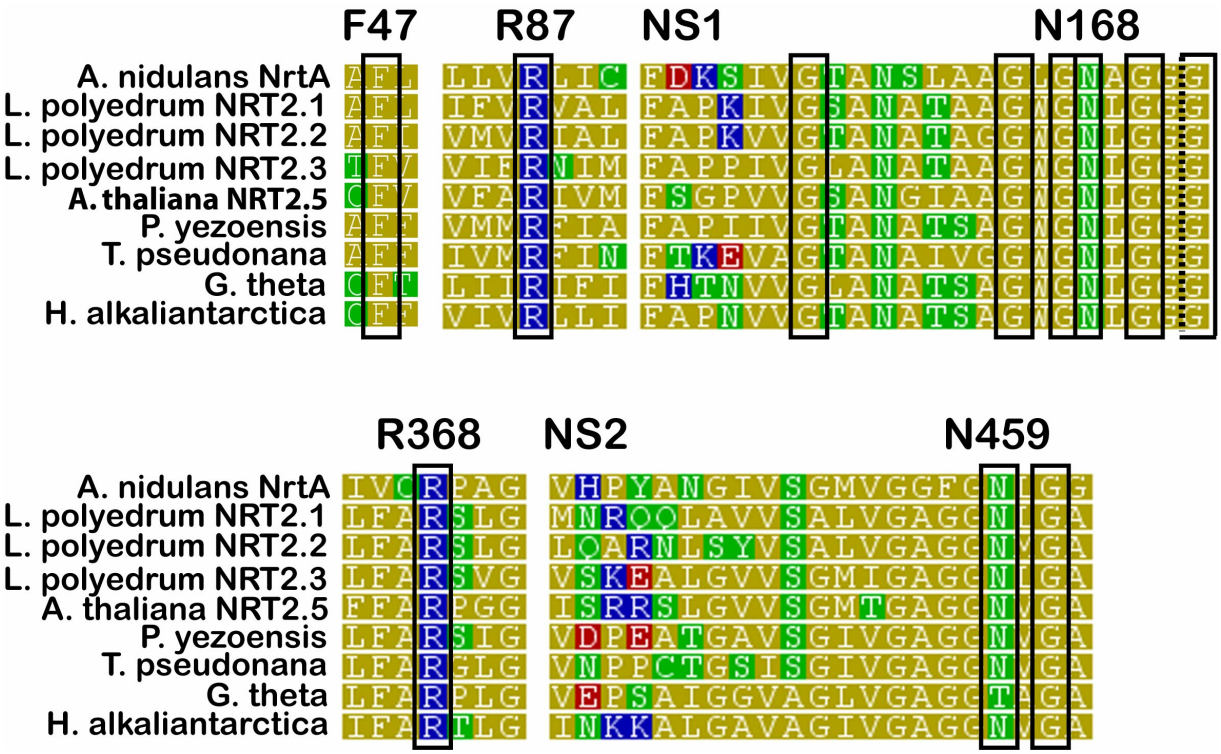
F47
R87
NS1
N168
A. nidulans NrtA
L. polyedrum NRT2.1
L. polyedrum NRT2.2
L. polyedrum NRT2.3
A. thaliana NRT2.5
P. yezoensis
T. pseudonana
G. theta
H. alkaliantarctica
R368
NS2
N459
A. nidulans NrtA
L. polyedrum NRT2.1
L. polyedrum NRT2.2
L. polyedrum NRT2.3
A. thaliana NRT2.5
P. yezoensis
T. pseudonana
G. theta
H. alkaliantarctica

Figure 3.5. Mature dinoflagellate NRT2 share the 12 predicted transmembrane domains.

NrtA from *Aspergillus* and NRT2.5 from *Arabidopsis* were compared to the NRT2 sequences of the dinoflagellates, *Symbiodinium*, *Alexandrium* and *Lingulodinium*. All sequences were submitted to TMHMM, TMPred and TopPred and a summary of their analysis is presented. Domains, which were either undetected or below the default threshold in one of the predictors, but detected in others, were marked as "Putative TM". The $N_{cytosolic}$: $C_{cytosolic}$ topology prediction of TMPred and TopPred was selected for presentation, because both predictors shared the same results for all sequences analysed. Corresponding positions for F47, R87, R368, NS1 and NS2 of *Aspergillus* NrtA to the other sequences were followed with dashed lines. R87 and R368 ; Arg^{87} and Arg^{368} of *A. nidulans* NrtA, NS ; Nitrate Signature, An ; *A. nidulans*, At ; *A. thaliana*, Ata ; *A. tamarense*, Ssp ; *Symbiodinium* sp. Freudenthal, Lp ; *L. polyedrum*

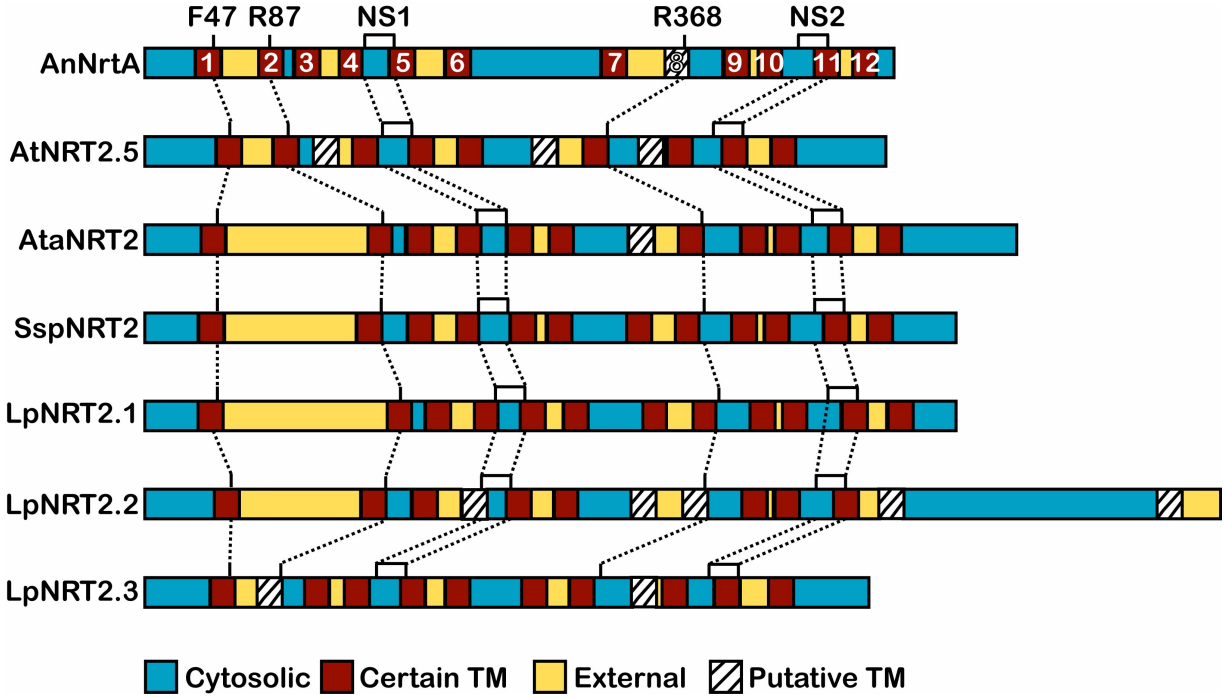
F47
R87
NS1
R368
NS2
AnNrtA
1
2
3
4
5
6
7
8
9
10
11
12
AtNRT2.5
AtaNRT2
SspNRT2
LpNRT2.1
LpNRT2.2
LpNRT2.3
Cytosolic
Certain TM
External
Putative TM

Figure 3.6. LpNRT2.1 is constitutively expressed.

Western blot analyses of LpNRT2.1 on 1D gels (A, C) or on 2D gels (B). Samples were taken at the indicated times over a daily cycle in normal f/2 medium (A, B) or after 2 h or 24 h growth in medium containing the indicated N source. RuBisCO was used as a loading control. Rub; RuBisCO, $+NO_3^-$; normal f/2 supplemented with 880 µM NO_3^-, $+NO2^-$; f/2 with 10 µM and no nitrate, $+NH_4^+$; f/2 with 40 µM NH_4^+ and no nitrate, -N; f/2 lacking added N, ZT; Zeitgeber time

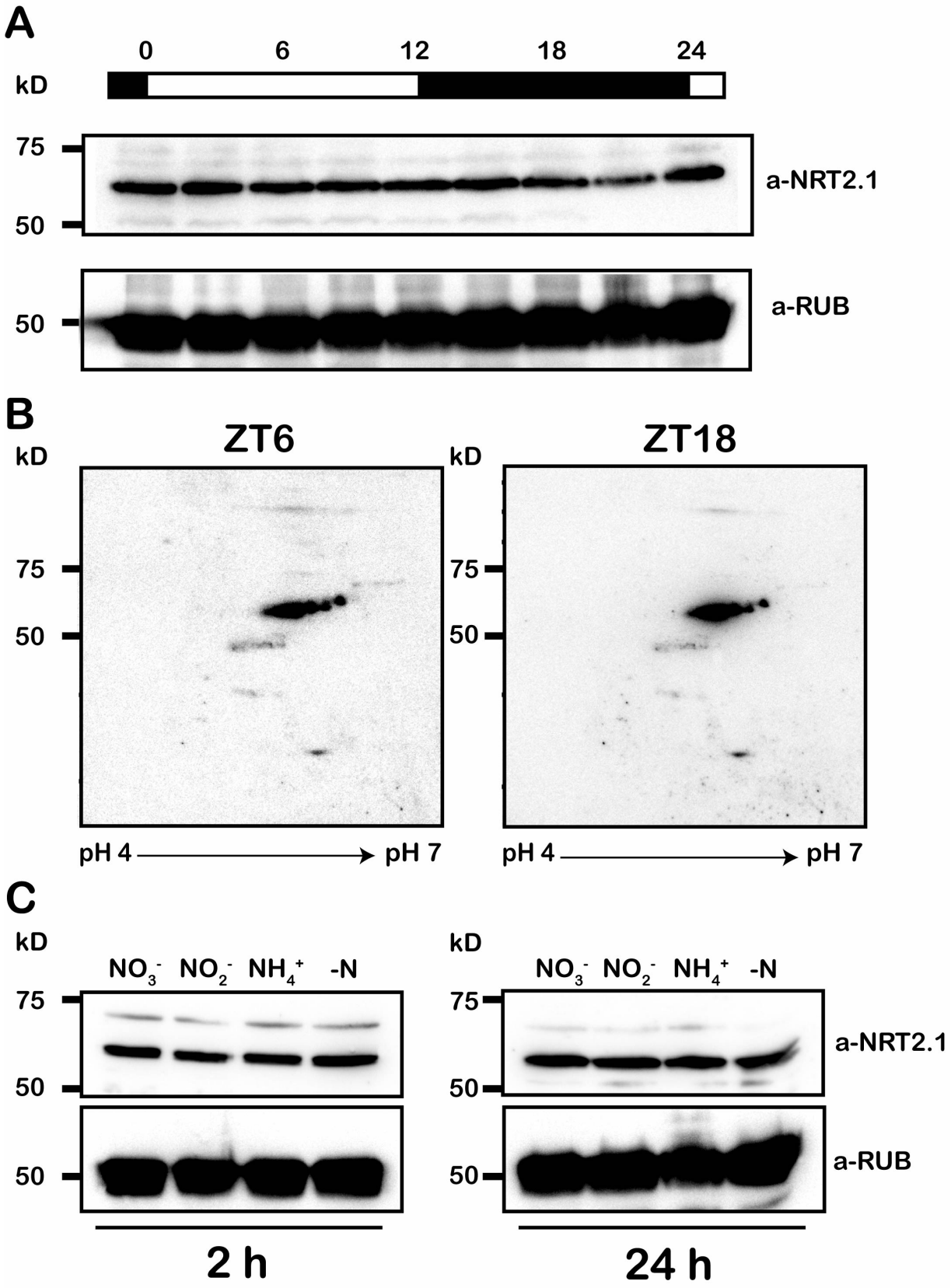
A
0
6
12
18
24
kD
75
50
a-NRT2.1
50
a-RUB
B
ZT6
ZT18
kD
kD
75
50
75
50
pH 4
pH 7
pH 4
pH 7
C
kD
kD
NO3- NO2- NH4+ -N
NO3- NO2- NH4+ -N
75
50
75
50
a-NRT2.1
50
50
a-RUB
2 h
24 h

Supplementary Figure legend

Figure 3.S1. Absolute nitrate uptake in *Lingulodinium* is the same over a 24 h period in ZT or CT.

Mean δ ^{15}N was obtained by combining data from Fig. 3.1A and 3.1B. Values for ZT were calculated by adding the means of δ ^{15}N in the light (white bar) and dark (black bar) phases divided by 2 to account for the difference in uptake observed between day and night. Values for CT were calculated by taking the mean of all time points in B). Results are mean ± SE (n=3). Data are not statistically different. ZT; Zeitgeber time, CT; Circadian time.

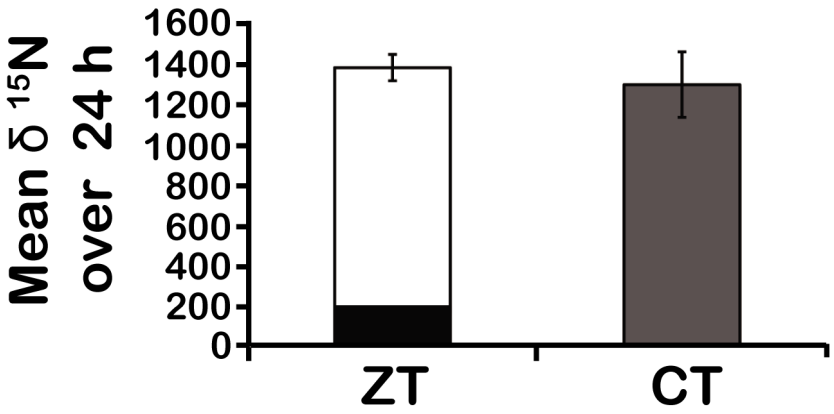
Mean δ 15N over 24 h
1600
1400
1200
1000
800
600
400
200
0
ZT
CT

Figure 3.S2. *Lingulodinium* putative CLC are predicted to be unselective for nitrate.

Lingulodinium polyedrum putative CLC (see table 1) were compared to *Arabidopsis thaliana* CLC-a and CLC-b, and *Rattus norvegicus* CLC-4. Position 160 from *Arabidopsis* CLC-a indicated the position of the selectivity filter. Instead of a proline residue found in plant and reported to be essential for nitrate selectivity, mammalian and all except one dinoflagellate sequences contain a serine residue, typically found in chloride specialized transporters.

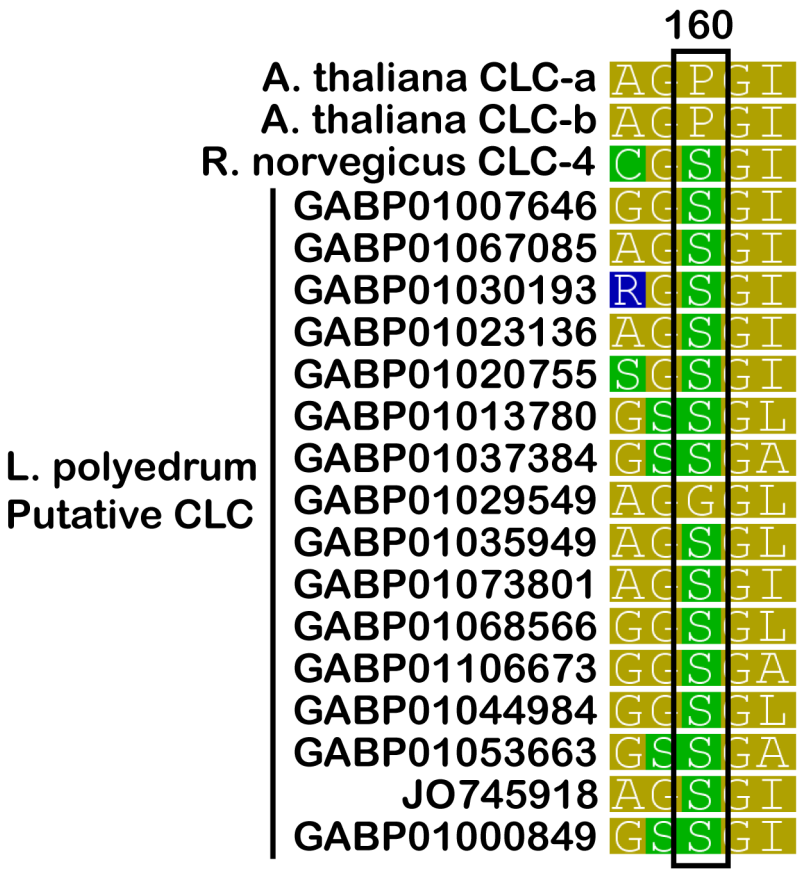
160
A. thaliana CLC-a
A. thaliana CLC-b
R. norvegicus CLC-4
L. polyedrum Putative CLC
GABP01007646
GABP01067085
GABP01030193
GABP01023136
GABP01020755
GABP01013780
GABP01037384
GABP01029549
GABP01035949
GABP01073801
GABP01068566
GABP01106673
GABP01044984
GABP01053663
JO745918
GABP01000849

Figure 3.S3. Transcripts of NRT2.1 are the most abundant, relative to all of *Lingulodinium* putative nitrate transporter sequences.

RPKM data for putative nitrate transporters from table 1 (A to W) were generated after mapping raw reads onto a Velvet assembly. Bars are: A; LpNRT2.1_GABP01091661, B; LpNRT2.2_JO755411, C; LpNRT2.3_GABP01019652, D; JO716588, E; JO704794, F; GABP01017364, G; GABP01007646, H; GABP01067085, I; GABP01030193, J; GABP01023136, K; GABP01020755, L; GABP01013780, M; GABP01037384, N; GABP01029549, O; GABP01035949, P; GABP01073801, Q; GABP01068566, R; GABP01106673, S; GABP01044984, T; GABP01064559, U; GABP01053663, V; JO745918, W; GABP01000849. Results are mean ± SE (n=8). Statistically different results ($p < 0.05$) are marked over the bars with a different lower case letter (Analysis of variance). RPKM; Reads Per Kilobase per Million

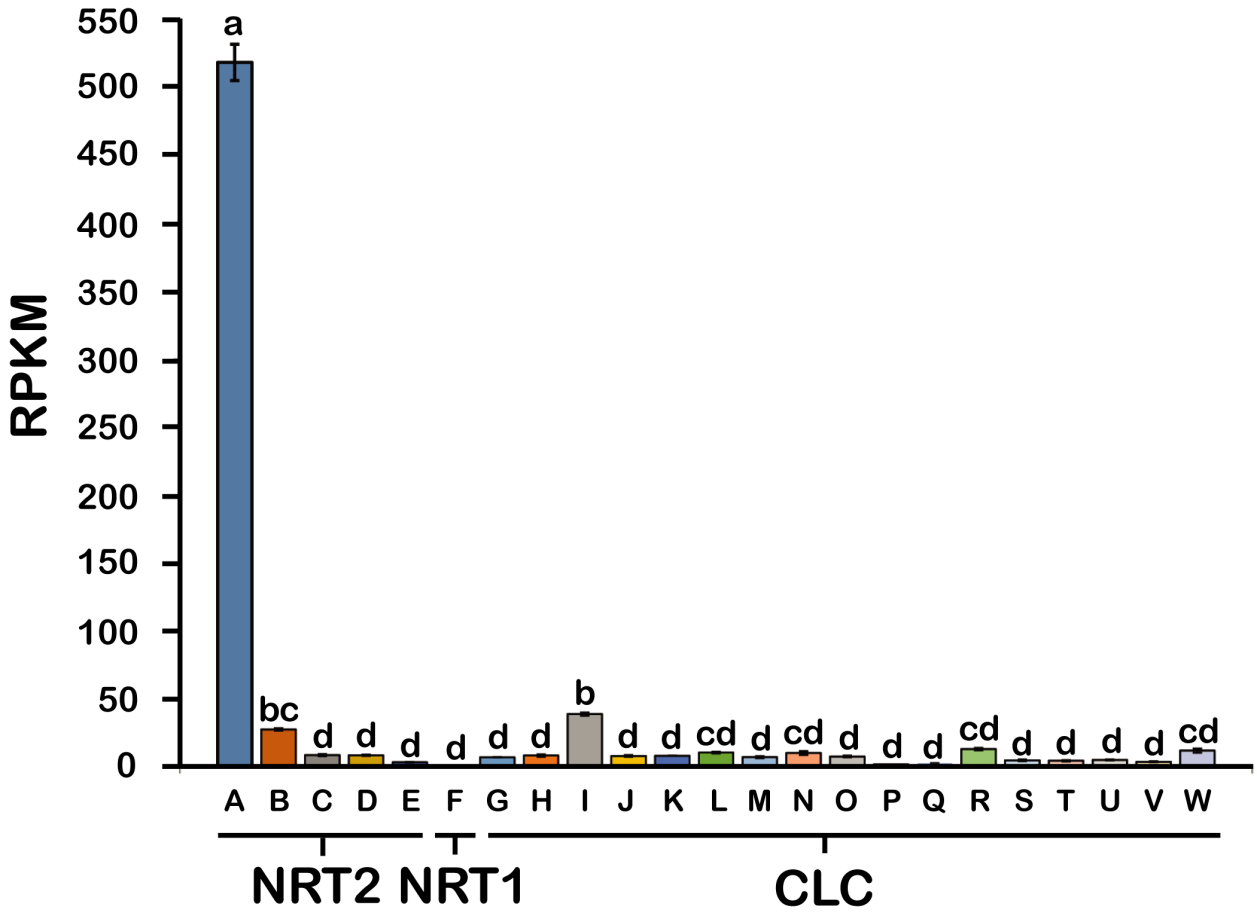
RPKM
550
500
450
400
350
300
250
200
150
100
50
0
a
bc
d
d
d
d
d
d
b
d
d
cd
d
cd
d
d
d
cd
d
d
d
d
cd
A B C D E F G H I J K L M N O P Q R S T U V W
NRT2
NRT1
CLC

3.7. Acknowledgements

We gratefully acknowledge the financial support of the Natural Sciences and Engineering Research Council of Canada (NSERC) for discovery grants to DM and of the Fond de Recherche du Québec- Nature et Technologies (FQRNT) for a studentship (SDB).

Chapter 4- Publication # 4

The *Lingulodinium* circadian system lacks rhythmic changes in transcript abundance

Sougata Roy*, Mathieu Beauchemin*, Steve Dagenais Bellefeuille*, Louis Letourneau, Mario Cappadocia and David Morse

Published in BMC Biology, 2014, 12:107 DOI 10.1186/s12915-014-0107-z

* These authors contributed equally to this work

Author contributions:

The project was designed by S. Roy, M. Beauchemin, S. Dagenais Bellefeuille, M. Cappadocia and D. Morse. The Trinity and Velvet sequence assemblies and read counts were performed by L. Letourneau with additional bioinformatics analysis performed by M. Beauchemin and D. Morse. Transcription inhibition was performed by S. Roy, rhythm measurements were carried out by S. Roy and S. Dagenais Bellefeuille, and Northern analyses were carried out by M. Beauchemin and S. Dagenais Bellefeuille. The article was written by S. Roy, M. Beauchemin, S. Dagenais Bellefeuille, M. Cappadocia and D. Morse.

RNA-seq is a high-throughput analysis method that gives a snapshot of the RNA profile and level of expression in a specific condition or time. We initially used this method to identify transcripts in *Lingulodinium* that showed changes in expression level through a daily or circadian cycle. My interest in this project was to find which components of the nitrate metabolism were under circadian-control at the RNA level. However, we were surprised to discover that no transcript in the complete transcriptome of *Lingulodinium* varied rhythmically. While the focus of this publication is on the absence of rhythmic transcription as a whole, I included it in my thesis, because it also points that circadian regulation of the nitrate metabolism in *Lingulodinium* is not at the transcriptional level.

4.1. Abstract

Background

Almost all cells display circadian rhythms, ~24 hour period changes in their biochemistry, physiology or behavior. These rhythms are orchestrated by an endogenous circadian clock whose mechanism is based on transcription-translation feedback loops (TTFL) where the translated products of clock genes act to inhibit their own transcription.

Methods

We have used RNA-Seq to measure the abundance of all transcripts in an RNA-Seq-derived *de novo* gene catalog in two different experiments. One compared midday and midnight in a light-dark cycle (ZT6 and ZT18) with similar times under constant light (CT6 and CT18). The second compared four times (ZT2, ZT6, ZT14 and ZT18) under a light dark cycle. The timing for the bioluminescence and photosynthesis rhythms were also determined in the presence of the transcription inhibitors actinomycin D and cordycepin.

Results

We show here that despite an elaborate repertoire of biological rhythms, the unicellular dinoflagellate *Lingulodinium* has no detectable daily variation in the abundance of any transcript in an RNA-Seq-derived *de novo* gene catalog. Furthermore, notwithstanding a marked decrease in rhythm amplitude, the timing of the two rhythms is unchanged in the presence of transcription inhibitors.

Conclusions

The lack of detectable daily variation in transcript levels indicates that the endogenous circadian timer of *Lingulodinium* does not require rhythmic RNA. If the circadian timer is considered as a limit cycle oscillator, then cellular time in this organism must be defined by variations in state variables that do not include the amount of a clock gene transcript.

4.2. Background

Circadian rhythms are changes in a cell's biochemistry, physiology or behavior that occur with a roughly 24-hour period. The rhythms are the observable outputs of a cell-autonomous and resettable timekeeper [374] called a circadian clock. This endogenous circadian clock is ubiquitous and organized as TTFL in eukaryotes, and although the genes that constitute the clock differ between plant, animal, and fungal model systems [375], transcriptional control is thought to be an integral component of the clock mechanism. Even in cyanobacteria, where a daily rhythm in the phosphorylation state of the clock protein KaiC has been proposed to be the pacemaker [269], a KaiC TTFL may be required for generating robust rhythms [376].

Recent observations, however, have indicated that transcription is not always required to produce circadian oscillations, as evidenced by the daily oscillation of redox cycles of peroxiredoxin in red blood cells [377] and the green algae *Ostreococcus tauri* [378]. Interestingly, when *O. tauri* is placed in prolonged darkness, transcription rates fall below detectable limits and the rhythm in luciferase fused with the clock component CCA dampens after one day. However, when rhythmicity is re-initiated by transfer to constant light, the phase of the rhythm varies depending on the time when cells are exposed to light [378]. Thus, either a timer driving the observed rhythm of this translational reporter continues even though the overt rhythm itself is undetectable, or the TTFL of *O. tauri* may be influenced by cross-talk with the non-transcriptional peroxiredoxin rhythm which has been shown to continue unabated in darkness.

The marine dinoflagellate *Lingulodinium* displays a large variety of overt rhythms, and has been a model for study of the mechanisms linking the clock with these rhythms for many years [379]. For example, the bioluminescence rhythm is correlated with rhythmic changes in the amount of the reaction catalyst (dinoflagellate luciferase) [279] and of a luciferin binding protein (LBP) [277] that protects the bioluminescence substrate luciferin from non-bioluminescent oxidation. In addition, the sequestration of the key carbon-fixing enzyme RuBisCO within the pyrenoid of the chloroplast is correlated with the capacity of the cell to efficiently fix carbon [29]. Both these different rhythms correlate with rhythms in the rate of protein synthesis *in vivo*, indicating that clock control over gene expression may regulate the

timing of the rhythms. Importantly, in these and other examples, the control over protein synthesis occurs at a translational level since levels of the corresponding mRNAs do not change over the daily cycle [277,380,381,382].

In contrast to the depth of knowledge concerning the rhythms, the mechanism of the circadian clock in *Lingulodinium* remains unknown. To compound the difficulty in characterizing the central timer, physiological studies have shown that these single celled organisms actually contain two different endogenous clocks, as the rhythms of bioluminescence and swimming behavior can run with different periods [383] and show different phase resetting behavior [384]. In the present study we sought to identify rhythmic transcripts in *Lingulodinium* in order to identify potential TTFL components. We used RNA-Seq to assess levels of all RNA species in a *Lingulodiunium* transcriptome [63] over both diurnal and circadian cycles. Surprisingly, our analyses indicate that *Lingulodinium* does not express any detectable rhythmic transcripts. This suggests that the mechanism of the endogenous timers in this organism will instead involve translational and post-translational mechanisms.

4.3. Results

To assess the possibility of isolating components of a transcription-based oscillator in a dinoflagellate, RNA-Seq was used to globally quantitate transcript levels at different times. Two different RNA-Seq experiments were performed, the first of which generated 252 million 76 bp paired end reads (using Zeitgeber times ZT 6, ZT 18, and circadian times CT 6 and CT 18) while the second generated 545 million 100 bp paired end reads (taken at times ZT 2, ZT 6, ZT 14 and ZT 18), of which 51% and 92%, respectively, mapped to our *de novo* gene assemblies. We first compared ZT 6 and ZT 18 by mapping the 100 bp reads to a 103,266 contig Trinity assembly [354] (Fig. 4.1A.), expecting to find both light-induced and circadian differences between the two times. Instead, read counts from the two times, normalized as reads per kilobase per million reads (RPKM) [385] show surprisingly few differences in mRNA levels. DESeq [386] analysis indicated only five contigs showed significantly different levels between the two times ($p_{adj} < 0.001$). A similar result was obtained when the reads were mapped to a 74,655 contig Velvet assembly [63] for which DESeq identified 13 significant differences ($p_{adj} < 0.001$) (Supplementary Fig. 4.S1A). Of the five significant differences uncovered using the Trinity assembly, three were also identified as significant using the Velvet assembly, while the remaining two do not have corresponding contigs in the Velvet assembly. The increased number of significant differences in the Velvet assembly is primarily due to slight differences in the read counts that move either the fold difference or the mean read counts above the significance threshold. Similar results were obtained using EdgeR [387] to assess significant differences, so DESeq was used for all further analyses.

To confirm the similarity in transcript levels between midday and midnight, the midday/midnight comparison was repeated using the 76 bp paired-end read experiment. This experiment included samples taken at both true (ZT 18) and at subjective (CT 18) midnight, so we first assessed the similarity between these two. DESeq analysis identified 9 and 6 significant differences when read counts were mapped to the Trinity (Fig. 4.1B) and Velvet (Supplementary Fig. 4.S1B) assemblies, respectively, with only one contig common to both. We conclude from this that constant light during the night phase does not cause a major alteration in gene expression, and thus the two midnight samples are essentially duplicates. We therefore compared the duplicate midday samples with these two midnight samples using

DESeq (Supplementary Fig. 4.S2). This analysis revealed no significant differences using the Trinity assembly and only three significant differences with the Velvet assembly. Since none of the differences found in this second experiment were in common with those found in the first experiment, we conclude that the mRNA complement of the cells at midday is the same as at midnight.

To test the possibility that cells might express rhythmic RNA with maxima lying between midday and midnight, we next compared the two additional times (ZT 2 and ZT 14) in the 100 bp read experiment. These times, immediately after the light/dark transitions, were chosen to maximize the chances of finding differentially accumulated RNAs. We determined significant differences from all possible pairwise comparisons of read counts mapped to the Trinity assembly using DESeq ($p_{adj}<0.001$) and combined all to yield a final list of 131 non-rRNA sequences (Fig. 4.2A). Those showing the greatest fold-differences were typically lower in abundance (Fig. 4.2B). Hierarchical clustering identified four main groups of sequences, with those peaking at ZT 14 containing the greatest number of significantly different RNAs (Fig. 4.2C). Surprisingly, however, among the 42 sequences that could be identified by sequence homology were found 2 of the 3 known mitochondrial protein-coding genes [388] and 9 of the 10 known plastid protein-coding genes [35], and all these organelle-encoded transcripts were among the group with peak expression at ZT 14. The plastid-encoded sequences included the *psbA* transcript that had been previously shown by Northern analyses to be arrhythmic [389], suggesting that at least some of the transcripts identified as significantly different in our high throughput approach might in fact be false positives. To assess this possibility, Northern analyses were performed using a random selection of 11 sequences (Fig. 4.2D). No rhythmicity was observed in the levels of any of these RNAs, as confirmed by densitometric scans (Fig. 4.2E). Taken together, the two RNA-Seq experiments thus indicate that the entire mRNA complement of the cell is maintained at constant levels over the 24-hour cycle, both under light/dark cycles or in constant light.

The absence of rhythmic RNAs suggested that the circadian clock would continue unabated in the presence of transcription inhibitors. To test this, we exposed cell cultures to a combination of the transcription inhibitors actinomycin D and cordycepin (3-doxyadenosine). Actinomycin D binds to DNA and interferes with transcription and replication [390] while cordycepin interferes with polyadenylation of mRNAs [391]. This combined treatment

reduced RNA synthesis to levels roughly 5% of vehicle-treated cultures (Fig. 4.3A) and is lethal after three days. Importantly, within this three-day time frame, the presence of the inhibitors does not change the timing of the bioluminescence rhythm in constant darkness (Fig. 4.3B) although the amplitude of the rhythm shows a marked decrease. Furthermore, the timing of the photosynthesis rhythm in constant light (Fig. 4.3C) appears similar in the presence of the drug, although again we note a marked decrease in the rhythmic amplitude, especially during the third day (the second day under constant conditions). We conclude from these experiments that, despite a strong effect on the amplitude of the two rhythms, robust transcription is not required for determining their circadian timing.

4.4. Discussion

The results described here indicate that none of the sequences in our *Lingulodinium* transcriptomes show circadian or diurnal variations in transcript levels (Figs. 4.1., 4.2.). These analyses rely on assemblies, derived from high throughput Illumina RNA-Seq experiments, that have been constructed using either Velvet or Trinity. The Velvet assembly has been most extensively characterized, with the 74,655 contigs estimated to represent ~94% of the total transcripts expressed by the cells [63]. The 103,266 contig Trinity transcriptome contains all the Velvet contigs as well as roughly 28,000 additional contigs [354]. Thus, it seems unlikely that *Lingulodinium* will express a rhythmic transcript in an RNA species that is not represented in either of the two assemblies. This conclusion is also supported by the finding that reducing the transcription rate to 5% of control levels does not affect the period of either the bioluminescence or the photosynthesis rhythms (Fig 4.3.).

The manifestation of eukaryotic circadian rhythms in the absence of transcription was first suggested by observations of the photosynthesis rhythm in enucleated *Acetabularia* [392]. More recently, the finding of a circadian rhythm in peroxiredoxin redox state in red blood cells [377], the demonstration of a FRQ-less oscillator in *Neurospora* [393] and the ability of transcription-incompetent *O. tauri* [378] to keep time in constant darkness have also provided support for this view. However, since these latter two organisms also have a canonical TTFL, the significance of a non-transcriptional oscillator operating in parallel remains unclear. In contrast, our findings indicate that the entire *Lingulodinium* circadian system has evolved to function without a TTFL, a particularly remarkable finding considering that there are at least two independent circadian timers in these cells [383]. It is unknown at this time if *Lingulodinium* will also show a circadian rhythm in peroxiredoxin redox state.

One possible explanation for the absence of transcriptional control in the *Lingulodinium* clock is the potential difficulty in regulating transcription in the dinoflagellates. Indeed, these organisms do not contain detectable levels of histone proteins [52], their chromosomes are permanently condensed [47], and the number and diversity of transcription factors is also much reduced compared to other eukaryotes [63,172]. In addition, a global analysis of mRNAs in the dinoflagellate *Karenia* has shown their half-lives to be substantially longer than reported in other organisms [394], as might be expected if little control was

exerted at the level of RNA synthesis rates. *Lingulodinium* also appears to have quite stable RNAs, as least for the few specific cases that have been examined [395].

How might timing signals be generated in *Lingulodinium* in the absence of rhythmic transcripts? Previous work with the system has show that inhibitors of translation (such as anisomycin, puromycin and cycloheximide) have major phase-shifting effects on the bioluminescence rhythm [396,397,398]. In particular, a specific dose of the inhibitor anisomycin given at a specific time, but not lower or higher doses, can induce arrhythmicity [398]. This has been interpreted by a limit cycle model to mean that the clock has been driven to a singularity and provides strong presumptive evidence that translation is a state variable in the clock mechanism. In addition to inhibitors of translation, the kinase inhibitors staurosporine and 6-dimethyl amino purine (6-DMAP) affect the period of the bioluminescence rhythm when administered chronically, and strongly affect light-induced phase shifts [399]. Similarly, a range of protein phosphatase inhibitors (okadaic acid, calyculin A and cantharidin) also affect the rhythmic period when given chronically, although they appear unable to block light-induced phase shifts [400]. We suggest that, in the absence of rhythmic transcripts, *Lingulodinium* may have evolved translational/posttranslational feedback loops with 24-hour rhythmicity that can act as the central timing mechanism. One intriguing possibility is that protein phosphorylation may be used to control translation, as *Lingulodinium* has casein kinase 2 (CK2) sites in a large number of RNA binding proteins [401]. CK2 is a kinase that has been implicated in animal, plant and fungal clock mechanisms [402].

There is growing awareness that RNA-binding proteins may play an important role in clock function. For example, the *Chlamydomonas* protein CHLAMY1 is involved in controlling both the period and phase of the circadian rhythms [226]. In addition, a cold-induced RNA-binding protein appears to be required for efficient translation of the clock gene *Clock* transcripts in mammalian cells [403]. Lastly, ATX (Ataxin-2) in *Drosophila* is an RNA-associated protein that, together with TYF (Twenty-four), is required for translating the transcripts from the clock gene *Period* (*Per*) [404,405]. TYF binds both to PABP, a factor binding the polyadenylated tail at the 3' end of mRNA, and to the eukaryotic translation initiation factor eIF4E, which binds the cap at the 5' end of the mRNA [405]. This circularization is thought to increase translation [406] which in this case would be targeted to the *Per* transcript. In mouse liver cells, changes in the length of the poly(A) tail occur

independently from the steady state level of the transcripts, and tail length is associated with circadian control over protein synthesis [407].

The lack of rhythmic transcripts over the daily cycle in *Lingulodinium* provides new impetus for an examination of translation and post-translational mechanisms in the clock. The former may be addressed by methods such as translating ribosome affinity purification, which has been used to demonstrate rhythmic translation from constant levels of mRNA in drosophila [408]. The latter, at least for modifications involving phosphorylation, is now becoming accessible through phosphoprotein purification and MS/MS de novo sequencing [401]. In any event, it is clear that the long-studied *Lingulodinium* circadian system has still some surprises in reserve.

4.5. Conclusions

The lack of oscillating RNAs over the circadian cycle of the dinoflagellate *Lingulodinium* indicates that the clock mechanism in this organism does not use or require rhythmic changes in RNA amounts.

4.6. Methods

4.6.1. Cell Culture

Unialgal but not axenic *Lingulodinium polyedrum* (CCMP 1936, previously *Gonyaulax polyedra*) was obtained from the Provasoli-Guillard National Center for Marine Algae and Microbiota (East Boothbay, ME, USA). Cell cultures were grown in normal f/2 medium prepared using Instant Ocean under a 12 h light (40 μmol photons m^{-2} s^{-1} cool white fluorescent light) and 12 h darkness at a temperature of 18 ± 1 °C. This light/dark regime is termed LD, with LD 0 corresponding to lights on and LD 12 to lights off. Cells were harvested by filtration on Whatman 541 paper and washed with 200 ml of sterile seawater to reduce bacterial contamination.

4.6.2. RNA extraction and RNA-Seq

RNA-Seq was performed for two different experiments. In one experiment, *Lingulodinium polyedrum* cells grown in f/2 seawater medium at 18°C under a 12:12 light:dark cycle [277] were isolated by centrifugation (500g for 1 min) at two times (Zeitgeber Time ZT 6, ZT 18) and two times under constant light (Circadian Time CT 6, CT 18). The onset of the light phase in a light dark cycle or under continuous light is termed ZT 0 or CT 0, respectively. In another experiment, cells were taken at ZT 2, ZT 6, ZT 14 and ZT 18. All cell pellets were washed twice with fresh seawater and recentrifuged, and the cell pellets were resuspended in 1 mL of Trizol reagent (Life Technologies) and total RNA was extracted as per the manufacturers' protocol. For the first experiment, RNA quality was assessed by Northern blots before and after purification of poly(A) RNA using the poly(A) tract mRNA isolation kit (Promega) and sequenced using a Genome Analyzer IIX (Illumina) at the McGill University and Génome Québec Innovation Center. For the second experiment, RNA pellets were dissolved in 50 μL DEPC treated H_2O, and a Bioanalyzer (Agilent) test performed to assess the quality of the extracted RNA samples. An mRNA-Seq Sample Preparation Kit (Illumina) was used prior to sequencing of the mRNAs using a HiSeq platform (Illumina) at the Institut de Recherche en Immunologie et Cancérologie (Université de Montréal).

Reads were mapped to both a Velvet assembly (accession nos. JO692619-JO767447) [63] and to a Trinity assembly (accession nos. GABP01000001-GABP01114492) [354] using BWA [409]. Sequencing produced 252 million 76 bp paired end reads (Illumina GAII, accession numbers SRR330443-6), of which 49.8% and 51.8% mapped to the Velvet and Trinity assemblies respectively, and 545 million 100 bp paired end reads (HiSeq, accession numbers SRR1184543, 1184608, 1184657, 1184666) of which 95.5 and 88.3% mapped to the Velvet and Trinity assemblies, respectively. Read counts were analyzed by DESeq [386] and EdgeR [387] to uncover statistically significant differences**.** All reads and assemblies are available as a part of the NCBI BioProject PRJNA69549.

Northern blots were performed using total RNA isolated by Trizol extraction as described by the manufacturer. From the 131 sequences with DESeq significant differences, 67 pairs of oligonucleotides were designed from the Trinity assembly sequences and tested by PCR, with 27 pairs producing sequence-validated amplicons. The majority of these were from the same group (maximal levels at ZT 14) so only 17 were tested by Northern blotting, and of these 9 (including a mitochondrial *cox1* probe) yielded a well-defined signal after exposure. An additional two probes were prepared from previously cloned plastid-encoded sequences *atpA* and *psbC* [35]. An actin probe was used to control for RNA loading.

4.6.3. Transcription Inhibition

All the inhibitors were dissolved in 100% DMSO to prepare the stock solution. To inhibit transcription, 20 µL from a stock of 10 mg/mL Cordycepin (final concentration 20 µg/mL) and 5 µL from a stock of 1 mM Actinomycin D (final concentration 0.5 µM) were added to a 10 mL culture of *Lingulodinium* cells. To monitor the inhibition of RNA synthesis, 5 µCi of ^{32}P radionuclide was added after 8 hours incubation with inhibitors. Total RNA was extracted using Trizol reagent (Life Technologies) after 8 hours of incubation with the label. RNA pellets were dissolved in 50 µL of DEPC treated water and 2 µL aliquots mixed with 2 mL of scintillation fluid and counted using a scintillation counter (Perkin Elmer TriCarb 2800TR). The control was prepared by adding only the vehicle (DMSO) to the culture.

4.6.4. Rhythm Measurements

To monitor the bioluminescence rhythm after inhibition of transcription, cordycepin and actinomycin D was added to the same concentrations as above. After 4 hours of incubation of the cultures with inhibitors, six 280 μL aliquots of cell culture were loaded in to a 96-well microtiter plate. Control cells in seawater or with the vehicle alone (DMSO) were also included in the plate. The bioluminescence rhythm was monitored in constant darkness as described [354] using a Spectramax M5 (Molecular Devices) microplate reader kept in the culture room at constant temperature. Bioluminescence output was recorded for one second every 2 min for the next 72 hours. Wells containing cultures were surrounded by wells filled with only seawater to limit evaporation. The pH rhythm was measured as described [297,410] using a pH electrode in a culture flask kept under constant light and temperature in the culture room. The treatments with DMSO alone or DMSO containing the inhibitors were repeated three times.

Figure 4.1. Transcript abundance does not change between midday (ZT 6) and midnight (ZT 18).

(A) Read counts from the two samples (as reads per kilobase per million, RPKM), obtained by mapping raw read data to 103,266 contig Trinity assembly, were plotted against each other. Contigs corresponding to rRNA were removed. Insets show (upper left) the fold difference for DESeq statistically significant differences ($p_{adj} < 0.001$) and (lower right) the MA plot used to determine statistically valid differences. (B) Transcript abundance does not change between true (ZT 18) and subjective (CT 18) midnight.

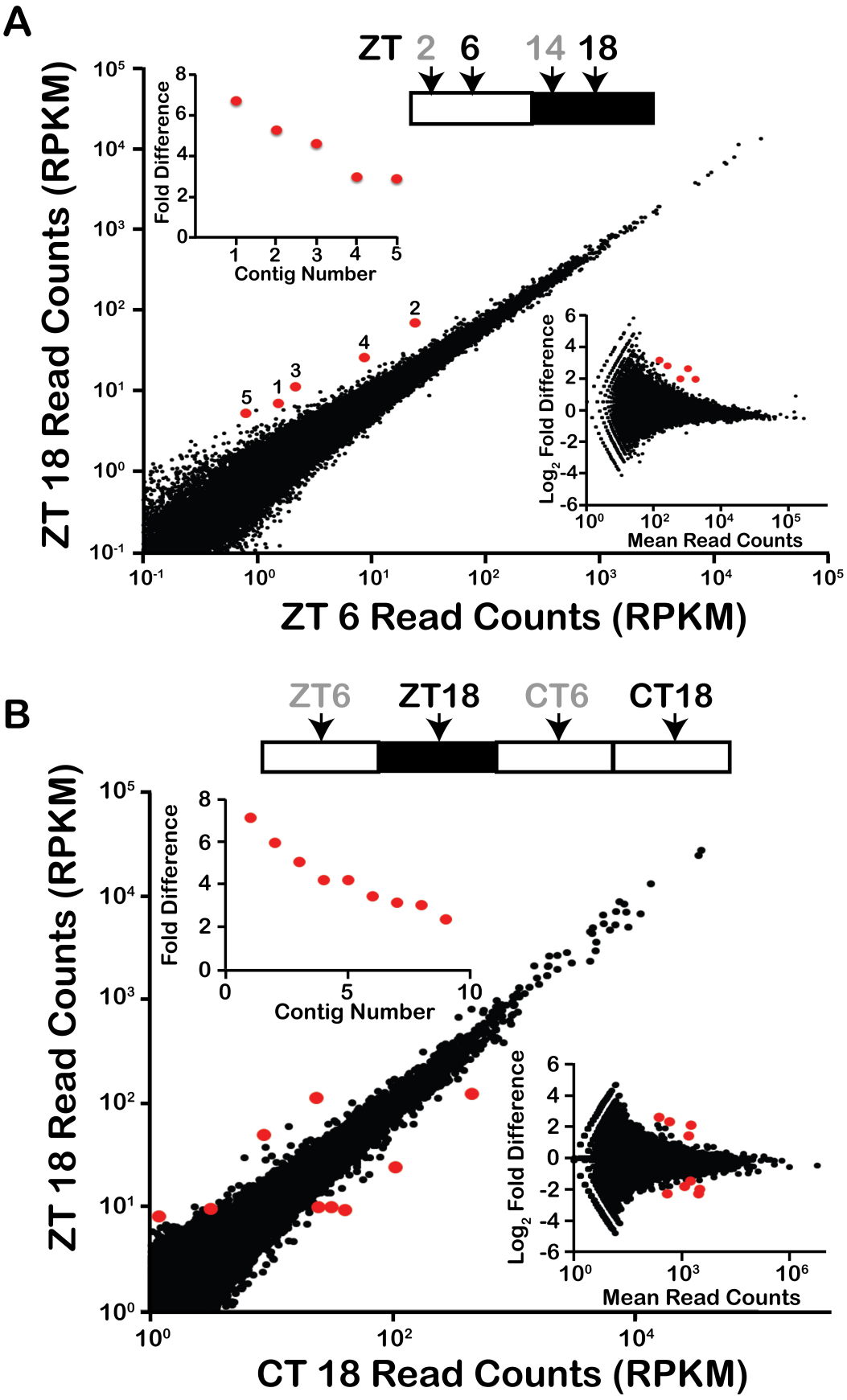
A
ZT 2 6 14 18
ZT 18 Read Counts (RPKM)
ZT 6 Read Counts (RPKM)
Fold Difference
Contig Number
Log2 Fold Difference
Mean Read Counts
B
ZT6 ZT18 CT6 CT18
CT 18 Read Counts (RPKM)

Figure 4.2. *Lingulodinium* does not have rhythmic transcripts over a 24 hour cycle.

(A) DESeq significant differences for all pairs of samples taken LD 2, 6, 14 and 18 under a light dark cycle were combined to a single list of 131 contigs. B) Contigs with more than five-fold maximum difference are typically those with lower mean read counts. (C) A heat map of all the significant differences detected shows a preponderance of contigs whose abundance appears greatest at ZT 14. Hierarchical clustering was performed only with rows to preserve the order of the time points. (D) Northern blots using probes prepared from a random selection of contigs indicate the RNA-Seq predicted differences are false positives. (E) Densitometric scans of Northerns relative to actin as a loading control (red) compared to normalized RNA-Seq data (blue).

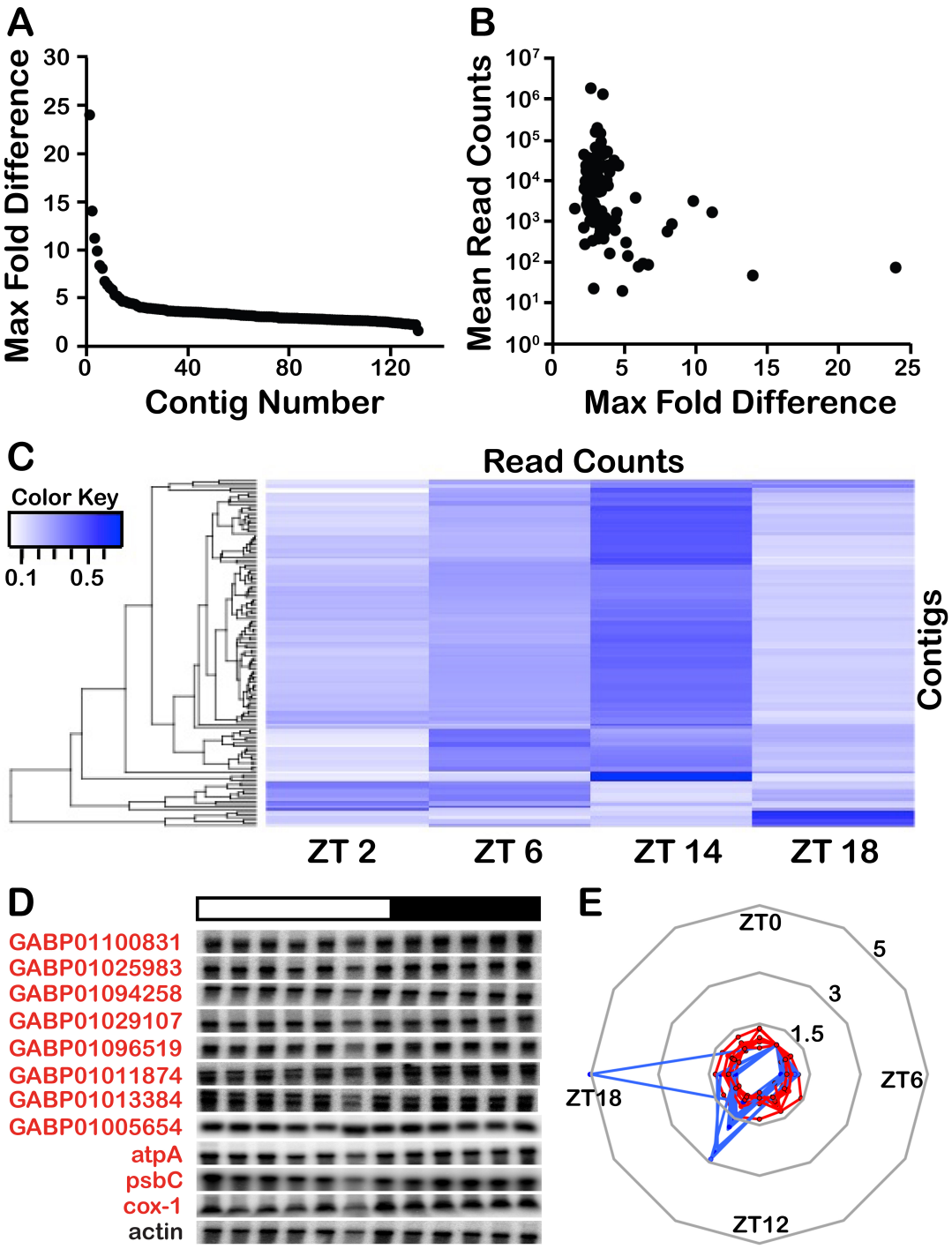
A
Max Fold Difference
Contig Number
B
Mean Read Counts
Max Fold Difference
C
Color Key
0.1
0.5
Read Counts
Contigs
ZT 2
ZT 6
ZT 14
ZT 18
D
GABP01100831
GABP01025983
GABP01094258
GABP01029107
GABP01096519
GABP01011874
GABP01013384
GABP01005654
atpA
psbC
cox-1
actin
E
ZT0
5
3
1.5
ZT6
ZT12
ZT18

Figure 4.3. Rhythms continue in the presence of transcription inhibitors.

A) A combination of actinomycin D and cordycepin reduces RNA synthesis rates to around 5% (mean ± SD, n=4) of the values of vehicle treated cultures. Cultures survive 3-5 days at these concentrations of inhibitors. (B) There is no change in the timing of the bioluminescence rhythm in constant dark. Horizontal bars indicate the light regime, with drugs were added to the cultures at the indicated times (red arrows). Each data point is the average of 3 samples. (C) There is no change in the timing of the pH rhythm used to monitor CO_2 fixation. A representative example of three different experiments is shown for each treatment. The amplitude of the rhythm is severely diminished by the third day of treatment.

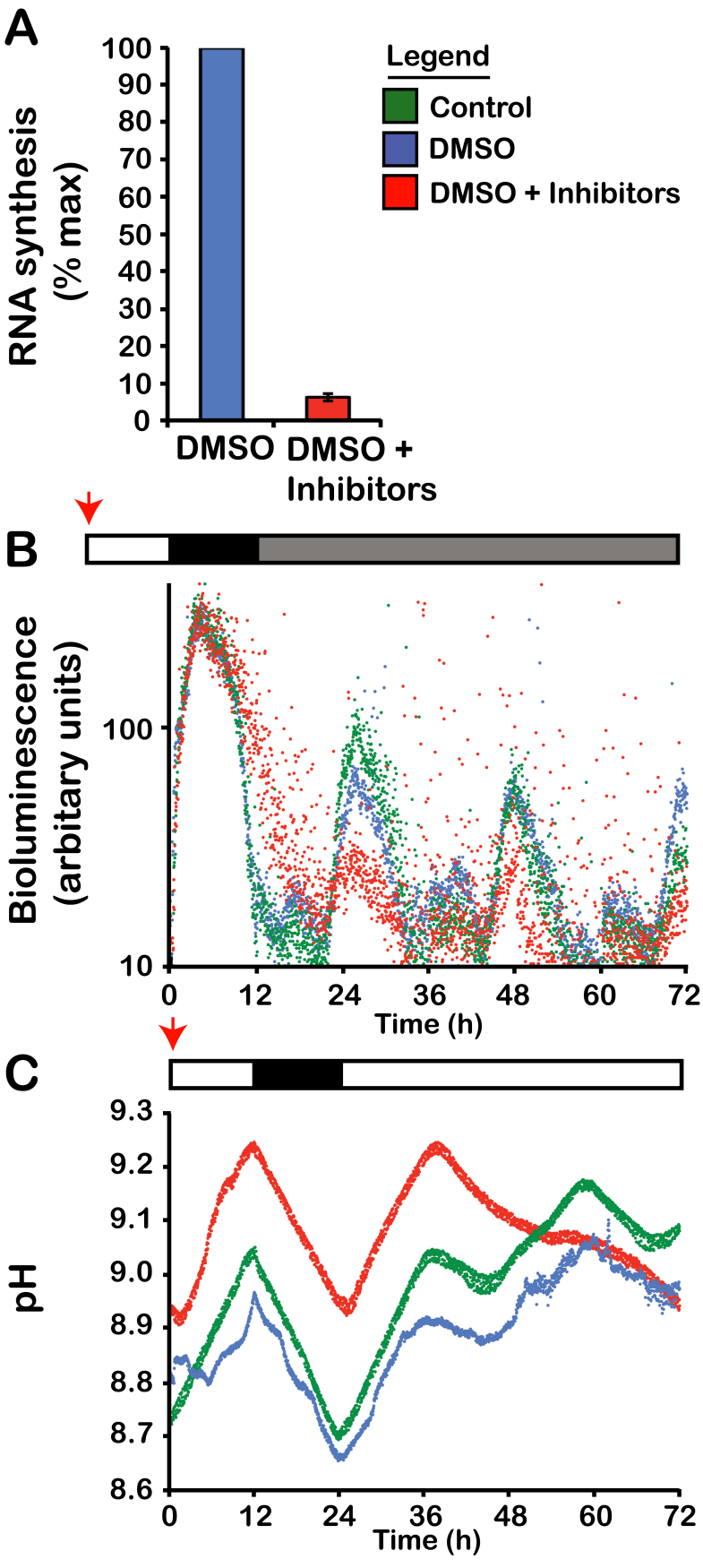
A
RNA synthesis (% max)
100
90
80
70
60
50
40
30
20
10
0
DMSO
DMSO + Inhibitors
Legend
Control
DMSO
DMSO + Inhibitors
B
Bioluminescence (arbitary units)
100
10
0
12
24
36
48
60
72
Time (h)
C
pH
9.3
9.2
9.1
9.0
8.9
8.8
8.7
8.6
0
12
24
36
48
60
72
Time (h)

Supplementary Figure legend

Figure 4.S1. Analysis using the Velvet assembly

(A) Transcript abundance for midday and midnight samples (as reads per kilobase per million, RPKM) obtained by mapping raw read data from the 100 bp read experiment to a 74,655 contig Velvet assembly. The fold difference for the contigs that showed a significant difference is shown as an inset (upper left) while the MA plot used to determine significant differences is at lower right. Contigs corresponding to rRNA have been removed. (B) Transcript abundance for ZT 18 and CT 18 analyzed as above for the 76 bp read experiment.

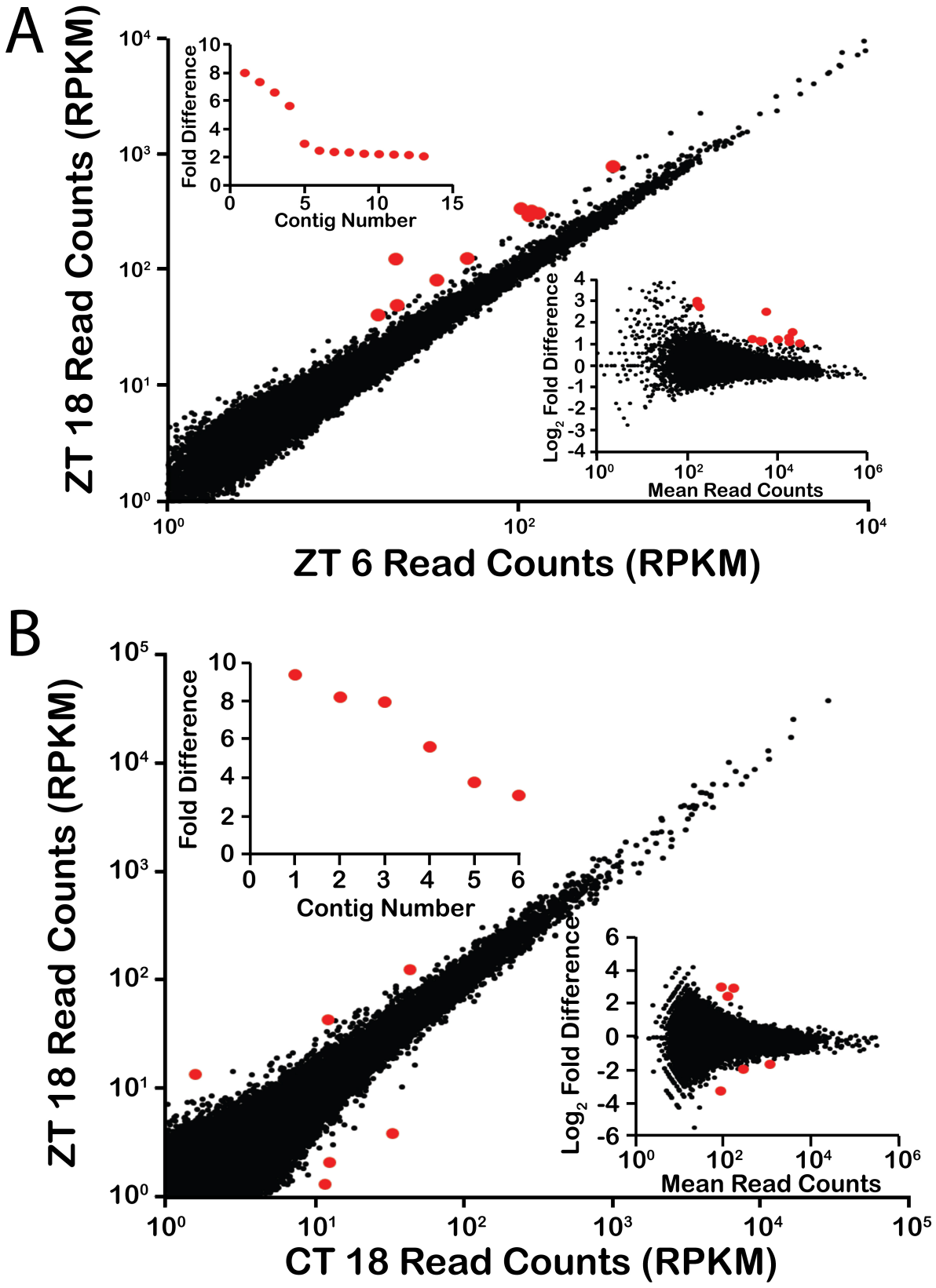
A
ZT 18 Read Counts (RPKM)
ZT 6 Read Counts (RPKM)
Fold Difference
Contig Number
Log2 Fold Difference
Mean Read Counts
B
ZT 18 Read Counts (RPKM)
CT 18 Read Counts (RPKM)
Fold Difference
Contig Number
Log2 Fold Difference
Mean Read Counts

Figure 4.S2. Analysis using duplicate ZT6 and ZT/CT18 samples

(A) Time of sampling in a light/dark cycle and constant light. (B) MA plots using ZT 6/CT 6 samples and ZT 18/CT 18 pairs as duplicates were analyzed by DESeq. There are no significant differences ($p_{adj} < 0.001$) when mapped to the Trinity assembly. (C) Three significant differences are identified when mapped to the Velvet assembly.

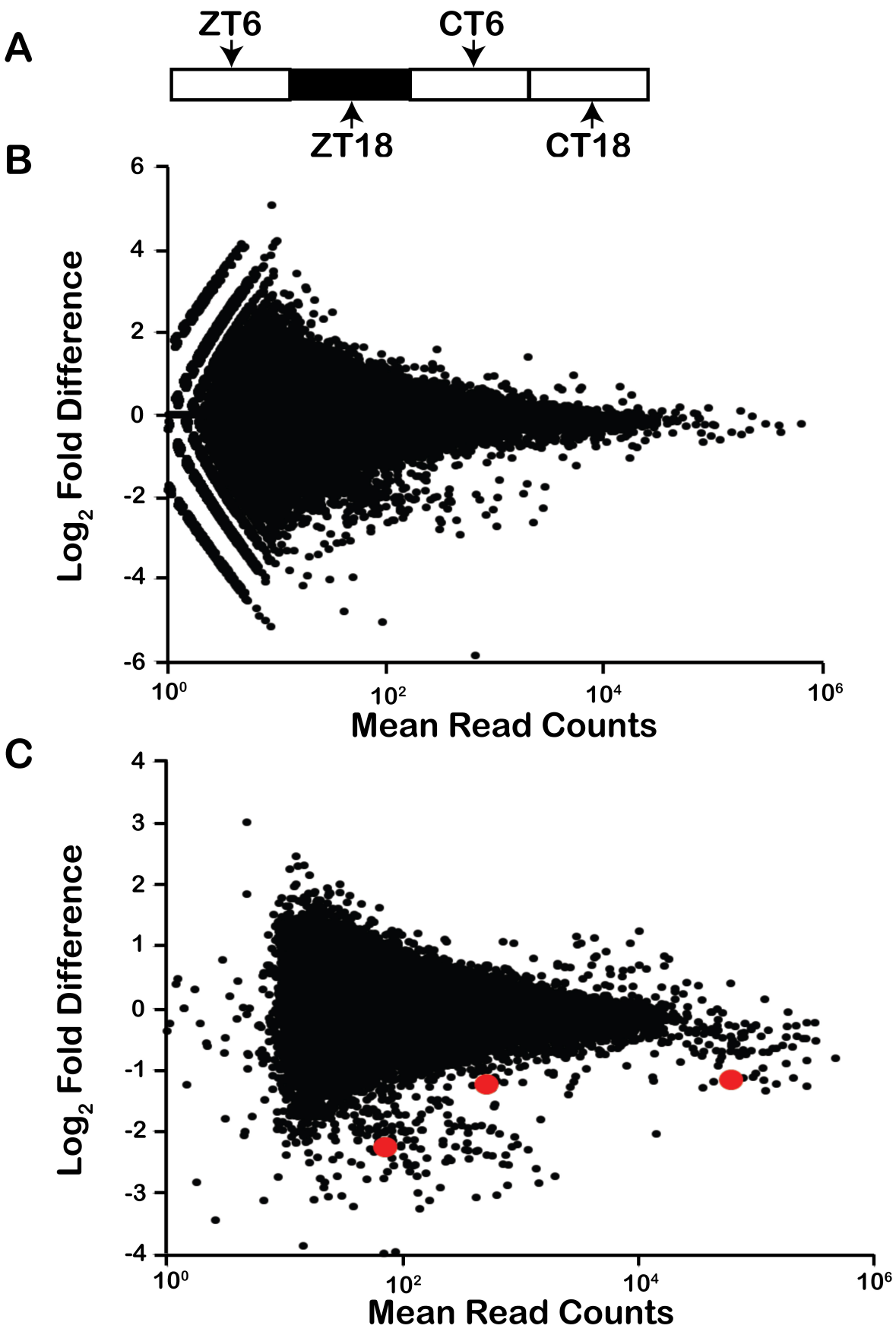
A
ZT6
CT6
ZT18
CT18
B
Log2 Fold Difference
6
4
2
0
-2
-4
-6
10^0
10^2
10^4
10^6
Mean Read Counts
C
Log2 Fold Difference
4
3
2
1
0
-1
-2
-3
-4
10^0
10^2
10^4
10^6
Mean Read Counts

Figure 4.S3. Individual bioluminescence traces.

The three individual bioluminescence traces used to determine the average of inhibitor-treated cultures shown in figure 4.3B.

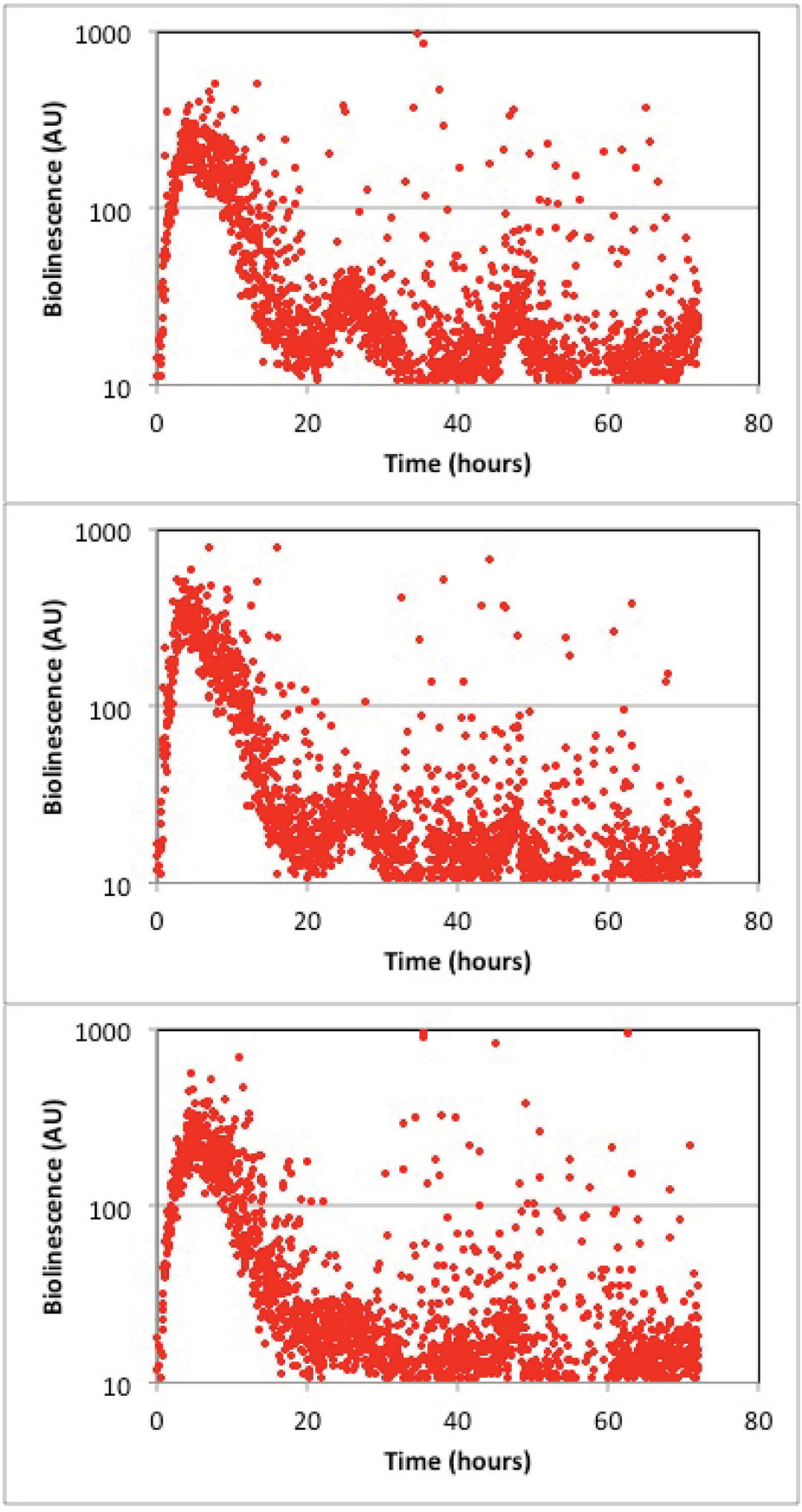
1000
100
10
Biolinescence (AU)
0
20
40
60
80
Time (hours)
1000
100
10
Biolinescence (AU)
0
20
40
60
80
Time (hours)
1000
100
10
Biolinescence (AU)
0
20
40
60
80
Time (hours)

4.7. Acknowledgements

We thank the Canadian National Science and Engineering Research Council for financial assistance in the form of a discovery grant (D.M.) and a research studentship (M.B.), and to the Fonds de Recherche du Quebec- Nature et Technologies for a research studentship (S.D.B.). We thank N. Cermakian and N. Luckhurst for review and comments on the manuscript. We dedicate this manuscript to the memory of J. Woodland Hastings, a pioneer of circadian biology and bioluminescence.

Chapter 5 - General discussion and perspectives

5.1. General discussion and perspectives

Since their appearance in the Mesoproterozoic Era, dinoflagellates were able to adapt to drastic changes in climate and periods of massive extinction and thus withstand the passage of time. Today, their ecological success in most marine and freshwater ecosystems is ascribed to the three trophic modes they have developed to acquire resources and energy. While most dinoflagellate species have a preference for heterotrophy or phototrophy, it appears that most of them can also combine both strategies (mixotrophy) in some conditions. For example, inorganic nitrogen depletion was shown to stimulate heterotrophic behaviors in the generally photosynthetic dinoflagellates *Gyrodinium galatheanum* and *Ceratium furca* [202,203]. Mixotrophy and/or organic nitrogen uptake has also been suggested to be possible means for *Karenia brevis* to sustain blooms in conditions of nitrogen depletion [206,287].

In addition to mixotrophy, I showed in this thesis that high-density populations of the photosynthetic dinoflagellate *Lingulodinium polyedrum* could be maintained for at least 2 weeks in near absence of inorganic nitrogen (Fig. 2.1A). Thus, this dinoflagellate can resist an episode of severe nitrogen depletion while waiting for N to become available again. Cells reacted to nitrogen stress by stopping or reducing the rates of metabolic pathways that required N, such as cell division (Fig. 2.1), protein synthesis (Fig. 2.3A) and chlorophyll synthesis (Fig. 2.4A). Photosynthesis remained high for roughly a week following nitrogen depletion (Fig. 2.4B), which resulted in an accumulation of reduced carbon in the form of starch granules (Fig.2.5). During the second week, the number of plastids decreased considerably (Fig. 2.4 C-K), while neutral lipids accumulated as lipid bodies (Fig. 2.6). Most likely, *Lingulodinium* used autophagy to degrade the chloroplast membranes and to recycle their components in the form of TAGs. Curiously, upon addition of new nitrate, cultures acclimated to nitrogen stress were able to outlive those that were not (Fig. 2.1B). It would thus be interesting to test if the increased survivability of acclimated cells was related to the accumulated starch and lipid bodies. More specifically, degradation rates of both carbon pools could be measured in acclimated cultures after addition of nitrate to verify if complete degradation correlates with the time of culture death or the moment where cell densities reach intermediate values. This latter observation is also intriguing, because one possible adaptation mechanism triggered during inorganic nitrogen stress could be the induction of organic transporters and/or

mixotrophy. In this case, acclimated cells that encountered a second episode of inorganic nitrogen depletion could rapidly react to the stress with an increased capacity for organic nitrogen uptake. Thus, survivor cells in acclimated cultures with intermediate density values might meet their daily N demands by taking up organic N from dead cells. This hypothesis could be verified by measuring the uptake rates of ^{15}N-labelled organic N, such as urea, in acclimated and non-acclimated cultures.

Curiously, starch granules and lipid bodies accumulated at opposite poles of *Lingulodinium* cells (Fig. 2.5 B-G; 2.6 B-J; 2.7). While the functional significance of this polarization will need further investigation, accumulation of these storage compounds could affect the swimming behavior of *Lingulodinium*. DVM in the water column is circadian-regulated in this dinoflagellate, such that every day cells rise to the surface near the end of the night and sink down several hours before dusk [373,411]. This rhythm is easily observed in culture flasks or Petri dishes, because cells form aggregation patterns at and below the cell surface during the day, while they form a "lawn" at the bottom of the flasks at night [373]. I observed that this rhythm was abolished in cultures that were nitrogen-depleted for 14 days. In fact, nitrogen-stressed cells that had accumulated starch and lipid bodies distributed evenly at all times within the culture flasks (unpublished). Since the maximum accumulation of starch in a nitrogen-sufficient cell can be observed at dusk (Fig. 2.5 A, C), starch granules might serve to help the downward migration of *Lingulodinium* at this time. Conversely, starch is almost completely degraded near dawn (Fig. 2.5 A-B), which coincides with the upward migration of cells. While an accumulation/degradation of lipid bodies anti-phase to starch could also help DVM by modifying buoyancy, this appears unlikely as I was unable to detect any difference in the amount of neutral lipids at LD0 or LD12 in either exponential or stationary nitrogen-sufficient cells (Appendix 1).

Nitrogen stress caused major metabolic changes in *Lingulodinium*, but did not affect expression of the nitrate transporter LpNRT2.1 (Fig. 3.6C). Protein expression was unresponsive to nitrate, nitrite or ammonium treatments (Fig. 3.6C), and did not show any daily variations (Fig. 3.6A). Because LpNRT2.1 is also the most abundant of the nitrate transporters in *Lingulodinium* (Fig. 3.2; Fig. 3.S3), global nitrate uptake appears to rely mainly on a constitutive process in this organism. A lack of regulation could indicate that in the environment this dinoflagellate never faces a complete deficiency in nitrate, which is

supported by the observation that *Lingulodinium* swims down to nitrate-enriched water at night and has a capacity for dark nitrate assimilation [147]. Thus, regulation of nitrate uptake might not be necessary for an organism that always expects some nitrate to be present in the environment. However, there is also a possibility that the rate of nitrate uptake is modulated through regulation of the other nitrate transporters, such as LpNRT2.2 and LpNRT2.3.

Chapter 3 presented a method for the identification and bioinformatic validation of nitrate transporters and it would be interesting to transfer this approach for the identification of other nitrogen transporters. For example, characterization of the most expressed ammonium and urea transporters could give a molecular explanation for the preference of these N forms over nitrate in blooming-populations of *Lingulodinium* [148]. Functional characterization in frog oocytes or yeast will be mandatory to determine transporter kinetics and confirm their substrates. To test if such heterologous systems could be used for *Lingulodinium* transporters, I injected and expressed LpNRT2.1 in oocytes and measured the uptake of $^{15}NO_3^-$ using stable isotope analysis (Appendix 2). Injected oocytes barely accumulated more ^{15}N than non-injected oocytes when incubated in the presence of 0.25 mM $^{15}NO_3^-$, while no statistical difference was detected when injected or non-injected oocytes were incubated with 10 mM $^{15}NO_3^-$. These preliminary results are consistent with a high-affinity transporter active when NO_3^- concentrations are low, but the experiment will require further optimization. For example, the amount of cRNA injected and the incubation time in $^{15}NO_3^-$ buffer, was 3 to 5 times less and 5 to 8 times shorter, respectively, than what is typically used when a similar nitrate uptake assay is carried with plant NRT2s [333,412]. The *Xenopus* expression system could also be used to test if LpNRT2.1 is able to carry NO_2^- and if this substrate is preferred to NO_3^-.

Unlike LBP and LCF in the bioluminescence rhythm, not all proteins of the nitrate pathway in *Lingulodinium* are circadian-controlled. In fact, activity of individual nitrate transporters should be dependant on light in this dinoflagellate, because global nitrate uptake was shown to be simply light-regulated (Fig. 3.1). Mechanisms for this regulation will require more research, but they do not rely on changes in the daily protein abundance, isoform patterns or phosphorylation states of LpNRT2.1 (Fig. 3.6A-B). Most impressively, daily uptake of nitrate is certainly not relying on rhythmic transcription of any transporters, since none of the transcripts in the *Lingulodinium* transcriptome showed any change in levels across

a daily cycle (Fig. 4.1A; 4.S1A). This also indicates that circadian variation in protein abundance and activity of the NR in this organism is unrelated to changes in mRNA levels, in contrast to what is observed in plants [413].

The observation that photosynthesis and bioluminescence in *Lingulodinium* run unabated for at least 2 days when RNA synthesis is reduced roughly to 5% of its normal levels (Fig. 4.3), strongly supports the contention that the clock of this dinoflagellate does not require a TTFL to generate circadian rhythms. Instead, this organism might use a central timing system based on translational/posttranslational feedback loops with a 24-h periodicity, because multiple translational, kinase and phosphatase inhibitors were shown to affect clock fundamental properties [396,397,398,399,400]. CK2 will be a promising candidate for characterization since multiple CK2 sites are observed in *Lingulodinium* RNA binding proteins [401] and that this kinase has been implicated in the clock mechanisms of animals, plants and fungi [402]. Interestingly, CK2 phosphorylation of *Nicotiana* NR was suggested to be involved in its inactivation and degradation in the dark [414]. A similar mechanism might explain the circadian regulation observed for *Lingulodinium* NR.

5.2. Conclusion

Dinoflagellates are fascinating organisms that have a remarkable capacity to adapt to environmental pressure, which was exemplified in this thesis by nitrogen stress. However, their adaptability also signifies that they will have major ecological and economical impacts into our future anthropogenically-altered aquatic ecosystems. Now that transcriptomic databases for multiple dinoflagellates and the *Symbiodinium* genome are available, it will be possible to expand our knowledge on dinoflagellate ecology on a molecular level. In particular, characterization of the proteins involved in the nitrogen pathway show great promises in predicting and understanding the dynamic of HABs.

References

1. Cavalier-Smith T (1991) Cell diversification in heterotrophic flagellates. In: DJ Patterson, Larson J, editors. The Biology of Free-living Heterotrophic Flagellates. Oxford: Clarendon Press. pp. 113-131.

2. Hackett JD, Yoon HS, Butterfield NJ, Sanderson MJ, Bhattacharya D (2007) Plastid endosymbiosis: sources and timing of the major events. Evolution of Primary Producers in the Sea. Burlington: Elsevier Academic Press. pp. 441.

3. Bhattacharya D, Yoo SH, Hedges SB, Hackett JD (2009) Eukaryotes (Eukaryota). In: Hedges S, Kumar S, editors. The Timetree of Life. Oxford: UK: Oxford Univ. Press. pp. 116-120.

4. Meng F, Zhou C, Yin L, Chen Z, Yuan X (2005) The oldest known dinoflagellates: Morphological and molecular evidence from Mesoproterozoic rocks at Yongji, Shanxi Province. Chinese Science Bulletin 50: 1230-1234.

5. Moestrup O, Daugbjerg N (2007) On dinoflagellate phylogeny and classification In: Brodie J, Lewis J, editors. Unraveling the Algae: The Past, Present, and Future of Algal Systematics. New York CRC press. pp. 215-230.

6. Wisecaver JH, Hackett JD (2011) Dinoflagellate genome evolution. Annu Rev Microbiol 65: 369-387.

7. Saldarriaga JF, McEwan ML, Fast NM, Taylor FJ, Keeling PJ (2003) Multiple protein phylogenies show that Oxyrrhis marina and Perkinsus marinus are early branches of the dinoflagellate lineage. Int J Syst Evol Microbiol 53: 355-365.

8. Saldarriaga JF, Taylor FJRM, Cavalier-Smith T, Menden-Deuer S, Keeling PJ (2004) Molecular data and the evolutionary history of dinoflagellates. Eur J Protistol 40: 85-111.

9. Zhang H, Bhattacharya D, Lin S (2007) A three-gene dinoflagellate phylogeny suggests monophyly of prorocentrales and a basal position for amphidinium and heterocapsa. J Mol Evol 65: 463-474.

10. Hoppenrath M, Leander BS (2010) Dinoflagellate Phylogeny as Inferred from Heat Shock Protein 90 and Ribosomal Gene Sequences. PLoS One 5.

11. Fensome RA, Taylor FJ, Norris G, Sarjeant WAS, Warton DI, et al. (1993) A classification of living fossil dinoflagellates Am Mus Nat Hist, Micropaleontol Spec Publ 7: 351.

12. Gaines G, Elbrachter M (1987) Heterotophic nutrition. In: Taylor FJR, editor. The Biology of Dinoflagellates. Oxford: Blackwell. pp. 224-268.

13. Prezelin B (1987) Photosynthetic physiology of dinoflagellates. In: Taylor F, editor. The biology of Dinoflagellates. pp. 174-223.

14. Lane CE, Archibald JM (2008) The eukaryotic tree of life: endosymbiosis takes its TOL. Trends Ecol Evol 23: 268-275.

15. Bodyl A, Stiller JW, Mackiewicz P (2009) Chromalveolate plastids: direct descent or multiple endosymbioses? Trends Ecol Evol 24: 119-121; author reply 121-112.

16. Archibald JM (2009) The puzzle of plastid evolution. Curr Biol 19: R81-88.

17. Cavalier-Smith T (2002) Chloroplast evolution: secondary symbiogenesis and multiple losses. Curr Biol 12: R62-64.

18. Bodyl A (2005) Do plastid-related characters support the Chromoalveolate hypothesis? J Phycol 41: 712-719.

19. Tengs T, Dahlberg OJ, Shalchian-Tabrizi K, Klaveness D, Rudi K, et al. (2000) Phylogenetic Analyses Indicate that the 19' Hexanoyloxy-fucoxanthin-Containing Dinoflagellates Have Tertiary Plastids of Haptophyte Origin. Mol Biol Evol 17: 718-729.

20. Yoon HS, Hackett JD, Van Dolah FM, Nosenko T, Lidie KL, et al. (2005) Tertiary Endosymbiosis Driven Genome Evolution in Dinoflagellate Algae. Mol Biol Evol 22: 1299-1308.

21. Schnepf E (1993) From prey via endosymbiont to plastid: comparative studies in dinoflagellates. In: Lewin R, editor. Origins of Plastids. New York: Chapman & Hall. pp. 53-76.

22. Yoon HS, Hackett JD, Ciniglia C, Pinto G, Bhattacharya D (2004) A molecular timeline for the origin of photosynthetic eukaryotes. Mol Biol Evol 21: 809-818.

23. Janouskovec J, Horak A, Obornik M, Lukes J, Keeling PJ (2010) A common red algal origin of the apicomplexan, dinoflagellate, and heterokont plastids. Proc Natl Acad Sci U S A 107: 10949-10954.

24. Palmer JD (2003) The symbiotic birth and spread of plastids: How many times and whodunit? . J Phycol 39: 4-12.

25. Slamovits CH, Keeling PJ (2008) Plastid-derived genes in the nonphotosynthetic alveolate Oxyrrhis marina. Mol Biol Evol 25: 1297-1306.

26. Morse D, Salois P, Markovic P, Hastings JW (1995) A nuclear encoded form II RuBisCO in dinoflagellates. Science 268: 1622-1624.

27. Badger MR, Bek EJ (2008) Multiple RuBisCO forms in proteobacteria: their functional significance in relation to CO2 acquisition by the CBB cycle. J Exp Bot 59: 1525-1541.

28. Lapointe M, MacKenzie T, Morse D (2008) An external delta-carbonic anhydrase in a free living marine dinoflagellate may circumvent diffusion limited carbon acquisition. Plant Physiol 147: 1427-1436.

29. Nassoury N, Fritz L, Morse D (2001) Circadian changes in ribulose-1,5-bisphosphate carboxylase/oxygenase distribution inside individual chloroplasts can account for the rhythm in dinoflagellate carbon fixation. Plant Cell 13: 923-934.

30. Howe CJ, Nisbet RE, Barbrook AC (2008) The remarkable chloroplast genome of dinoflagellates. J Exp Bot 59: 1035-1045.

31. Bachvaroff TR, Concepcion GT, Rogers CR, Herman EM, Delwiche CF (2004) Dinoflagellate expressed sequence tag data indicate massive transfer of chloroplast genes to the nuclear genome. Protist 155: 65-78.

32. Zhang Z, Green BR, Cavalier-Smith T (1999) Single gene circles in dinoflagellate chloroplast genomes. Nature 400: 155-159.

33. Koumandou VL, Nisbet RE, Barbrook AC, Howe CJ (2004) Dinoflagellate chloroplasts--where have all the genes gone? Trends Genet 20: 261-267.

34. Dang Y, Green BR (2010) Long transcripts from dinoflagellate chloroplast minicircles suggest "rolling circle" transcription. J Biol Chem 285: 5196-5203.

35. Wang Y, Morse D (2006) Rampant polyuridylylation of plastid gene transcripts in the dinoflagellate Lingulodinium. Nucleic Acids Res 34: 613-619.

36. Nosenko T, Lidie KL, Van Dolah FM, Lindquist E, Cheng JF, et al. (2006) Chimeric plastid proteome in the Florida "red tide" dinoflagellate Karenia brevis. Mol Biol Evol 23: 2026-2038.

37. Patron NJ, Waller RF, Keeling PJ (2006) A tertiary plastid uses genes from two endosymbionts. J Mol Biol 357: 1373-1382.

38. Jackson CJ, Norman JE, Schnare MN, Gray MW, Keeling PJ, et al. (2007) Broad genomic and transcriptional analysis reveals a highly derived genome in dinoflagellate mitochondria. BMC Biol 5: 41.

39. Kamikawa R, Nishimura H, Sako Y (2009) Analysis of the mitochondrial genome, transcripts, and electron transport activity in the dinoflagellate Alexandrium catenella (Gonyaulacales, Dinophyceae). Phycol Res 57: 1-11.

40. Nash EA, Barbrook AC, Edwards-Stuart RK, Bernhardt K, Howe CJ, et al. (2007) Organization of the mitochondrial genome in the dinoflagellate Amphidinium carterae. Mol Biol Evol 24: 1528-1536.

41. Feagin J (1994) The extrachromosomal DNAs of apicomplexan parasites. Annu Rev Microbiol 48: 81-104.

42. Feagin JE, Mericle BL, Werner E, Morris M (1997) Identification of additional rRNA fragments encoded by the Plasmodium falciparum 6 kb element. Nucleic Acids Res 25: 438-446.

43. Waller RF, Jackson CJ (2009) Dinoflagellate mitochondrial genomes: stretching the rules of molecular biology. Bioessays 31: 237-245.

44. Slamovits CH, Saldarriaga JF, Larocque A, Keeling PJ (2007) The highly reduced and fragmented mitochondrial genome of the early-branching dinoflagellate Oxyrrhis marina shares characteristics with both apicomplexan and dinoflagellate mitochondrial genomes. J Mol Biol 372: 356-368.

45. Lin S, Zhang H, Spencer DF, Norman JE, Gray MW (2002) Widespread and extensive editing of mitochondrial mRNAS in dinoflagellates. J Mol Biol 320: 727-739.

46. Dodge JD, editor (1966) The Dinophyceae. 96-115 p.

47. Rizzo P (1991) The enigma of the dinoflagellate chromosome. J Protozool 38: 246-252.

48. Rizzo PJ, Burghardt RC (1982) Histone-like protein and chromatin structure in the wall-less dinoflagellate Gymnodinium nelsoni. Biosystems 15: 27-34.

49. Bouligand Y, Norris V (2001) Chromosome separation and segregation in dinoflagellates and bacteria may depend on liquid crystalline states. Biochimie 83: 187-192.

50. Chow MH, Yan KT, Bennett MJ, Wong JT (2010) Birefringence and DNA condensation of liquid crystalline chromosomes. Eukaryot Cell 9: 1577-1587.

51. Lin SJ, Zhang HA, Zhuang YY, Tran B, Gill J (2010) Spliced leader-based metatranscriptomic analyses lead to recognition of hidden genomic features in dinoflagellates. Proc Natl Acad Sci USA 107: 20033-20038.

52. Roy S, Morse D (2012) A full suite of histone and histone modifying genes are transcribed in the dinoflagellate Lingulodinium. PLoS One.

53. Veldhuis MJW, Cucci TL, Sieracki ME (1997) Cellular DNA content of marine phytoplankton using two new fluorochromes: Taxonomic and ecological implications. J Phycol 33: 527-541.

54. Hou Y, Lin S (2009) Distinct gene number-genome size relationships for eukaryotes and non-eukaryotes: gene content estimation for dinoflagellate genomes. PLoS One 4: e6978.

55. Liu LY, Hastings JW (2006) Novel and rapidly diverging intergenic sequences between tandem repeats of the luciferase genes in seven dinoflagellate species. J Phycol 42: 96-103.

56. Lee D-H, Mittag M, Sczekan S, Morse D, Hastings JW (1993) Molecular cloning and genomic organization of a gene for luciferin binding protein from the dinoflagellate *Gonyaulax polyedra*. J Biol Chem 268: 8842-8850.

57. Le QH, Markovic P, Jovine R, Hastings J, Morse D (1997) Structure and organization of the peridinin-chlorophyll a-protein gene in *Gonyaulax polyedra*. Mol Gen Genet 255: 595-604.

58. Zhang H, Hou Y, Miranda L, Campbell DA, Sturm NR, et al. (2007) Spliced leader RNA trans-splicing in dinoflagellates. Proc Natl Acad Sci USA 104: 4618-4623.

59. Lidie KB, Van Dolah FM (2007) Spliced leader RNA-Mediated trans-splicing in a dinoflagellate, Karenia brevis. J Eukaryot Microbiol 54: 427-435.

60. Zhang H, Lin S (2008) mRNA editing and spliced-leader RNA trans-splicing groups Oxyrrhis, noctiluca, Heterocapsa, and Amphidinium as basal lineages of dinoflagellates. J Phycol 44: 703-711.

61. Bachvaroff TR, Place AR, Coats DW (2009) Expressed Sequence Tags from Amoebophrya sp Infecting Karlodinium veneficum: Comparing Host and Parasite Sequences. J Eukaryot Microbiol 56: 531-541.

62. Parsons M, Nelson RG, Watkins KP, Agabian N (1984) Trypanosome mRNAs share a common 5' spliced leader sequence. Cell 38: 309-316.

63. Beauchemin M, Roy S, Daoust P, Dagenais-Bellefeuille S, Bertomeu T, et al. (2012) Dinoflagellate tandem array gene transcripts are highly conserved and not polycistronic. Proc Natl Acad Sci U S A 109: 15793-15798.

64. Lin S (2011) Genomic understanding of dinoflagellates. Res Microbiol 162: 551-569.

65. Guillebault D, Sasorith S, Derelle E, Wurtz JM, Lozano JC, et al. (2002) A new class of transcription initiation factor, intermediate between TBPs and TLFs is present in the marine unicellular organism: The dinoflagellate *Crypthecodinium cohnii*. J Biol Chem 1: 1.

66. Lin S, Cheng S, Song B, Zhong X, Lin X, et al. (2015) The Symbiodinium kawagutii genome illuminates dinoflagellate gene expression and coral symbiosis. Science 350: 691-694.

67. Okamoto OK, Hastings JW (2003) Novel dinoflagellate circadian-clock genes identified through microarray analysis of a phase shifted clock. J Phycol 39: 1-9.

68. Okamoto OK, Hastings JW (2003) Genome-wide analysis of redox-regulated genes in a dinoflagellate. Gene 321: 73-81.

69. Van Dolah FM, Lidie KB, Morey JS, Brunelle SA, Ryan JC, et al. (2007) Microarray analysis of diurnal and circadian regulated genes in the florida red-tide dinoflagellate *Karenia brevis* (Dinophyceae). J Phycol 43: 741-752.

70. Erdner DL, Anderson DM (2006) Global transcriptional profiling of the toxic dinoflagellate Alexandrium fundyense using massively parallel signature sequencing. BMC Genomics 7.

71. Moustafa A, Evans AN, Kulis DM, Hackett JD, Erdner DL, et al. (2010) Transcriptome profiling of a toxic dinoflagellate reveals a gene-rich protist and a potential impact on gene expression due to bacterial presence. PLoS One 5: e9688.

72. Dale B (1983) Dinoflagellate resting cysts: "bentic plankton". In: Fryxell GA, editor. Survival Strategies of the Algae Cambridge: Cambridge University Press. pp. 69-136.

73. Ribeiro S, Berge T, Lundholm N, Andersen TJ, Abrantes F, et al. (2011) Phytoplankton growth after a century of dormancy illuminates past resilience to catastrophic darkness. Nat Commun 2.

74. Pospelova V, Pedersen TF, de Vernal A (2006) Dinoflagellate cysts as indicators of climatic and oceanographic changes during the past 40 kyr in the Santa Barbara Basin, southern California. Paleoceanography 21.

75. Mertens KN, Gonzalez C, Delusina I, Louwye S (2009) 30 000 years of productivity and salinity variations in the late Quaternary Cariaco Basin revealed by dinoflagellate cysts. Boreas 38: 647-662.

76. Londeix L, Herreyre Y, Turon JL, Fletcher W (2009) Last Glacial to Holocene hydrology of the Marmara Sea inferred from a dinoflagellate cyst record. Rev Palaeobot Palyno 158: 52-71.

77. Kunz-Pirrung M, Matthiessen J, De Vernal A (2001) Late Holocene dinoflagellate cysts as indicators for short-term climate variability in the eastern Laptev Sea (Arctic Ocean). J Quaternary Sci 16: 711-716.

78. Ellegaard M (2000) Variations in dinoflagellate cyst morphology under conditions of changing salinity during the last 2000 years in the Limfjord, Denmark. Rev Palaeobot Palyno 109: 65-81.

79. de Vernal A, Eynaud F, Henry M, Hillaire-Marcel C, Londeix L, et al. (2005) Reconstruction of sea-surface conditions at middle to high latitudes of the Northern Hemisphere during the Last Glacial Maximum (LGM) based on dinoflagellate cyst assemblages. Quaternary Sci Rev 24: 897-924.

80. Bonnet S, de Vernal A, Hillaire-Marcel C, Radi T, Husum K (2010) Variability of sea-surface temperature and sea-ice cover in the Fram Strait over the last two millennia. Mar Micropaleontol 74: 59-74.

81. Mertens KN, Rengefors K, Moestrup O, Ellegaard M (2012) A review of recent freshwater dinoflagellate cysts: taxonomy, phylogeny, ecology and palaeocology. Phycologia 51: 612-619.

82. Davy SK, Allemand D, Weis VM (2012) Cell Biology of Cnidarian-Dinoflagellate Symbiosis. Microbiol Mol Biol R 76: 229-261.

83. Hansen PJ (2011) The Role of Photosynthesis and Food Uptake for the Growth of Marine Mixotrophic Dinoflagellates. J Eukaryot Microbiol 58: 203-214.

84. Smayda T (1997) Harmful algal blooms: their ecophysiology and general relevance to phytoplankton blooms in the sea. Limnol Oceanogr 42: 1137-1153.

85. Rein KS, Snyder RV (2006) The biosynthesis of polyketide metabolites by dinoflagellates. Adv Appl Microbiol, Vol 59 59: 93-125.

86. Anderson DM, Burkholder JM, Cochlan WP, Glibert PM, Gobler CJ, et al. (2008) Harmful algal blooms and eutrophication: Examining linkages from selected coastal regions of the United States. Harmful Algae 8: 39-53.

87. Bodeanu N, Ruta G (1998) Development of the planktonic algae in the Romanian Black Sea sector in 1981-1996; Reguera B, Blanco J, Fernandez M, Wyatt T, editors. Paris, France: Paris-Xunta de Galicia & Intergovernmental Oceanographic Commission of UNESCO.

88. Okaichi T (1997) Red tides in the Seto Inland Sea.; Okaichi T, Yanagi Y, editors. Tokyo, Japan: Terra Scientific Publishing Company. p. 327.

89. Zhou M-j, Shen Z-l, Yu R-c (2008) Responses of a coastal phytoplankton community to increased nutrient input from the Changjiang (Yangtze) River. Cont Shelf Res 28: 1483-1489.

90. Smayda TJ (1990) Novel and Nuisance Phytoplankton Blooms in the Sea - Evidence for a Global Epidemic. Toxic Marine Phytoplankton: 29-40.

91. Egge JK, Aksnes DL (1992) Silicate as Regulating Nutrient in Phytoplankton Competition. Mar Ecol Prog Ser 83: 281-289.

92. Egge JK (1998) Are diatoms poor competitors at low phosphate concentrations? J Marine Syst 16: 191-198.

93. Officer CB, Ryther JH (1980) The Possible Importance of Silicon in Marine Eutrophication. Mar Ecol Prog Ser 3: 83-91.

94. Fensome RA, Saldarriaga JF, Taylor FJRM (1999) Dinoflagellate phylogeny revisited: reconciling morphological and molecular based phylogenies. Grana 38: 66-80.

95. Gestal C, Novoa B, Posada D, Figueras A, Azevedo C (2006) Perkinsoide chabelardi n. gen., a protozoan parasite with an intermediate evolutionary position: possible cause of the decrease of sardine fisheries? Environ Microbiol 8: 1105-1114.

96. Guillou L, Viprey M, Chambouvet A, Welsh RM, Kirkham AR, et al. (2008) Widespread occurrence and genetic diversity of marine parasitoids belonging to Syndiniales (Alveolata). Environ Microbiol 10: 3349-3365.

97. Harada H, Nakajima K, Sakaue K, Matsuda Y (2006) CO2 sensing at ocean surface mediated by cAMP in a marine diatom. Plant Physiol 142: 1318 - 1328.

98. Park MG, Cooney SK, Yih W, Coats DW (2002) Effects of two strains of the parasitic dinoflagellate Amoebophrya on growth, photosynthesis, light absorption, and quantum yield of bloom-forming dinoflagellates. Mar Ecol Prog Ser 227: 281-292.

99. Skovgaard A, Massana R, Balague V, Saiz E (2005) Phylogenetic position of the copepod-infesting parasite Syndinium turbo (Dinoflagellata, Syndinea). Protist 156: 413-423.

100. Small HJ, Shields JD, Reece KS, Bateman K, Stentiford GD (2012) Morphological and Molecular Characterization of Hematodinium perezi (Dinophyceae: Syndiniales), a Dinoflagellate Parasite of the Harbour Crab, Liocarcinus depurator. J Eukaryot Microbiol 59: 54-66.

101. Vila M, Garces E, Maso M (2001) Potentially toxic epiphytic dinoflagellate assemblages on macroalgae in the NW Mediterranean. Aquat Microb Ecol 26: 51-60.

102. Stoecker D, Johnson M, deVargas C, Not F (2009) Acquired phototrophy in aquatic protists. Aquat Microb Ecol 57: 279-310.

103. Stoecker DK (1999) Mixotrophy among Dinoflagellates. J Eukaryot Microbiol 46: 397-401.

104. Steidinger KA, Burkholder JM, Glasgow HB, Hobbs CW, Garrett JK, et al. (1996) Pfiesteria piscicida gen. et sp. nov. (Pfiesteriaceae fam. nov.) a new toxic dinoflagellate with a complex life cycle and behavior. J Phycol 32: 157-164.

105. Anderson DM, Cembella AD, Hallegraeff GM (2012) Progress in understanding harmful algal blooms: paradigm shifts and new technologies for research, monitoring, and management. Ann Rev Mar Sci 4: 143-176.

106. Lee YS (2006) Factors affecting outbreaks of high-density Cochlodinium polykrikoides red tides in the coastal seawaters around Yeosu and Tongyeong, Korea. Mar Pollut Bull 52: 1249-1259.

107. San Diego-McGlone ML, Azanza RV, Villanoy CL, Jacinto GS (2008) Eutrophic waters, algal bloom and fish kill in fish farming areas in Bolinao, Pangasinan, Philippines. Mar Pollut Bull 57: 295-301.

108. Anderson DM, Alpermann TJ, Cembella AD, Collos Y, Masseret E, et al. (2012) The globally distributed genus Alexandrium: multifaceted roles in marine ecosystems and impacts on human health. Harmful Algae 14: 10-35.

109. Wang DZ (2008) Neurotoxins from marine dinoflagellates: a brief review. Mar Drugs 6: 349-371.

110. Hu HH, Chen WD, Shi YJ, Cong W (2006) Nitrate and phosphate supplementation to increase toxin production by the marine dinoflagellate Alexandrium tamarense. Mar Pollut Bull 52: 756-760.

111. Gruber N (2008) The Marine Nitrogen Cycle: Overview and Challenges. Nitrogen in the Marine Environment (2nd Edition). San Diego: Academic Press. pp. 1-50.

112. Beman MJ, Arrigo KR, Matson PA (2005) Agricultural runoff fuels large phytoplankton blooms in vulnerable areas of the ocean. Nature 434: 211-214.

113. Rabalais NN (2002) Nitrogen in Aquatic Ecosystems. Ambio 31: 102-112.

114. Galloway JN, Dentener FJ, Capone DG, Boyer EW, Howarth RW, et al. (2004) Nitrogen Cycles: Past, Present, and Future. Biogeochemistry 70: 153-226.

115. Epstein E, Hagen CE (1952) A Kinetic Study of the Absorption of Alkali Cations by Barley Roots. Plant Physiol 27: 457-474.

116. Epstein E, Rains DW, Elzam OE (1963) Resolution of Dual Mechanisms of Potassium Absorption by Barley Roots. Proc Natl Acad Sci USA 49: 684-692.

117. Doddema H, Telkamp GP (1979) Uptake of Nitrate by Mutants of Arabidopsis thaliana, Disturbed in Uptake or Reduction of Nitrate. Physiol Plantarum 45: 332-338.

118. Franco AR, Cardenas J, Fernandez E (1988) Two different carriers transport both ammonium and methylammonium in Chlamydomonas reinhardtii. J Biol Chem 263: 14039-14043.

119. Galvan A, Quesada A, Fernandez E (1996) Nitrate and Nitrite Are Transported by Different Specific Transport Systems and by a Bispecific Transporter in Chlamydomonas reinhardtii. J Biol Chem 271: 2088-2092.

120. Howitt SM, Udvardi MK (2000) Structure, function and regulation of ammonium transporters in plants. Biochim Biophys Acta 1465: 152-170.

121. Rentsch D, Schmidt S, Tegeder M (2007) Transporters for uptake and allocation of organic nitrogen compounds in plants. FEBS Lett 581: 2281-2289.

122. Siddiqi MY, Glass AD, Ruth TJ, Rufty TW (1990) Studies of the Uptake of Nitrate in Barley: I. Kinetics of NO(3) Influx. Plant Physiol 93: 1426-1432.

123. Wilson MR, Walker NA (1988) The Transport and Metabolism of Urea in Chara australis: I. Passive diffusion, specific transport and metabolism of urea, thiourea and methylurea. J Exp Bot 39: 739-751.

124. Galvan A, Fernandez E (2001) Eukaryotic nitrate and nitrite transporters. Cell Mol Life Sci 58: 225-233.

125. Liu KH, Tsay YF (2003) Switching between the two action modes of the dual-affinity nitrate transporter CHL1 by phosphorylation. EMBO J 22: 1005-1013.

126. Ho C-H, Lin S-H, Hu H-C, Tsay Y-F (2009) CHL1 Functions as a Nitrate Sensor in Plants. Cell 138: 1184-1194.

127. Gaspar M, Bousser A, Sissoeff I, Roche O, Hoarau J, et al. (2003) Cloning and characterization of ZmPIP1-5b, an aquaporin transporting water and urea. Plant Science 165: 21-31.

128. Jahn TP, Moller AL, Zeuthen T, Holm LM, Klaerke DA, et al. (2004) Aquaporin homologues in plants and mammals transport ammonia. FEBS Lett 574: 31-36.

129. Liu LH, Ludewig U, Gassert B, Frommer WB, von Wiren N (2003) Urea transport by nitrogen-regulated tonoplast intrinsic proteins in Arabidopsis. Plant Physiol 133: 1220-1228.

130. Loque D, Ludewig U, Yuan L, von Wiren N (2005) Tonoplast intrinsic proteins AtTIP2;1 and AtTIP2;3 facilitate NH3 transport into the vacuole. Plant Physiol 137: 671-680.

131. Fernandez E, Galvan A (2007) Inorganic nitrogen assimilation in Chlamydomonas. J Exp Bot 58: 2279-2287.

132. De Angeli A, Monachello D, Ephritikhine G, Frachisse JM, Thomine S, et al. (2006) The nitrate/proton antiporter AtCLCa mediates nitrate accumulation in plant vacuoles. Nature 442: 939-942.

133. Liu L-H, Ludewig U, Frommer WB, von Wiren N (2003) AtDUR3 Encodes a New Type of High-Affinity Urea/H+ Symporter in Arabidopsis. Plant Cell 15: 790-800.

134. Sugiura M, Georgescu MN, Takahashi M (2007) A nitrite transporter associated with nitrite uptake by higher plant chloroplasts. Plant Cell Physiol 48: 1022-1035.

135. Bhattacharyya P, Volcani BE (1980) Sodium-dependent silicate transport in the apochlorotic marine diatom Nitzschia alba. Proc Natl Acad Sci USA 77: 6386-6390.

136. Boyd CM, Gradmann D (1999) Electrophysiology of the marine diatom Coscinodiscus wailesii III. Uptake of nitrate and ammonium. J Exp Bot 50: 461-467.

137. Hellebust JA (1978) Uptake of organic substrates by Cyclotella cryptica (Bacillariophyceae): Effects of ions, ionophores and metabolic and transport inhibitors J Phycol 14: 79-83.

138. Raven JA, Smith FA (1980) Intracellular pH Regulation in the Giant-Celled Marine Alga Chaetomorpha darwinii. J Exp Bot 31: 1357-1369.

139. Gimmler H (2000) Primary sodium plasma membrane ATPases in salt-tolerant algae: facts and fictions. J Exp Bot 51: 1171-1178.

140. Bisson MA, Beilby MJ, Shepherd VA (2006) Electrophysiology of turgor regulation in marine siphonous green algae. J Membr Biol 211: 1-14.

141. Ullrich WR, Glaser E (1982) Sodium-phosphate cotransport in the green alga Ankistrodesmus braunii. Plant Sci Lett 27: 155-161.

142. Reid RJ, Mimura T, Ohsumi Y, Walker NA, Smith FA (2000) Phosphate uptake in Chara: membrane transport via Na/Pi cotransport. Plant Cell Environ 23: 223-228.

143. Sanders D, Smith FA, Walker NA (1985) Proton/chloride cotransport in Chara: mechanism of enhanced influx after rapid external acidification. Planta 163: 411-418.

144. Walker NA, Reid RJ, Smith FA (1993) The uptake and metabolism of urea by Chara australis: IV. Symport with sodium--a slip model for the high and low affinity systems. J Membr Biol 136: 263-271.

145. Collos Y, Vaquer A, Laabir M, Abadie E, Laugier T, et al. (2007) Contribution of several nitrogen sources to growth of Alexandrium catenella during blooms in Thau lagoon, southern France. Harmful Algae 6: 781-789.

146. Fan C, Glibert PM, Burkholder JM (2003) Characterization of the affinity for nitrogen, uptake kinetics, and environmental relationships for Prorocentrum minimum in natural blooms and laboratory cultures. Harmful Algae 2: 283-299.

147. Harrison WG (1976) Nitrate metabolism of the red tide dinoflagellate Gonyaulax polyedra Stein. J Exp Mar Biol Ecol 21: 199-209.

148. Kudela R, Cochlan W (2000) Nitrogen and carbon uptake kinetics and the influence of irradiance for a red tide bloom off southern California. Aquat Microb Ecol 21: 31-47.

149. Lee YS (2008) Utilization of various nitrogen, phosphorus, and selenium compounds by Cochlodinium polykrikoides. J Environ Biol 29: 799-804.

150. Leong SC, Taguchi S (2004) Response of the dinoflagellate Alexandrium tamarense to a range of nitrogen sources and concentrations: growth rate, chemical carbon and nitrogen, and pigments. Hydrobiologia 515: 215-224.

151. Leong SCY, Maekawa M, Taguchi S (2010) Carbon and nitrogen acquisition by the toxic dinoflagellate Alexandrium tamarense in response to different nitrogen sources and supply modes. Harmful Algae 9: 48-58.

152. Loureiro S, Garces E, Collos Y, Vaque D, Camp J (2009) Effect of marine autotrophic dissolved organic matter (DOM) on Alexandrium catenella in semi-continuous cultures. J Plankton Res 31: 1363-1372.

153. Maguer J-F, L'Helguen S, Madec C, Labry C, Le Corre P (2007) Nitrogen uptake and assimilation kinetics in Alexandrium minutum (Dynophyceae): Effect of N-limited growth rate on nitrate and ammonium interactions J Phycol 43: 295-303.

154. Pernice M, Meibom A, Van Den Heuvel A, Kopp C, Domart-Coulon I, et al. (2012) A single-cell view of ammonium assimilation in coral-dinoflagellate symbiosis. ISME J 6: 1314-1324.

155. Collos Y, Vaquer A, Souchu P (2005) Acclimation of nitrate uptake by phytoplankton to high substrate levels . J Phycol 41: 466-478.

156. Chang FH, McClean M (1997) Growth responses of Alexandrium minutum (Dinophyceae) as a function of three different nitrogen sources and irradiance. New Zeal J Mar Fresh 31: 1-7.

157. Flynn K, Jones KJ, Flynn KJ (1996) Comparisons among species of Alexandrium (Dinophyceae) grown in nitrogen- or phosphorus-limiting batch culture. Mar Biol 126: 9-18.

158. Collos Y, Gagne C, Laabir M, Vaquer A, Cecchi P, et al. (2004) Nitrogenous nutrition of alexandrium catenella (Dinophyceae) in cultures and in Thau Lagoon, Southern France J Phycol 40: 96-103.

159. Dortch Q, Clayton JR, Jr., Thoresen SS, Ahmed SI (1984) Species differences in accumulation of nitrogen pools in phytoplankton. Mar Biol 81: 237-250.

160. Fauchot J, Levasseur M, Roy S, Gagnon R, Weise AM (2005) Environmental factors controlling Alexandrium tamarense (Dinophyceae) growth rate during a red tide in the St-Lawrence estuary (Canada) J Phycol 41: 263-272.

161. Kopp C, Pernice M, Domart-Coulon I, Djediat C, Spangenberg JE, et al. (2013) Highly Dynamic Cellular-Level Response of Symbiotic Coral to a Sudden Increase in Environmental Nitrogen. mBio 4.

162. Cookson SJ, Williams LE, Miller AJ (2005) Light-dark changes in cytosolic nitrate pools depend on nitrate reductase activity in Arabidopsis leaf cells. Plant Physiol 138: 1097-1105.

163. Paasche E, Bryceson I, Tangen K (1984) Interspecific variation in dark nitrogen uptake by dinoflagellates J Phycol 20: 394-401.

164. Armbrust EV, Berges JA, Bowler C, Green BR, Martinez D, et al. (2004) The genome of the diatom Thalassiosira pseudonana: ecology, evolution, and metabolism. Science 306: 79-86.

165. Bowler C, Allen A, Badger J, Grimwood J, Jabbari K, et al. (2008) The Phaeodactylum genome reveals the evolutionary history of diatom genomes. Nature 456: 239 - 244.

166. Lommer M, Specht M, Roy AS, Kraemer L, Andreson R, et al. (2012) Genome and low-iron response of an oceanic diatom adapted to chronic iron limitation. Genome Biol 13: R66.

167. Bender SJ, Parker MS, Armbrust EV (2012) Coupled effects of light and nitrogen source on the urea cycle and nitrogen metabolism over a diel cycle in the marine diatom Thalassiosira pseudonana. Protist 163: 232-251.

168. Allen AE (2005) Beyond sequence homology: redundant ammonium transporters in a marine diatom are not functionally equivalent J Phycol 41: 4-6.

169. Hildebrand M (2005) Cloning and functional characterization of ammonium transporters from the marine diatom Cylindrotheca fusiformis (Bacillariophyceae) J Phycol 41: 105-113.

170. Hildebrand M, Dahlin K (2000) Nitrate transporter genes from the diatom Cylindrotheca fusiformis (Bacillariophyceae): mRNA levels controlled by nitrogen source and by the cell cycle J Phycol 36: 702-713.

171. Shoguchi E, Shinzato C, Kawashima T, Gyoja F, Mungpakdee S, et al. (2013) Draft Assembly of the Symbiodinium minutum Nuclear Genome Reveals Dinoflagellate Gene Structure. Curr Biol 23: 1399-1408.

172. Bayer T, Aranda M, Sunagawa S, Yum LK, DeSalvo MK, et al. (2012) Symbiodinium Transcriptomes: Genome Insights into the Dinoflagellate Symbionts of Reef-Building Corals. PLoS One 7: e35269.

173. Hackett JD, Wisecaver JH, Brosnahan ML, Kulis DM, Anderson DM, et al. (2013) Evolution of Saxitoxin Synthesis in Cyanobacteria and Dinoflagellates. Mol Biol Evol 30: 70-78.

174. Morey JS, Monroe EA, Kinney AL, Beal M, Johnson JG, et al. (2011) Transcriptomic response of the red tide dinoflagellate, *Karenia brevis*, to nitrogen and phosphorus depletion and addition. BMC Genomics 12: 346.

175. Jeong H, Yoo Y, Kim J, Seong K, Kang N, et al. (2010) Growth, feeding and ecological roles of the mixotrophic and heterotrophic dinoflagellates in marine planktonic food webs. Ocean Sci J 45: 65-91.

176. Fenchel T (1987) Ecology of protozoa: the biology of free-living phagotrophic protists. Madison, WI; Science Tech Publishers; Berlin: Springer-Verlag. x + 197pp.

177. Jacobson DM (1987) The ecology and feeding biology of thecate heterotrophic dinoflagellates: Massachusetts Institute of Technology 210 p.

178. Jeong HJ, Yoo YD, Park JY, Song JY, Kim ST, et al. (2005) Feeding by phototrophic red-tide dinoflagellates: five species newly revealed and six species previously known to be mixotrophic. Aquat Microb Ecol40: 133-150.

179. Adolf JE, Krupatkina D, Bachvaroff T, Place AR (2007) Karlotoxin mediates grazing by Oxyrrhis marina on strains of Karlodinium veneficum. Harmful Algae 6: 400-412.

180. Berge T, Hansen P, Moestrup O (2008) Feeding mechanism, prey specificity and growth in light and dark of the plastidic dinoflagellate Karlodinium armiger. Aquat Microb Ecol 50: 279-288.

181. Bockstahler KR, Coats DW (1993) Spatial and Temporal Aspects of Mixotrophy In Chesapeake Bay Dinoflagellates. J Eukaryot Microbiol 40: 49-60.

182. Hansen PJ (1991) Quantitative importance and trophic role of heterotrophic dinoflagellates in coastal pelagial food web. Mar Ecol Prog Ser 73: 253-261.

183. Jacobson DM, Anderson DM (1986) Thecate Heterotrophic Dinoflagellates - Feeding-Behavior and Mechanisms. J Phycol 22: 249-258.

184. Jeong HJ, Park JY, Nho JH, Park MO, Ha JH, et al. (2005) Feeding by red-tide dinoflagellates on the cyanobacterium Synechococcus. Aquat Microb Ecol 41: 131-143.

185. Jeong HJ, Seong KA, Du Yoo Y, Kim TH, Kang NS, et al. (2008) Feeding and grazing impact by small marine heterotrophic dinoflagellates on heterotrophic bacteria. J Eukaryot Microbiol 55: 271-288.

186. Menden-Deuer S, Lessard EJ, Satterberg J, Grunbaum D (2005) Growth rates and starvation survival of three species of the pallium-feeding, thecate dinoflagellate genus Protoperidinium. Aquat Microb Ecol41: 145-152.

187. Nakamura Y, Suzuki S, Hiromi J (1995) Population dynamics of heterophytic dinoflagellates during a Gymnodinium mikimotoi red tide in the Seto Inland Sea. Mar Ecol Prog Ser 125: 269-277.

188. Strom SL, Buskey EJ (1993) Feeding, growth, and behavior of the thecate heterotrophic dinoflagellate Oblea rotunda Limnol Oceanogr 38: 965-977.

189. Tillmann U (2004) Interactions between planktonic microalgae and protozoan grazers. J Eukaryot Microbiol 51: 156-168.

190. Jeong HJ, Ha JH, Yoo YD, Park JY, Kim JH, et al. (2007) Feeding by the Pfiesteria-like heterotrophic dinoflagellate Luciella masanensis. J Eukaryot Microbiol 54: 231-241.

191. Miller TR, Belas R (2003) Pfiesteria piscicida, P-shumwayae, and other Pfiesteria-like dinoflagellates. Res Microbiol 154: 85-90.

192. Parrow MW, Burkholder JM (2004) The sexual life cycles of Pfiesteria piscicida and cryptoperidiniopsoids (Dinophyceae). J Phycol 40: 664-673.

193. Stoecker DK (1998) Conceptual models of mixotrophy in planktonic protists and some ecological and evolutionary implications. Eur J Protistol 34: 281-290.

194. Bockstahler KR, Coats DW (1993) Grazing of the mixotrophic dinoflagellate Gymnodinium sanguineum on ciliate populations of Chesapeake Bay. Mar Biol 116: 477-487.

195. Smalley GW, Coats DW (2002) Ecology of the red-tide dinoflagellate Ceratium furca: distribution, mixotrophy, and grazing impact on ciliate populations of Chesapeake Bay. J Eukaryot Microbiol 49: 63-73.

196. Qiu D, Huang L, Liu S, Lin S (2011) Nuclear, mitochondrial and plastid gene phylogenies of Dinophysis miles (Dinophyceae): evidence of variable types of chloroplasts. PLoS One 6: e29398.

197. Garcia-Cuetos L, Moestrup ò, Hansen PJ, Daugbjerg N (2010) The toxic dinoflagellate Dinophysis acuminata harbors permanent chloroplasts of cryptomonad origin, not kleptochloroplasts. Harmful Algae 9: 25-38.

198. Kim S, Kang Y, Kim H, Yih W, Coats D, et al. (2008) Growth and grazing responses of the mixotrophic dinoflagellate Dinophysis acuminata as functions of light intensity and prey concentration. Aquat Microb Ecol 51: 301-310.

199. Nishitani GOH, Nagai S, Sakiyama S, Kamiyama T (2008) Successful cultivation of the toxic dinoflagellate Dinophysis caudata (Dinophyceae). Plankton and Benthos Research 3: 78-85.

200. Nishitani G, Nagai S, Takano Y, Sakiyama S, Baba K, et al. (2008) Growth characteristics and phylogenetic analysis of the marine dinoflagellate Dinophysis infundibulus (Dinophyceae). Aquat Microb Ecol 52: 209-221.

201. Park M, Kim S, Kang Y, Yih W (2006) First successful culture of the marine dinoflagellate Dinophysis acuminata. Aquat Microb Ecol 45: 101-106.

202. Li A, Stoecker DK, Coats DW (2000) Mixotrophy in *Gyrodinium galatheanum* (Dinophyceae): grazing responses to light intensity and inorganic nutrients. J Phycol 36: 33-45.

203. Smalley GW, Coats DW, Stoecker DK (2003) Feeding in the mixotrophic dinoflagellate *Ceratium furca* is influenced by intracellular nutrient concentrations. Mar Ecol Prog Ser 262: 137-151.

204. Stoecker D, Li A, Coats D, Gustafson D, Nannen M (1997) Mixotrophy in the dinoflagellate *Prorocentrum minimum*. Mar Ecol Prog Ser 152: 1-12.

205. Jeong HJ, Shim JH, Kim JS, Park JY, Lee CW, et al. (1999) Feeding by the mixotrophic thecate dinoflagellate Fragilidium cf. mexicanum on red-tide and toxic dinoflagellates. Mar Ecol Prog Ser 176: 263-277.

206. Glibert PM, Burkholder JM, Kana TM, Alexander J, Skelton H, et al. (2009) Grazing by Karenia brevis on Synechococcus enhances its growth rate and may help to sustain blooms. Aquat Microb Ecol 55: 17-30.

207. Seong KA, Jeong HJ, Kim S, Kim GH, Kang JH (2006) Bacterivory by co-occurring red-tide algae, heterotrophic nanoflagellates, and ciliates. Mar Ecol Prog Ser 322: 85-97.

208. Risgaard-Petersen N, Langezaal AM, Ingvardsen S, Schmid MC, Jetten MS, et al. (2006) Evidence for complete denitrification in a benthic foraminifer. Nature 443: 93-96.

209. Shoun H, Tanimoto T (1991) Denitrification by the fungus Fusarium oxysporum and involvement of cytochrome P-450 in the respiratory nitrite reduction. J Biol Chem 266: 11078-11082.

210. Usuda K, Toritsuka N, Matsuo Y, Kim DH, Shoun H (1995) Denitrification by the fungus Cylindrocarpon tonkinense: anaerobic cell growth and two isozyme forms of cytochrome P-450nor. Appl Environ Microbiol 61: 883-889.

211. Preisler A, de Beer D, Lichtschlag A, Lavik G, Boetius A, et al. (2007) Biological and chemical sulfide oxidation in a Beggiatoa inhabited marine sediment. ISME J 1: 341-353.

212. Kamp A, de Beer D, Nitsch JL, Lavik G, Stief P (2011) Diatoms respire nitrate to survive dark and anoxic conditions. Proc Natl Acad Sci USA 108: 5649-5654.

213. Howard WD, Solomonson LP (1982) Quaternary structure of assimilatory NADH:nitrate reductase from Chlorella. J Biol Chem 257: 10243-10250.

214. Guerrero MG, Vega JM, Losada M (2003) The Assimilatory Nitrate-Reducing System and its Regulation. Ann Rev Plant Physiol 32: 169-204.

215. Heldt H-W, Piechulla B (2011) Nitrate assimilation is essential for the synthesis of organic matter. Plant Biochemistry (Fourth Edition). San Diego: Academic Press. pp. 273-305.

216. Moreno-Vivian C, Cabello P, Martinez-Luque M, Blasco R, Castillo F (1999) Prokaryotic Nitrate Reduction: Molecular Properties and Functional Distinction among Bacterial Nitrate Reductases. J Bacteriol 181: 6573-6584.

217. Chen Q, Silflow CD (1996) Isolation and characterization of glutamine synthetase genes in Chlamydomonas reinhardtii. Plant Physiol 112: 987-996.

218. Forde BG, Lea PJ (2007) Glutamate in plants: metabolism, regulation, and signalling. J Exp Bot 58: 2339-2358.

219. Leggat W, Hoegh-Guldberg O, Dove S, Yellowlees D (2007) Analysis of an EST library from the dinoflagellate (Symbiodinium sp.) symbiont of reef-building corals1. J Phycol 43: 1010-1021.

220. Anderson SL, Burris JE (1987) Role of glutamine synthetase in ammonia assimilation by symbiotic marine dinoflagellates (zooxanthellae). Mar Biol 94: 451-458.à

221. Rahav O, Dubinsky Z, Achituv Y, Falkowski PG (1989) Ammonium Metabolism in the Zooxanthellate Coral, Stylophora pistillata. P Roy Soc Lond B Biol 236: 325-337.

222. Summons RE, Osmond CB (1981) Nitrogen assimilation in the symbiotic marine alga Gymnodinium microadriaticum: direct analysis of 15N incorporation by gc-ms methods. Phytochemistry 20: 575-578.

223. Ramalho CB, Hastings JW, Colepicolo P (1995) Circadian oscillation of nitrate reductase activity in Gonyaulax polyedra is due to changes in cellular protein levels. Plant Physiol 107: 225-231.

224. Roenneberg T, Rehman J (1996) Nitrate, a nonphotic signal for the circadian system. FASEB J 10: 1443-1447.

225. Dortch Q, Maske H (1982) Dark Uptake of Nitrate and Nitrate Reductase Activity of a Red-Tide Population Off Peru. Mar Ecol Prog Ser 9: 299-303.

226. Iliev D, Voytsekh O, Schmidt EM, Fiedler M, Nykytenko A, et al. (2006) A heteromeric RNA-binding protein is involved in maintaining acrophase and period of the circadian clock. Plant Physiol 142: 797-806.

227. Pilgrim ML, Caspar T, Quail PH, McClung CR (1993) Circadian and light-regulated expression of nitrate reductase in Arabidopsis. Plant Mol Biol 23: 349-364.

228. Allen AE, Dupont CL, Obornik M, Horak A, Nunes-Nesi A, et al. (2011) Evolution and metabolic significance of the urea cycle in photosynthetic diatoms. Nature 473: 203-207.

229. Gupta KJ, Fernie AR, Kaiser WM, van Dongen JT (2011) On the origins of nitric oxide. Trends Plant Sci 16: 160-168.

230. Carpenter EJ, Montoya JP, Burns J, Mulholland MR, Subramaniam A, et al. (1999) Extensive bloom of a N2-fixing diatom/cyanobacterial association in the tropical Atlantic Ocean. Mar Ecol Prog Ser 185: 273-283.

231. Venrick EL (1974) The distribution and significance of Richelia intracellularis Schmidt in the North Pacific central gyre. Limnol Oceanogr 19: 437-444.

232. Tarangkoon W, Hansen G, Hansen P (2010) Spatial distribution of symbiont-bearing dinoflagellates in the Indian Ocean in relation to oceanographic regimes. Aquat Microb Ecol 58: 197-213.

233. Lesser MP, Mazel CH, Gorbunov MY, Falkowski PG (2004) Discovery of symbiotic nitrogen-fixing cyanobacteria in corals. Science 305: 997-1000.

234. Rosenberg E, Koren O, Reshef L, Efrony R, Zilber-Rosenberg I (2007) The role of microorganisms in coral health, disease and evolution. Nat Rev Microbiol 5: 355-362.

235. Lema KA, Willis BL, Bourne DG (2012) Corals form characteristic associations with symbiotic nitrogen-fixing bacteria. Appl Environ Microbiol 78: 3136-3144.

236. Lesser MP, Falcon LI, Rodriguez-Roman A, Enriquez S, Hoegh-Guldberg O, et al. (2007) Nitrogen fixation by symbiotic cyanobacteria provides a source of nitrogen for the scleractinian coral Montastraea cavernosa. Mar Ecol Prog Ser 346: 143-152.

237. Olson ND, Ainsworth TD, Gates RD, Takabayashi M (2009) Diazotrophic bacteria associated with Hawaiian Montipora corals: Diversity and abundance in correlation with symbiotic dinoflagellates. J Exp Mar Biol Ecol 371: 140-146.

238. Hockin NL, Mock T, Mulholland F, Kopriva S, Malin G (2012) The response of diatom central carbon metabolism to nitrogen starvation is different from that of green algae and higher plants. Plant Physiol 158: 299-312.

239. Lei QY, Lu SH (2011) Molecular ecological responses of dinoflagellate, *Karenia mikimotoi* to environmental nitrate stress. Mar Pollut Bull 62: 2692-2699.

240. Pleissner D, Eriksen NT (2012) Effects of phosphorous, nitrogen, and carbon limitation on biomass composition in batch and continuous flow cultures of the heterotrophic dinoflagellate *Crypthecodinium cohnii*. Biotechnol Bioeng 109: 2005-2016.

241. Leong SC, Murata A, Nagashima Y, Taguchi S (2004) Variability in toxicity of the dinoflagellate Alexandrium tamarense in response to different nitrogen sources and concentrations. Toxicon 43: 407-415.

242. Vanucci S, Pezzolesi L, Pistocchi R, Ciminiello P, Dell'Aversano C, et al. (2012) Nitrogen and phosphorus limitation effects on cell growth, biovolume, and toxin production in *Ostreopsis cf. ovata*. Harmful Algae 15: 78-90.

243. Wang DZ, Hsieh D (2002) Effects of nitrate and phosphate on growth and C2 toxin productivity of Alexandrium tamarense CI01 in culture. Mar Pollut Bull 45: 286-289.

244. Lin S, Mulholland MR, Zhang H, Feinstein TN, Jochem FJ, et al. (2004) Intense grazing and prey-dependent growth of *Pfiesteria piscicida* (Dinophyceae) J Phycol 40: 1062-1073.

245. Olson RJ, Chisholm SW (1986) Effect of light and nitrogen limitation on the cell cycle of the dinoflagellate *Amphidinium carteri*. J Plankton Res 8: 785-793.

246. Wang ZT, Ullrich N, Joo S, Waffenschmidt S, Goodenough U (2009) Algal lipid bodies: stress induction, purification, and biochemical characterization in wild-type and starchless Chlamydomonas reinhardtii. Eukaryot Cell 8: 1856-1868.

247. Wingler A, Purdy S, MacLean JA, Pourtau N (2006) The role of sugars in integrating environmental signals during the regulation of leaf senescence. J Exp Bot 57: 391-399.

248. Fuentes-Grunewald C, Garces E, Alacid E, Sampedro N, Rossi S, et al. (2012) Improvement of lipid production in the marine strains Alexandrium minutum and Heterosigma akashiwo by utilizing abiotic parameters. J Ind Microbiol Biotechnol 39: 207-216.

249. Kroth PG, Chiovitti A, Gruber A, Martin-Jezequel V, Mock T, et al. (2008) A model for carbohydrate metabolism in the diatom Phaeodactylum tricornutum deduced from comparative whole genome analysis. PLoS One 3: e1426.

250. Yang ZK, Niu YF, Ma YH, Xue J, Zhang MH, et al. (2013) Molecular and cellular mechanisms of neutral lipid accumulation in diatom following nitrogen deprivation. Biotechnol Biofuels 6: 67.

251. Allen A, Vardi A, Bowler C (2006) An ecological and evolutionary context for integrated nitrogen metabolism and related signaling pathways in marine diatoms. Curr Opin Plant Biol 9: 264 - 273.

252. Jeong HJ, Yoo YD, Kang NS, Lim AS, Seong KA, et al. (2012) Heterotrophic feeding as a newly identified survival strategy of the dinoflagellate Symbiodinium. Proc Natl Acad Sci USA 109: 12604-12609.

253. Lewitus AJ, Willis BM, Hayes KC, Burkholder JM, Glasgow Jr HB, et al. (1999) Mixotrophy and nitrogen uptake by Pfiesteria piscicida (Dinophyceae) J Phycol 35: 1430-1437.

254. Fernandez E, Galvan A (2008) Nitrate Assimilation in Chlamydomonas. Eukaryotic Cell 7: 555-559.

255. Lillo C (2008) Signalling cascades integrating light-enhanced nitrate metabolism. Biochem J 415: 11-19.

256. Maheswari U, Jabbari K, Petit J-L, Porcel B, Allen A, et al. (2010) Digital expression profiling of novel diatom transcripts provides insight into their biological functions. Genome Biol 11: R85.

257. Poulsen N, Kröger N (2005) A new molecular tool for transgenic diatoms. FEBS Journal 272: 3413-3423.

258. Lewis J, Hallet R (1997) Lingulodinium polyedrum (Gonyaulax polyedra) a blooming dinoflagellate. Oceanogr Mar Biol Annu Rev 35: 97-161.

259. Paz B, Daranas AH, Norte M, Riobo P, Franco JM, et al. (2008) Yessotoxins, a group of marine polyether toxins: An overview. Mar Drugs 6: 73-102.

260. Schmitter R (1971) The fine structure of *Gonyaulax polyedra*, a bioluminescent marine dinoflagellate. J Cell Sci 9: 147-173.

261. Spector D, editor (1984) Dinoflagellate nuclei. New York: Academic Press. 107-147 p.

262. Hastings JW (2007) The Gonyaulax clock at 50: translational control of circadian expression. Cold Spring Harb Symp Quant Biol 72: 141-144.

263. Woelfle MA, Ouyang Y, Phanvijhitsiri K, Johnson CH (2004) The Adaptive Value of Circadian Clocks: An Experimental Assessment in Cyanobacteria. Curr Biol 14: 1481-1486.

264. Dodd AN, Salathia N, Hall A, Kevei E, Toth R, et al. (2005) Plant circadian clocks increase photosynthesis, growth, survival, and competitive advantage. Science 309: 630-633.

265. Beaver LM, Gvakharia BO, Vollintine TS, Hege DM, Stanewsky R, et al. (2002) Loss of circadian clock function decreases reproductive fitness in males of Drosophila melanogaster. Proc Natl Acad Sci USA 99: 2134-2139.

266. DeCoursey PJ, Walker JK, Smith SA (2000) A circadian pacemaker in free-living chipmunks: essential for survival? J Comp Physiol A 186: 169-180.

267. Dunlap JC, Loros JJ, DeCoursey PJ, editors (2004) Chronobiology: Biological Timekeeping. Sunderland, Massachusetts, USA: Sinauer Associates, Inc. Publishers. 382 p.

268. Dunlap JC (1999) Molecular bases for circadian clocks. Cell 96: 271-290.

269. Nakajima M, Imai K, Ito H, Nishiwaki T, Murayama Y, et al. (2005) Reconstitution of circadian oscillation of cyanobacterial KaiC phosphorylation in vitro. Science 308: 414-415.

270. Dunlap J (1998) An end in the beginning. Science 280: 1548-1549.

271. Young MW, Kay SA (2001) Time zones: a comparative genetics of circadian clocks. Nat Rev Genet 2: 702-715.

272. Nicolas MT, Nicolas G, Johnson CH, Bassot JM, Hastings JW (1987) Characterization of the bioluminescent organelles in *Gonyaulax polyedra* (dinoflagellates) after fast-freeze fixation and antiluciferase immunogold staining. J Cell Biol 105: 723-735.

273. Morse D, Pappenheimer AM, Jr., Hastings JW (1989) Role of a luciferin-binding protein in the circadian bioluminescent reaction of *Gonyaulax polyedra*. J Biol Chem 264: 11822-11826.

274. Hastings JW (2001) Cellular and molecular mechanisms of circadian regulation in the unicellular dinoflagellate *Gonyaulax polyedra*. In: Takahashi JS, Turek F, Moore RY, editors. Handbood of Behavioral Neurobiology. New York N.Y.: Plenum Press. pp. 321-334.

275. Fogel M, Hastings JW (1972) Bioluminescence: mechanism and mode of control of scintillon activity. Proc Natl Acad Sci USA 69: 690-693.

276. Fritz L, Morse D, Hastings JW (1990) The circadian bioluminescence rhythm of Gonyaulax is related to daily variations in the number of light-emitting organelles. J Cell Sci 95 (Pt 2): 321-328.

277. Morse D, Milos PM, Roux E, Hastings JW (1989) Circadian regulation of bioluminescence in Gonyaulax involves translational control. Proc Natl Acad Sci USA 86: 172-176.

278. Dunlap JC, Hastings JW (1981) The biological clock in *Gonyaulax* controls luciferase activity by regulating turnover. J Biol Chem 256: 10509-10518.

279. Johnson CH, Roeber JF, Hastings JW (1984) Circadian Changes in Enzyme Concentration Account for Rhythm of Enzyme Activity in Gonyaulax. Science 223: 1428-1430.

280. Mittag M, Li L, Hastings JW (1998) The mRNA level of the circadian regulated Gonyaulax luciferase remains constant over the cycle. Chronobiol Int 15: 93-98.

281. Sweeney BM (1960) The photosynthetic rhythm in single cells of *Gonyaulax polyedra*. Cold Spring Harbor Symp Quant Biol 25: 145-148.

282. Hastings JW, Astrachan L, Sweeney BM (1961) A persistent daily rhythm in photosynthesis. J Gen Physiol 45: 69-76.

283. Le Q, Jovine R, Markovic P, Morse D (2001) PCP is not implicated in the photosynthesis rhythm of Gonyaulax despite circadian regulation of its translation. Biol Rhythm Research 32: 579-594.

284. Bush KJ, Sweeney BM (1972) The activity of ribulose diphosphate carboxylase in extracts of *Gonyaulax polyedra* in the day and the night phases of the circadian rhythm of photosynthesis. Plant Physiol 50: 446-451.

285. Rensing L, Taylor WR, Dunlap J, Hastings JW (1980) The effects of protein synthesis inhibitors on the *Gonyaulax* clock II: the effect of cycloheximide on ultrastructural parameters. J Comp Physiol 138: 9-18.

286. Sweeney BM, Folli SI (1984) Nitrate deficiency shortens the circadian period in gonyaulax. Plant Physiol 75: 242-245.

287. Vargo GA, Heil CA, Fanning KA, Dixon LK, Neely MB, et al. (2008) Nutrient availability in support of *Karenia brevis* blooms on the central West Florida Shelf: What keeps *Karenia* blooming? Cont Shelf Res 28: 73-98.

288. Vitousek P, Howarth R (1991) Nitrogen limitation on land and in the sea: How can it occur? Biogeochemistry 13: 87-115.

289. Dagenais-Bellefeuille S, Morse D (2013) Putting the N in dinoflagellates. Front Microbiol 4: 369.

290. Walsh JJ, Weisberg RH, Lenes JM, Chen FR, Dieterle DA, et al. (2009) Isotopic evidence for dead fish maintenance of Florida red tides, with implications for coastal fisheries over both source regions of the West Florida shelf and within downstream waters of the South Atlantic Bight. Prog Oceanogr 80: 51-73.

291. Moorthi S, Countway P, Stauffer B, Caron D (2006) Use of Quantitative Real-Time PCR to Investigate the Dynamics of the Red Tide Dinoflagellate Lingulodinium polyedrum. Microb Ecol 52: 136-150.

292. Atkinson M, Bingman C (1994) Elemental composition of commercial seasalts. J Aquari & Aqua Sci 8: 39-43.

293. Liu B, Lo SC, Matton DP, Lang BF, Morse D (2012) Daily changes in the phosphoproteome of the dinoflagellate *Lingulodinium*. Protist 163: 746-754.

294. Dorion S, Clendenning A, Jeukens J, Salas JJ, Parveen N, et al. (2012) A large decrease of cytosolic triosephosphate isomerase in transgenic potato roots affects the distribution of carbon in primary metabolism. Planta 236: 1177-1190.

295. Rivoal J, Hanson AD (1993) Evidence for a Large and Sustained Glycolytic Flux to Lactate in Anoxic Roots of Some Members of the Halophytic Genus *Limonium*. Plant Physiol 101: 553-560.

296. Jeffrey S, Humphrey G (1975) New spectrophotometric equations for determining chlorophylls a, b, c1 and c2 in higher plants, algae and natural phytoplankton. Biochem Physiol Pflanz: 191-194.

297. Mackenzie TD, Morse D (2011) Circadian photosynthetic reductant flow in the dinoflagellate Lingulodinium is limited by carbon availability. Plant Cell Environ 34: 669-680.

298. Trethewey RN, Geigenberger P, Riedel K, Hajirezaei MR, Sonnewald U, et al. (1998) Combined expression of glucokinase and invertase in potato tubers leads to a dramatic reduction in starch accumulation and a stimulation of glycolysis. Plant J 15: 109-118.

299. Chen W, Zhang C, Song L, Sommerfeld M, Hu Q (2009) A high throughput Nile red method for quantitative measurement of neutral lipids in microalgae. J Microbiol Methods 77: 41-47.

300. Kolter R, Siegele DA, Tormo A (1993) The stationary phase of the bacterial life cycle. Annu Rev Microbiol 47: 855-874.

301. Foyer CH, Parry M, Noctor G (2003) Markers and signals associated with nitrogen assimilation in higher plants. J Exp Bot 54: 585-593.

302. Hicks GR, Hironaka CM, Dauvillee D, Funke RP, D'Hulst C, et al. (2001) When Simpler Is Better. Unicellular Green Algae for Discovering New Genes and Functions in Carbohydrate Metabolism. Plant Physiol 127: 1334-1338.

303. Hu Q, Sommerfeld M, Jarvis E, Ghirardi M, Posewitz M, et al. (2008) Microalgal triacylglycerols as feedstocks for biofuel production: perspectives and advances. Plant J 54: 621-639.

304. Jiang PL, Pasaribu B, Chen CS (2014) Nitrogen-deprivation elevates lipid levels in *Symbiodinium* spp. by lipid droplet accumulation: morphological and compositional analyses. PLoS One 9: e87416.

305. Graf A, Smith AM (2011) Starch and the clock: the dark side of plant productivity. Trends Plant Sci 16: 169-175.

306. Ball S, Colleoni C, Cenci U, Raj JN, Tirtiaux C (2011) The evolution of glycogen and starch metabolism in eukaryotes gives molecular clues to understand the establishment of plastid endosymbiosis. J Exp Bot 62: 1775-1801.

307. Dauvillée D, Deschamps P, Ral JP, Plancke C, Putaux JL, et al. (2009) Genetic dissection of floridean starch synthesis in the cytosol of the model dinoflagellate *Crypthecodinium cohnii*. Proc Natl Acad Sci USA 106: 21126-21130.

308. Deschamps P, Guillebeault D, Devassine J, Dauvillee D, Haebel S, et al. (2008) The heterotrophic dinoflagellate *Crypthecodinium cohnii* defines a model genetic system to investigate cytoplasmic starch synthesis. Eukaryot Cell 7: 872-880.

309. Holmes R, Williams P, Eppley R (1967) Red water in La Jolla Bay, 1964-1967. Limnol Oceanogr 12: 503-512.

310. Turpin DH (1991) Effects of inorganic N availability on algal photosynthesis and carbon metabolism J Phycol 27: 14-20.

311. Evans J (1989) Photosynthesis and nitrogen relationships in leaves of C3 plants. Oecologia 78: 9-19.

312. Kolber Z, Zehr J, Falkowski P (1988) Effects of Growth Irradiance and Nitrogen Limitation on Photosynthetic Energy Conversion in Photosystem II. Plant Physiol 88: 923-929.

313. Prézelin BB, Samuelsson G, Matlick HA (1986) Photosystem II photoinhibition and altered kinetics of photosynthesis during nutrient-dependent high-light photoadaptation in *Gonyaulax polyedra*. Mar Biol 93: 1-12.

314. Pérez-Pérez ME, Florencio FJ, Crespo JL (2010) Inhibition of Target of Rapamycin Signaling and Stress Activate Autophagy in *Chlamydomonas reinhardtii*. Plant Physiol 152: 1874-1888.

315. Thompson AR, Doelling JH, Suttangkakul A, Vierstra RD (2005) Autophagic nutrient recycling in *Arabidopsis* directed by the ATG8 and ATG12 conjugation pathways. Plant Physiol 138: 2097-2110.

316. Davey MP, Horst I, Duong GH, Tomsett EV, Litvinenko AC, et al. (2014) Triacylglyceride production and autophagous responses in *Chlamydomonas reinhardtii* depend on resource allocation and carbon source. Eukaryot Cell 13: 392-400.

317. Siaut M, Cuine S, Cagnon C, Fessler B, Nguyen M, et al. (2011) Oil accumulation in the model green alga *Chlamydomonas reinhardtii*: characterization, variability between common laboratory strains and relationship with starch reserves. BMC Biotechnol 11: 7.

318. Zhou J, Fritz L (1994) The PAS/ACCUMULATION bodies in *Prorocentrum lima* and *Prorocentrum maculosum* (Dinophyceae) are dinoflagellate lysosomes J Phycol 30: 39-44.

319. Schmitter RE (1971) The fine structure of *Gonyaulax polyedra*, a bioluminescent marine dinoflagellate. J Cell Sci 9: 147-173.

320. Eroglu E, Okada S, Melis A (2011) Hydrocarbon productivities in different Botryococcus strains: comparative methods in product quantification. J Appl Phycol 23: 763-775.

321. Campbell RW, Dower JF (2003) Role of lipids in the maintenance of neutral buoyancy by zooplankton. Mar Ecol Prog Ser 263: 93-99.

322. Heldt H-W, Piechulla B (2011) 9 - Polysaccharides are storage and transport forms of carbohydrates produced by photosynthesis. In: Heldt H-W, Piechulla B, editors. Plant Biochemistry (Fourth Edition). San Diego: Academic Press. pp. 241-271.

323. Viola R, Nyvall P, Pedersen M (2001) The unique features of starch metabolism in red algae. Proc Biol Sci 268: 1417-1422.

324. Deschamps P, Haferkamp I, Dauvillee D, Haebel S, Steup M, et al. (2006) Nature of the periplastidial pathway of starch synthesis in the cryptophyte *Guillardia theta*. Eukaryot Cell 5: 954-963.

325. Plancke C, Colleoni C, Deschamps P, Dauvillee D, Nakamura Y, et al. (2008) Pathway of cytosolic starch synthesis in the model glaucophyte *Cyanophora paradoxa*. Eukaryot Cell 7: 247-257.

326. Pierce RH, Henry MS, Blum PC, Lyons J, Cheng YS, et al. (2003) Brevetoxin Concentrations in Marine Aerosol: Human Exposure Levels During a Karenia brevis Harmful Algal Bloom. B Environ Contam Tox 70: 161-165.

327. Crawford NM, Forde BG (2002) Molecular and developmental biology of inorganic nitrogen nutrition. Arabidopsis Book 1: e0011.

328. Moir JW, Wood NJ (2001) Nitrate and nitrite transport in bacteria. Cell Mol Life Sci 58: 215-224.

329. Unkles SE, Hawker KL, Grieve C, Campbell EI, Montague P, et al. (1991) crnA encodes a nitrate transporter in Aspergillus nidulans. Proc Natl Acad Sci USA 88: 204-208.

330. Unkles SE, Zhou D, Siddiqi MY, Kinghorn JR, Glass AD (2001) Apparent genetic redundancy facilitates ecological plasticity for nitrate transport. EMBO J 20: 6246-6255.

331. Krapp A, David LC, Chardin C, Girin T, Marmagne A, et al. (2014) Nitrate transport and signalling in Arabidopsis. J Exp Bot 65: 789-798.

332. Tsay YF, Chiu CC, Tsai CB, Ho CH, Hsu PK (2007) Nitrate transporters and peptide transporters. FEBS Lett 581: 2290-2300.

333. Kotur Z, Mackenzie N, Ramesh S, Tyerman SD, Kaiser BN, et al. (2012) Nitrate transport capacity of the Arabidopsis thaliana NRT2 family members and their interactions with AtNAR2.1. New Phytol 194: 724-731.

334. Orsel M, Chopin F, Leleu O, Smith SJ, Krapp A, et al. (2006) Characterization of a two-component high-affinity nitrate uptake system in Arabidopsis. Physiology and protein-protein interaction. Plant Physiol 142: 1304-1317.

335. Zhou JJ, Fernandez E, Galvan A, Miller AJ (2000) A high affinity nitrate transport system from Chlamydomonas requires two gene products. FEBS Lett 466: 225-227.

336. Zhou JJ, Trueman LJ, Boorer KJ, Theodoulou FL, Forde BG, et al. (2000) A high affinity fungal nitrate carrier with two transport mechanisms. J Biol Chem 275: 39894-39899.

337. Leran S, Varala K, Boyer JC, Chiurazzi M, Crawford N, et al. (2014) A unified nomenclature of Nitrate Transporter 1/ Peptide Transporter family members in plants. Trends Plant Sci 19: 5-9.

338. Slot JC, Hallstrom KN, Matheny PB, Hibbett DS (2007) Diversification of NRT2 and the Origin of Its Fungal Homolog. Mol Biol Evol 24: 1731-1743.

339. Jentsch TJ (2008) CLC chloride channels and transporters: from genes to protein structure, pathology and physiology. Crit Rev Biochem Mol Biol 43: 3-36.

340. von der Fecht-Bartenbach J, Bogner M, Dynowski M, Ludewig U (2010) CLC-b-Mediated NO3-/H+ Exchange Across the Tonoplast of Arabidopsis Vacuoles. Plant Cell Physiol 51: 960-968.

341. Geiger D, Maierhofer T, Al-Rasheid KA, Scherzer S, Mumm P, et al. (2011) Stomatal closure by fast abscisic acid signaling is mediated by the guard cell anion channel SLAH3 and the receptor RCAR1. Sci Signal 4: ra32.

342. Geiger D, Scherzer Sn, Mumm P, Stange A, Marten I, et al. (2009) Activity of guard cell anion channel SLAC1 is controlled by drought-stress signaling kinase-phosphatase pair. Proc Natl Acad Sci USA 106: 21425-21430.

343. Stamatakis A (2014) RAxML version 8: a tool for phylogenetic analysis and post-analysis of large phylogenies. Bioinformatics 30: 1312-1313.

344. Huson DH, Scornavacca C (2012) Dendroscope 3: an interactive tool for rooted phylogenetic trees and networks. Syst Biol 61: 1061-1067.

345. Kinghorn JR, Sloan J, Kana'n GJM, DaSilva ER, Rouch DA, et al. (2005) Missense Mutations That Inactivate the Aspergillus nidulans nrtA Gene Encoding a High-Affinity Nitrate Transporter. Genetics 169: 1369-1377.

346. Unkles SE, Karabika E, Symington VF, Cecile JL, Rouch DA, et al. (2012) Alanine scanning mutagenesis of a high-affinity nitrate transporter highlights the requirement for glycine and asparagine residues in the two nitrate signature motifs. Biochem J 447: 35-42.

347. Unkles SE, Rouch DA, Wang Y, Siddiqi MY, Glass AD, et al. (2004) Two perfectly conserved arginine residues are required for substrate binding in a high-affinity nitrate transporter. Proc Natl Acad Sci USA 101: 17549-17554.

348. Forde BG (2000) Nitrate transporters in plants: structure, function and regulation. BBA-Biomembranes 1465: 219-235.

349. Krogh A, Larsson B, von Heijne G, Sonnhammer EL (2001) Predicting transmembrane protein topology with a hidden Markov model: application to complete genomes. J Mol Biol 305: 567-580.

350. Hofmann K, Stoffel W (1993) TMBASE- A database of membrane spanning protein segments Biol Chem 374: 166.

351. Claros MG, von Heijne G (1994) TopPred II: an improved software for membrane protein structure predictions. Comput Appl Biosci 10: 685-686.

352. von Heijne G (1992) Membrane protein structure prediction. Hydrophobicity analysis and the positive-inside rule. J Mol Biol 225: 487-494.

353. Roy S, Beauchemin M, Dagenais-Bellefeuille S, Letourneau L, Cappadocia M, et al. (2014) The Lingulodinium circadian system lacks rhythmic changes in transcript abundance. BMC Biol 12: 107.

354. Roy S, Letourneau L, Morse D (2014) Cold-induced cysts of the photosynthetic dinoflagellate Lingulodinium polyedrum have an arrested circadian bioluminescence rhythm and lower levels of protein phosphorylation. Plant Physiol 164: 966-977.

355. Gasteiger E, Gattiker A, Hoogland C, Ivanyi I, Appel RD, et al. (2003) ExPASy: the proteomics server for in-depth protein knowledge and analysis. Nucleic Acids Res 31: 3784-3788.

356. Bergsdorf E-Y, Zdebik AA, Jentsch TJ (2009) Residues Important for Nitrate/Proton Coupling in Plant and Mammalian CLC Transporters. J Biol Chem 284: 11184-11193.

357. Wege S, Jossier M, Filleur S, Thomine S, Barbier-Brygoo H, et al. (2010) The proline 160 in the selectivity filter of the Arabidopsis NO3−/H+ exchanger AtCLCa is essential for nitrate accumulation in planta. Plant J 63: 861-869.

358. Trueman LJ, Richardson A, Forde BG (1996) Molecular cloning of higher plant homologues of the high-affinity nitrate transporters of Chlamydomonas reinhardtii and Aspergillus nidulans. Gene 175: 223-231.

359. Glass AD, Britto DT, Kaiser BN, Kinghorn JR, Kronzucker HJ, et al. (2002) The regulation of nitrate and ammonium transport systems in plants. J Exp Bot 53: 855-864.

360. Wang R, Xing X, Crawford N (2007) Nitrite Acts as a Transcriptome Signal at Micromolar Concentrations in Arabidopsis Roots. Plant Physiol 145: 1735-1745.

361. Derelle E, Ferraz C, Rombauts S, Rouze P, Worden AZ, et al. (2006) Genome analysis of the smallest free-living eukaryote Ostreococcus tauri unveils many unique features. Proc Natl Acad Sci USA 103: 11647-11652.

362. Nassoury N, Cappadocia M, Morse D (2003) Plastid ultrastructure defines the protein import pathway in dinoflagellates. J Cell Sci 116: 2867-2874.

363. Bertomeu T, Hastings JW, Morse D (2003) Vectorial labeling of dinoflagellate cell surface proteins J Phycol 39: 1254-1260.

364. Kotur Z, Glass AD (2015) A 150 kDa plasma membrane complex of AtNRT2.5 and AtNAR2.1 is the major contributor to constitutive high-affinity nitrate influx in Arabidopsis thaliana. Plant Cell Environ 38: 1490-1502.

365. Lezhneva L, Kiba T, Feria-Bourrellier AB, Lafouge F, Boutet-Mercey S, et al. (2014) The Arabidopsis nitrate transporter NRT2.5 plays a role in nitrate acquisition and remobilization in nitrogen-starved plants. Plant J 80: 230-241.

366. Clement CR, Hopper MJ, Jones LHP, Leafe EL (1978) The Uptake of Nitrate by Lolium perenne from Flowing Nutrient Solution: II. Effect of light, defoliation, and relationship to CO_2 flux. J Exp Bot 29: 1173-1183.

367. Macduff JH, Bakken AK, Dhanoa MS (1997) An analysis of the physiological basis of commonality between diurnal patterns of NH_4^+, NO_3^- and K^+ uptake by Phleum pratense and Festuca pratensis. J Exp Bot 48: 1691-1701.

368. Peuke AD, Jeschke WD (1998) The effects of light on induction, time courses, and kinetic patterns of net nitrate uptake in barley. Plant Cell Environ 21: 765-774.

369. Lejay L, Tillard P, Lepetit M, Olive F, Filleur S, et al. (1999) Molecular and functional regulation of two NO3- uptake systems by N- and C-status of Arabidopsis plants. Plant J 18: 509-519.

370. Matt P, Geiger M, Walch-Liu P, Engels C, Krapp A, et al. (2001) The immediate cause of the diurnal changes of nitrogen metabolism in leaves of nitrate-replete tobacco: a major imbalance between the rate of nitrate reduction and the rates of nitrate uptake and ammonium metabolism during the first part of the light period. Plant Cell Environ 24: 177-190.

371. Ono F, Frommer WB, von Wirén N (2000) Coordinated Diurnal Regulation of Low- and High-Affinity Nitrate Transporters in Tomato. Plant Biol 2: 17-23.

372. Slamovits CH, Okamoto N, Burri L, James ER, Keeling PJ (2011) A bacterial proteorhodopsin proton pump in marine eukaryotes. Nat Commun 2: 183.

373. Roenneberg T, Colfax GN, Hastings JW (1989) A circadian rhythm of population behavior in Gonyaulax polyedra. J Biol Rhythms 4: 201-216.

374. Dunlap JC, Loros JJ, DeCoursey PJ (2004) Chronobiology : Biological Timekeeping. Sunderland MA: Sinauer Associates. 406 p.

375. Bell-Pedersen D, Cassone VM, Earnest DJ, Golden SS, Hardin PE, et al. (2005) Circadian rhythms from multiple oscillators: lessons from diverse organisms. Nat Rev Genet 6: 544-556.

376. Teng SW, Mukherji S, Moffitt JR, de Buyl S, O'Shea EK (2013) Robust circadian oscillations in growing cyanobacteria require transcriptional feedback. Science 340: 737-740.

377. O'Neill JS, Reddy AB (2011) Circadian clocks in human red blood cells. Nature 469: 498-503.

378. O'Neill JS, van Ooijen G, Dixon LE, Troein C, Corellou F, et al. (2011) Circadian rhythms persist without transcription in a eukaryote. Nature 469: 554-558.

379. Nassoury N, Hastings JW, Morse D (2005) Biochemistry and circadian regulation of output from the *Gonyaulax* clock: are there many clocks or simply many hands? In: Kippert F, editor. The circadian clock in eukaryotic microbes: Kluwer Academic and Plenum.

380. Milos P, Morse D, Hastings JW (1990) Circadian control over synthesis of many *Gonyaulax* proteins is at a translational level. Naturwiss 77: 87-89.

381. Fagan T, Morse D, Hastings J (1999) Circadian synthesis of a nuclear encoded chloroplast Glyceraldehyde-3-phosphate dehydrogenase in the dinoflagellate *Gonyaulax polyedra* is translationally controlled. Biochemistry 38: 7689-7695.

382. Hollnagel HC, Pinto E, Morse D, Colepicolo P (2002) The oscillation of photosynthetic capacity in *Gonyaulax polyedra* is not related to differences in RuBisCO, peridinin or chlorophyll *a* amounts. Biol Rhythms Res 33: 443-458.

383. Roenneberg T, Morse D (1993) Two circadian clocks in a single cell. Nature 362: 362-364.

384. Morse D, Hastings JW, Roenneberg T (1994) Different phase responses of the two circadian oscillators in *Gonyaulax*. J Biol Rhythms 9: 263-274.

385. Mortazavi A, Williams BA, McCue K, Schaeffer L, Wold B (2008) Mapping and quantifying mammalian transcriptomes by RNA-Seq. Nat Methods 5: 621-628.

386. Anders S, Huber W (2010) Differential expression analysis for sequence count data. Genome Biol 11: R106.

387. Robinson MD, McCarthy DJ, Smyth GK (2010) edgeR: a Bioconductor package for differential expression analysis of digital gene expression data. Bioinformatics 26: 139-140.

388. Chaput H, Wang Y, Morse D (2002) Polyadenylated transcripts containing random gene fragments are expressed in dinoflagellate mitochondria. Protist 153: 111-122.

389. Wang Y, Jensen L, Hojrup P, Morse D (2005) Synthesis and degradation of dinoflagellate plastid-encoded psbA proteins are light-regulated, not circadian-regulated. Proc Natl Acad Sci USA 102: 2844-2849.

390. Sobell HM (1985) Actinomycin and DNA transcription. Proc Natl Acad Sci USA 82: 5328-5331.

391. Muller WE, Seibert G, Beyer R, Breter HJ, Maidhof A, et al. (1977) Effect of cordycepin on nucleic acid metabolism in L5178Y cells and on nucleic acid-synthesizing enzyme systems. Cancer Res 37: 3824-3833.

392. Woolum JC (1991) A re-examination of the role of the nucleus in generating the circadian rhythm in Acetabularia. J Biol Rhythms 6: 129-136.

393. Lakin-Thomas PL (2006) Transcriptional feedback oscillators: maybe, maybe not. J Biol Rhythms 21: 83-92.

394. Morey JS, Van Dolah FM (2013) Global analysis of mRNA half-lives and de novo transcription in a dinoflagellate, Karenia brevis. PLoS One 8: e66347.

395. Rossini C, Taylor W, Fagan T, Hastings JW (2003) Lifetimes of mRNAs for clock regulated proteins in a dinoflagellate. Chronobiol Int 20: 963-976.

396. Karakashian MW, Hastings JW (1963) The effects of inhibitors of macromolecular biosynthesis upon the persistent rhythm of luminescence in *Gonyaulax*. J Gen Physiol 47: 1-12.

397. Dunlap JC, Taylor WR, Hastings JW (1980) The effects of protein synthesis inhibitors on the Gonyaulax clock I: Phase shifting effects of cycloheximide. J Comp Physiol 138: 1-8.

398. Taylor W, Krasnow T, Dunlap JC, Broda H, Hastings JW (1982) Critical pulses of anisomycin drive the circadian oscillator in Gonyaulax towards its singularity. J Comp Physiol B 148: 11-25.

399. Comolli J, Taylor W, Hastings JW (1994) An inhibitor of protein phosphorylation stops the circadian oscillator and blocks light-induced phase shifting in Gonyaulax polyedra. J Biol Rhythms 9: 13-26.

400. Comolli J, Taylor W, Rehman J, Hastings JW (1996) Inhibitors of serine/threonine phosphoprotein phosphatases alter circadian properties in Gonyaulax polyedra. Plant Physiol 111: 285-291.

401. Roy S, Morse D (2014) The Dinoflagellate Lingulodinium has Predicted Casein Kinase 2 Sites in Many RNA Binding Proteins. Protist 165: 330-342.

402. Allada R, Meissner RA (2005) Casein kinase 2, circadian clocks, and the flight from mutagenic light. Mol Cell Biochem 274: 141-149.

403. Morf J, Rey G, Schneider K, Stratmann M, Fujita J, et al. (2012) Cold-inducible RNA-binding protein modulates circadian gene expression posttranscriptionally. Science 338: 379-383.

404. Zhang Y, Ling J, Yuan C, Dubruille R, Emery P (2013) A role for Drosophila ATX2 in activation of PER translation and circadian behavior. Science 340: 879-882.

405. Lim C, Allada R (2013) ATAXIN-2 activates PERIOD translation to sustain circadian rhythms in Drosophila. Science 340: 875-879.

406. Tarun SJ, Sachs A (1996) Association of the yeast poly(A) tail binding protein with translation initiation factor eIF-4G. EMBO J 15: 7168-7177.

407. Kojima S, Sher-Chen EL, Green CB (2012) Circadian control of mRNA polyadenylation dynamics regulates rhythmic protein expression. Genes Dev 26: 2724-2736.

408. Huang Y, Ainsley JA, Reijmers LG, Jackson FR (2013) Translational profiling of clock cells reveals circadianly synchronized protein synthesis. PLoS Biol 11: e1001703.

409. Li H, Durbin R (2009) Fast and accurate short read alignment with Burrows-Wheeler transform. Bioinformatics 25: 1754-1760.

410. Eisensamer B, Roenneberg T (2004) Extracellular pH is under circadian control in *Gonyaulax polyedra* and forms a metabolic feedback loop. Chronobiol Int 21: 27-41.

411. Eppley RW, Holm-Hansen O, Strickland JDH (1968) Some observations on the vertical migration of dinoflagellates. J Phycol 4: 333-340.

412. Kiba T, Feria-Bourrellier AB, Lafouge F, Lezhneva L, Boutet-Mercey S, et al. (2012) The Arabidopsis nitrate transporter NRT2.4 plays a double role in roots and shoots of nitrogen-starved plants. Plant Cell 24: 245-258.

413. Lillo C, Meyer C, Ruoff P (2001) The nitrate reductase circadian system. The central clock dogma contra multiple oscillatory feedback loops. Plant Physiol 125: 1554-1557.

414. Pigaglio E, Durand N, Meyer C (1999) A conserved acidic motif in the N-terminal domain of nitrate reductase is necessary for the inactivation of the enzyme in the dark by phosphorylation and 14-3-3 binding. Plant Physiol 119: 219-230.

Appendix 1

TAG levels are not different at dawn or dusk in stationary or exponential phase *Lingulodinium* cell cultures.

Cells from cultures in stationary or exponential phases were harvested either at dawn (LD0) or at dusk (LD12) and neutral lipids were quantified with Nile Red. Results are mean ± SE (n=3). Statistically different results ($p < 0.05$) are marked with a different letter (Analysis of variance). FW; Fresh weight.

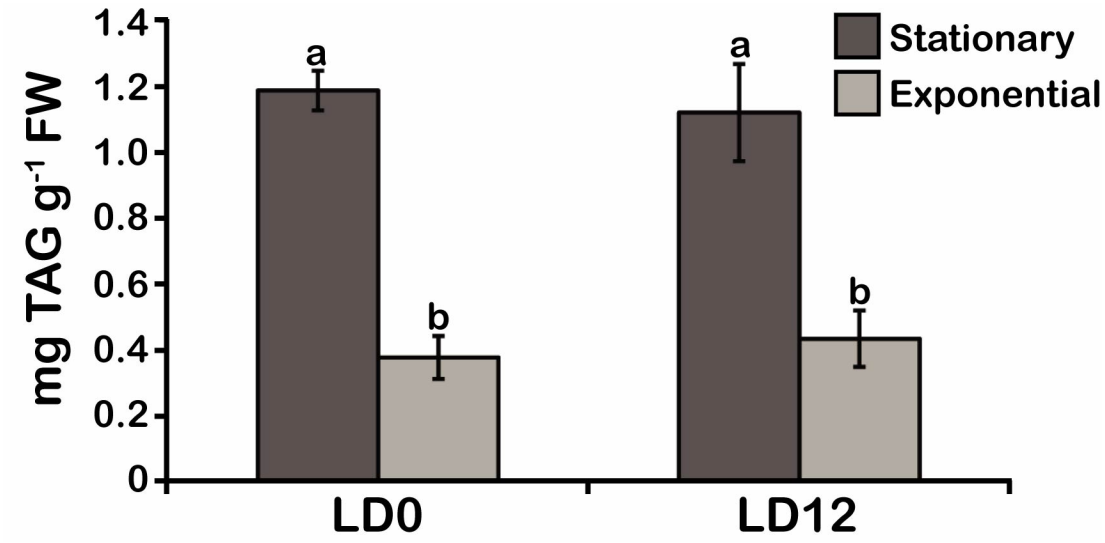

Appendix 2

$^{15}NO_3^-$ uptake in *Xenopus* oocytes injected or not with LpNRT2.1 mRNA.

Oocytes were surgically removed from frogs and defolliculated as described previously [20]. One to three days after defolliculation, oocytes were injected with 46 nl of water containing 10 ng of LpNRT2.1 cRNA. Oocytes were maintained in Barth's solution (in mM: 90 NaCl, 3 KCl, 0.82 $MgSO_4$, 0.41 $CaCl_2$, 0.33 $Ca(NO_3)_2$, 5 HEPES, pH 7.6) supplemented with 5% horse serum, 2.5 mM Na pyruvate, 100 U/ml penicillin, and 0.1 mg/ml streptomycin for 3–5 days post-injection to achieve maximum expression of LpNRT2.1. For nitrate uptake assays, injected or uninjected oocytes were incubated for 3 h in $^{15}NO_3^-$ buffer (in mM: 230 mannitol, 0.3 $CaCl_2$, 10 Mes-Tris pH 5.5) containing either 0.25 mM or 10 mM $Na^{15}NO_3^-$. Oocytes were lyophilized, weighed and inserted into tin capsules before stable isotope analysis. ^{15}N enrichment is expressed as $\delta\ ^{15}N$. Results are mean ± SE (n=3). Statistically different results ($p < 0.05$) are marked with an asterisk (Student's t-test).